Ibn Al-Haitham International Conference for Pure and Applied Sciences, University of Baghdad, Baghdad, Iraq (IHICPAS)

Ibn Al-Haitham International Conference for Pure and Applied Sciences, University of Baghdad, Baghdad, Iraq (IHICPAS).

Ahmed J. Obaid[1], Firas Abdulhameed Abdullatif [2], Moneer Hameed Tolephih[3], Hassan Ahmad Hasan [4], Salah Albermany[5], Hiba A. Ahmed[6]

[1, 5] Faculty of Computer Science and Mathematics, University of Kufa, Najaf, Iraq.
[2,3,4] Advanced Materials Science and Energy, CSIR Institute, RCED, India.
[6] Faculty of Science, University of Baghdad, Iraq.

E-Mails: [1]ahmedj.aljanaby@uokufa.edu.iq,

IHICPAS Conference Proceeding volume contain the novel contributions that were reviewed and presented through the Ibn Al-Haitham International Conference for Pure and Applied Sciences (IHICPAS) will be held in College of Education for Pure Science (Ibn al-Haitham), University of Baghdad on 20 and 21 December, 2020., where the conference covers 6 tracks which includes (Track1 Chemistry, Track 2: Mathematics, Track3: Computer Science, Track 4: Biology Sciences, Track 5: Physics, and Track 6: Remote Sensing and GIS). IHICPAS aims to gathering together all the new trends, projects, technologies, and recent research works in many fields in pure and Applied Sciences. The received papers which passed the double-blind reviews which successfully passed the reviewers comments and editorial board decisions comes from various authors around the world, where the authors are either working in academics centers, universities, research institutes, corporations, industries, and other agencies or postgraduate students where the presented works refers to their novelty in their research works.

IHICPAS Conference got very significant interesting from authors that comes from several countries like: UK, India, French, Morocco, Turkey, Nepal, Philippines, Indonesia, Australia, Egypt, Lebanon, Algeria, Iran, Pakistan, Malaysia, and Many other Countries where the authors are successfully presented their works and attend the sessions who managed by our scientific and organizing committee Members, and answered all the questions and dotes that directed by session chairs and attendances. We successfully held this conference within 2 days (20 and 21 December 2020), where in the first day we successfully listen to the keynote speakers' presentations then the session started from 10:00 AM based on Iraq Standard Time till 10:00PM. We would like to express our thanks and appreciation to all our session chairs for their hard work and attend our (12) sessions through two days and more than 10 hours per day to deliver the presented works in successful manner.

IHICPAS conference hosted 6 plenary sessions per day, where in the first day (20th December 2020) the Inauguration program started from (9:00 AM) till (10:00 AM). Then Sessions Started directly by dividing the authors into their certain session who managed by 4 Chairs (2 From Scientific Committee board, 1 from Organizing committee board and 1 from Conference Editors chairs board). The manuscripts which have presented and published in the IOP Conference Series: Journal of Physics under the peer-reviewed process. We love to express our gratitude for all of the participants, keynote speakers, organizing committee members, Scientific Committee members, and other Guest Chairs and Patrons for their supports and achievement, and we extend our thankful to all our reviewers (230+) reviewers, for their times and valuable notes. We extend our thanks to our international committee members for gaudiness of their participators and promote this conference in their regions, and successfully present very attractive presents. Also, we thank our authors for their effective contribution in our conference and participating with us in this conference proceeding. We also, acknowledge SICC Center at University of Kufa, Dijla Co. Pvt. Ltd., for their hospitality and sponsoring the conference. Furthermore, would like to thank SICC Center for supporting us to held this conference in successful manner.

Venue of the Conference

The conference has been organized Physically and virtually in College of Education for Pure Science (Ibn al-Haitham), University of Baghdad, in 20-21 December 2020. IHICPAS organizers aims through their scientific departments, and preparing a generation of students armed with knowledge and looking forward to building their country according to the new scientific developments. The university endeavors towards making use of them in an appropriate cultural means as well as building good and new scientific establishments for the sake of developing the present through scientific research.

The Reason(s) why IHICPAS Conference Held virtually:

Due Covid-19 Pandemic Situation in many countries around the world and the incredible increases cases through this Pandemic is very dangerous, and per day the number of cases in our peoples that infected by Covid-19 in the world and in Iraq, and due to the World Health Organization and Ministry of Health Recommendations, the conference organizers decided to conduct and held this conference Virtually to keep the life of participants and also due the challenges of lock down. Conduct IHICPAS virtually bring huge number of participants that non expected due many peoples are unable to attend conference physically, they able to attend our online Conference due to the friendly uses of Virtual Software without spending money for flight tickets or other matters to attend that type of conferences. However, we feel those peoples by attend our conference achieved our goal by inviting very attractive authors and participants who are interest to attending this conference, they will not able to attend it if it's held in non-virtually, However, The organizing committee have achieved these tasks and all sessions organized and managed successfully through Zoom Conference Meeting, where the team attend physically to use the University of Baghdad, College of Education for Pure Science (Ibn al-Haitham), infrastructure to achieve this conference Successfully.

Technology, Technical Difficulties and Drawbacks of Conference Virtually.

IHICPAS Conference Consider the ZOOM Meeting Software as the main software to conduct this conference, as the Main Software for delivering the Session discussions and Meeting information to all participants in Iraq and Other countries. The main advantages of this Technology is to reduce the time and space when someone would like to attend any scientific event and also broken the limitations for the peoples and authors who would like to attend this event from far away countries, in which the provide a facility to provide a platform that able to manage and control large number of participants is the main challenge of choosing the best software, we find Zoom meeting is the best software that fulfill our

requirements and provide amazing virtual platform to manage our authors and participants through our conference sessions.

The main technical difficulty in virtual software is the internet connection, due to covid-19 band, many peoples sitting at home and many jobs transformed from physical to virtual mode, However, internet connection and ISP infrastructure may affected due the large number of traffic devices that join to the network recently and may the ISP companies do not have good infrastructure to provide stable connection through the meeting or sessions. Hence, we conducted our sessions in the early morning time where the Babylon university, SICC, and Dijla Jewel Pvt. Ltd. Infrastructure used to achieve this task successfully. With Blessing of God, we held this conference successfully without any issue and we are looking to conduct this conference in future in physical manner after the world remedy from Covid-19 pandemic.

The Main Technical Difficulties of Virtual Meetings can be summarizing as follow:

Virtual Techniques and software that used to achieve these types of events and conferences in virtual mode, many software can be used, which can be offered by many companies either in free or paid own services. The main challenge to use online technique is to find the good software that able to manage large number of attendees with varied number of traffic data, we feel that the internet connections is the main source for any challenge in any online event. However, if the internet connection became slow, where many users are forced to exit and rejoin many times through the session. So many software's can used to achieve high quality meeting, need some certain limitations, like number of users, to keep the bandwidth little good, however not all interested peoples can attend meeting, difficulty of join and attend the meeting rooms, view and share the content, etc.

Drawbacks of virtual conference, we do not feel the virtual conference have much drawbacks than physical conferences, in which many peoples can avoid many fees payment for travels and hosting, registration fees, as well as flight tickets in which virtual conferences gives free offer for all the above issues. Another thing is, some famous figures and professors can easily join and attend without consider their fees in which they can attend and speak for hours when they sitting at home.

The main drawback we feel that if some authors would like to visit the conference venue for direct discussion and made good collaboration, so virtual meeting can also achieve this task easily, at the current time where all world suffer from Covid-19 pandemic.

Conference Chairs

- Prof. Dr. Firas Abdulhameed Abdullatif.
- Prof. Dr. Moneer Hameed Tolephih.

Conference Secretariat Chairs

- Prof. Dr. Salah Albermany
- Dr. Shubham Sharma
- A. Prof. Dr. **Ahmed J. Obaid.**

International Program Chairs

- Prof. Dr. Sandeep Kautish
- Prof. Dr Pradeep Kumar
- Prof. Dr. Macario G. Gayeta
- Prof. Dr. Tanusree Chatterjee
- Asst. Prof. Dr. Kamran Yeganegi

Scientific Committee

- Prof. Dr. Hasan Ahmed Hasan.
- Prof. Dr. Ghassan H. Abdulmajeed.
- Prof. Dr. Abdulkareem M. A. Alsammarraie.
- Prof. Dr.Nahla A.Al-Bakri.
- Prof. Dr. Alia A. Shehab.
- Prof. Dr. Mohamad J. Al-Jeboori.
- Prof. Dr. Ihsan Arfan Hussein.
- Prof. Dr. Ibrahim Mahdi Azooz Al-Salman.
- Prof. Dr. Luma N. Mohammed Tawfiq.
- Prof. Dr. Kareem Ali Jasim
- Prof. Dr. Dhafir T.A.Al-Heetimi
- Prof. Dr. Alaa A. Abdullatif
- Assist. Prof. Dr. Majeed Ahmed Weli
- Assist. Prof. Dr. Raied Mustafa Shakir
- Assist. Prof. Dr. Hanady Salim Abd Al-Sahib
- Assist. Prof. Dr. Wathiq Najah Abdullah
- Assist. Prof. Alaa Badr Hasan
- Assist.Prof. Dr. Rasha Naser Majeed
- Assist. Prof. Dr. Hussein Lefta Hussein
- Lect. Dr. Saba Naser Majeed

Organizing Committee

- Asst. Prof. Dr. Mohammed Mahdi Jawad
- Prof. Dr. Ahmed Waheed Nasir
- Prof. Dr. Tagreed Muslim Marush
- Prof. Dr. Bushra Hashim Hussein
- Asst. Prof Dr. Estabraq A. Mahmoud
- Asst. Prof. Dr. Salim Abdullah salman
- Asst.Prof.Dr. Ismaeel Yaseen Majeed
- Asst. Prof. Dr. Muazaz Azeez Hasan
- Asst. Prof. Dr. Auday Hattem Shaban
- Asst. Prof. Dr. Ahmed Mohammed Abbas
- Lec.Dr. Ali Adnan Nemah
- Lec.Dr. Sameer Sami Al-Obaidi
- Dr. Ahmed J. Obaid
- Lec.Dr. Ali Yahya Gheni
- Lec.Dr. Adel Rashed Abd Ali
- Lec.Dr. Mohammed Ali Ahmed
- Asst.Prof. Faisal Shallal Abbas
- Lec. Saad Ali Ahmed

- Asst. Lec. Harith Qasim Mahdi

Invited Speakers

- **Prof. Richard Winpenny,** Professor of Inorganic Chemistry, Materials Chemistry / Department of Chemistry Photon Science Institute / FSE Research Institutes Molecular Magnets Group.
- **Prof. Dr.Jure Ravnik**, Faculty of Mechanical, Slovenia Engineering, University of Maribor, Maribor, Slovenia.
- **Prof. Divya Maitreyi Chari,** Professor of Neural Tissue Engineering, University of Keele School of Medicine.
- **Prof. Dr. Sherein Salah el din Mohamed Ghaleb,** professor of forensic medicine and clinical toxicology, Cairo university, Egypt.
- **Ass.Prof. Ahmed saeed Alabed**, Ahmed Bin Mohammed Military college.

Organizing Institutions

- Ministry of Higher Education and Scientific Research
- University of Baghdad
- College of Education for Pure Science (Ibn al-Haitham).

Special Thanks to Conference Partners:

- **DIJLAH GOLDON JEWEL Company, Iraq, for their Supports and Sponsorship.**
- **SICC Center for Technical Supports.**

Conference Flyers and Posters:


ابن الهيثم
قاعة المرحوم الأستاذ الدكتور
فهد علي حسين الجبوري
رئيس
الجلسة

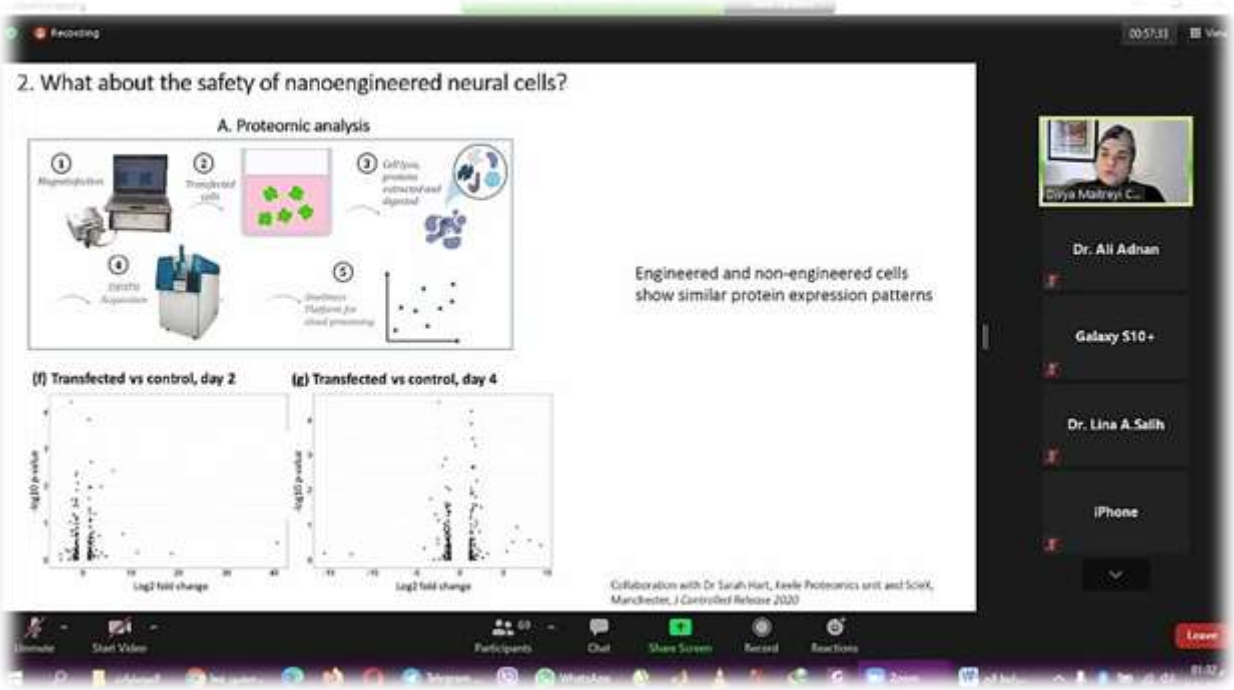
2. What about the safety of nanoengineered neural cells?
A. Proteomic analysis
Engineered and non-engineered cells show similar protein expression patterns
(f) Transfected vs control, day 2
(g) Transfected vs control, day 4
Dr. Ali Adnan
Galaxy S10+
Dr. Lina A.Salih
iPhone


Dr. Ali Adnan
Dr. Lina A.Salih
Dr.Ahmed Moha...
proff.dr.satar ab...
Suhasahib
Sawsan Sorchee
Dr. Nahla Al-Bakri
Huda Ahmed H...
Galaxy A70
Esraa ahmed
Amel Ghanim
Farkad Hawas...
kareem
Shatha Moham...
Jacqueline Tickle
Tamadher Arif
Baraa jafaar
Dr. Rawaa Salim...
Drshaimaa's Gal...
Abbas (Galaxy...
Dr.Maha Abduln...
Dr. Zahraa Huss...
Aisha Sulaiman...
Taqwa
Dr.shaimaa abe...
Dr.waheeda ras...
Dr .Huda Ali H...
Dr. Hanan Jame...
Wasan Abdulam...
Saba Naser
Baghdad1
dr.Zahraa Asim...
Hadeel Hadi Ja...
Galaxy A70
Noor Idan Jarad
atiaf ghanim

With our pleasure to attend our next conferences in Future

Dr. Ahmed J. Obaid, Conference Publication Chair

Peer review declaration

Peer review declaration

All papers published in this volume of Journal of Physics: Conference Series have been peer reviewed through processes administered by the Editors. Reviews were conducted by expert referees to the professional and scientific standards expected of a proceedings journal published by IOP Publishing.

- **Type of peer review: Single-blind / Double-blind / Triple-blind / Open / Other (please describe)**
  ICMAICT Conference follow Double-Blind Review where all received articles are checked for similarity through the official account of Turnitin All the Articles passed the similarity given to random authors for evaluation and given us their reports in certain forms, according to double review decision and Editors decision the paper either accepted, revised or rejected.

- **Conference submission management system:**
  At the beginning of Conference CFP has been received through Easy chair, then we are considering our own design system where the paper can be submitted, and tracked through this system, all papers has its own ID, for evaluation progress later.

- **Number of submissions received:**
  At the Beginning we received more than 525 submissions from all authors that comes from more than 8 countries, we consider only 290 papers for further progress, the conference organizers, scientific committee, guest Editors consider only the suitable submission (289) for further process.

- **Number of submissions sent for review:**
  Total Number sent for reviews was 420 and based on scientific committee decision and guest editor decision and alternative reviewers.

- **Number of submissions accepted:**
  Out of 525, papers we select 420 papers as initial Accepted Articles, we processed only 290 Articles due to the following reasons:
    - Some Corresponding authors do not complete the revision in well.
    - Some Papers do not complete the Copyright and Payments.
    - Some papers either published somewhere.
    - Some papers rejected based on editor's decision.

- **Acceptance Rate (Number of Submissions Accepted / Number of Submissions Received X 100):**

  Total Number of Received Papers = 525.

  Total Number of Accepted Papers = 290

Acceptance Rate = $\frac{Number\ of\ Submission\ Accepted}{Number\ of\ Submission\ Received} \times \% = \frac{290}{525}$ **= 55%**

- **Average number of reviews per paper:** 2 Reviewers for Each Paper
- **Total number of reviewers involved:** 188 Reviewers
- **Any additional info on review process:**
  - Each paper Assigned to 2 reviewers once passed the technical check.
  - Once Review Reports received the decision of Guest Editor will be as 3rd reviewer on each certain paper.
- **Contact person for queries:**

Main Guest Editors:

- **A. Prof. Dr. Ahmed J. Obaid, Bsc., M.Tech, PhD**
  Faculty of Computer Science and Mathematics, University of Kufa, Iraq
  ahmedj.aljanaby@uokufa.edu.iq
  Mobile (personal): (+964) 7802686683

- **Firas Ahmed Abdullatif,**
  Dean of College of Education for Pure Science (Ibn al-Haitham), Baghdad,
  dean@ihcoedu.uobaghdad.edu.iq

  Prof. Dr. Hassan Ahmad Hasan
  Head of Scientific Committee, Professor at Ibn alHaitham College, Baghdad,
  sci.assist.dean@ihcoedu.uobaghdad.edu.iq

- **Prof Dr. Salah Albermany,**
  Faculty of Computer Science and Mathematics, University of Kufa, Iraq
  salah.albermany@uokufa.edu.iq

- **Dr. Shubham Sharma,**
  Advanced Materials Science and Energy,
  CSIR-Central Leather Research Institute, RCED.
  shubhamsharmacsirclri@gmail.com

Published: 2021-06-01

BIOLOGY

CHEMISTRY

MATHEMATICS

A New Approach of Morgan-Voyce Polynomial to Solve Three Point Boundary Value Problems (https://jih.uobaghdad.edu.iq/index.php/j/article/view/2654)

Bushra Esaa Kashem 76-81

PDF (HTTPS://JIH.UOBAGHDAD.EDU.IQ/INDEX.PHP/J/ARTICLE/VIEW/2654/1682)

COMPUTER

Improved Certificate-Based Encryption Scheme in the Big Data: Combining AES and (ECDSA – ECDH) (https://jih.uobaghdad.edu.iq/index.php/j/article/view/2655)

Omar Salah F. Shareef, Ali Makki Sagheer 82-95

PDF (HTTPS://JIH.UOBAGHDAD.EDU.IQ/INDEX.PHP/J/ARTICLE/VIEW/2655/1683)

MAKE A SUBMISSION (HTTPS://JIH.UOBAGHDAD.EDU.IQ/INDEX.PHP/J/ABOUT/SUBMISSIONS)

INFORMATION

For Readers (https://jih.uobaghdad.edu.iq/index.php/j/information/readers)

For Authors (https://jih.uobaghdad.edu.iq/index.php/j/information/authors)

For Librarians (https://jih.uobaghdad.edu.iq/index.php/j/information/librarians)

REGISTER AS A REVIEWER (HTTPS://JIH.UOBAGHDAD.EDU.IQ/INDEX.PHP/J/REGFORM)

OPEN ACCESS

This is an open access Journal all content of the journal is available for reader free of charge immediately upon publication

LICENSED WORK

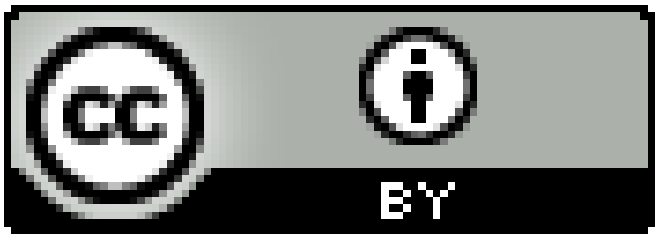

JOURNAL INFO

Journal: Ibn Al Haitham Journal for Pure and Applied sciences

Publisher: College of Education for Pure Science Ibn Al Haitham, University of Baghdad

IHJPAS is peer-reviewed and open access
PISSN: 1609-4042
EISSN: 2521-3407
Publishing Frequency: quarterly

Launch Date: 1989

Abbreviation: Ibn Al Haitham J. for Pure and Appl. Sci. OR IHJPAS

JOURNAL INDEXING

http://dx.doi.org/ (https://dx.doi.org/)

DOAJ

https://doaj.org/toc/2521-3407 (https://doaj.org/toc/2521-3407?source=%7B%22query%22%3A%7B%22filtered%22%3A%7B%22filter%22%3A%7B%22bool%22%3A%7B%22must%22%3A%5B%7B%22terms%22%3A%7B%22index.issn.exact%22%3A%5404042%22%2C%222521-3407%22%5D%7D%7D%7D%2C%7B%22term%22%3A%7B%22_type%22%3A%22article%22%7D%7D%5D%7D%7D%2C%22query%22%3A%7B%22match_all%22%3A%7B%7D%7D%7D%7D%

ORCID ID

ORCID ID ( )

RESEARCHERID

Researcher ID ( )

GOOGLE SCHOLAR

(https://scholar.google.com/citations?user=lyo0hnEAAAAJ&hl=ar&authuser=1)

FLAG COUNTER

Open Journal Systems (http://pkp.sfu.ca/ojs/)

Ibn Al-Haitham Journal for Pure and Applied Science (IHJPAS) is an academic journal established in 1989 and sponsored by the College of Education for pure Science-Al-Haitham, University of Baghdad, Ministry of Higher Education and Scientific Research-Iraq.

CONTACT

Email : jih@ihcoedu.uobaghdad.edu.iq (mailto:jih@ihcoedu.uobaghdad.edu.iq)

Phone : +964 07715613235 (+964 07715613235)

Website : http://jih.uobaghdad.edu.iq (https://jih.uobaghdad.edu.iq)

location : Baghdad / Adhamiya (https://www.google.iq/maps/place/%D9%83%D9%84%D9%8A%D8%A9+%D8%A7%D9%84%D8%AA%D8%B1%D8%A8%D9%8A%D8%A9+%D9%84%D9%84%D8%B9%D9%84%D9%
hl=ar&authuser=0)

IMPORTANT LINKS

About the Journal (/index.php/j/about)

Editorial Journal (/index.php/j/about/editorialTeam)

Submissions (/index.php/j/about/submissions)

Contact Us (/index.php/j/about/contact)

LOCATION

Ibn Al-Haitham Journal for Pure and Applied science https://doi.org/10.30526/2021.IHICPAS.2643

Relationships of Osmolality and Oxidative Stress with Semen Quality and Their Effects on Male Fertility

Edrees Mohammad Ameen
edrees.ameen@su.edu.krd
Department of Biology, College of Science, Salahaddin University, Erbil, Kurdistan Region, Iraq.

Abstract

The objective of this study was to investigate and find the relationships between human semen osmolality and oxidative stress with semen quality. Semen analysis was determined to evaluate semen quality and fertility. The concentration of semen malondialdehyde (MDA) was measured to assess oxidative stress. For this purpose, one hundred seventy healthy adult males were used in this study. The study was conducted from September 2018 to November 2019 in the Infertility care and in vitro fertilization center (IVF) and the Biology department of the College of Science at Salahaddin University in Erbil city. A significant positive correlation was observed between the total sperm motility, grade activity, and sperm motility index with semen osmolality less than 300 mOsm kg^{-1} ($r= 0.62$, $r = 0.64$, and $r= 0.75$ $p\leq0.01$ respectively) and osmolality 300-350 ($r= 0.53$, $p\leq0.05$ $r= 0.52$ $p\leq0.05$, and $r= 0.56$ $p\leq0.01$ respectively). Total sperm motility, grade activity, and sperm motility index are negatively correlated with osmolality 351-400 mOsm kg^{-1} ($r= -0.65$ $p\leq0.05$, $r= -0.56$ $p\leq0.05$, and $r= -0.67$ $p\leq0.01$) and more than 400 mOsm kg^{-1} ($r= -0.86$, $r = -0.74$ and $r= -0.88$ $p\leq0.01$). Regarding the relation between oxidative stress and sperm motility kinetics, total sperm motility, grade activity, and sperm motility index is negatively correlated with MDA more than 2 µmol/L ($r= -0.56$ $p\leq0.05$, $r= -0.52$ $p\leq0.05$, and $r= -0.67$ $p\leq0.01$ respectively). No significant correlation was found between semen osmolality and MDA concentration with sperm concentration, total sperm count, sperm viability, and normal sperm morphology.

Keywords: Osmolality, Semen Quality, Fertility, Oxidative stress, Semen analysis.

1. Introduction

Infertility has become a global health problem in recent years and is affecting 25-30% of reproductive-age couples worldwide to varying degrees [1]. An estimated 70 million people worldwide, suffer from subfertility or infertility [2, 3]. About 15% of couples are infertile and over 10% are subfertile. Comparison with females, males responsible for infertility and subfertility in about 40% to 50% of cases [4, 5]. A meta-analysis of recent studies carried out between 1973 and 2011, that was reported a decrease in sperm counts by more than 50%. The same goes for several other studies that have also recorded a continuous decline in semen quality [6, 7]. Low quality of semen is well known as a large disorder causing male fertility [8, 9]. The study of semen quality is the most important and most commonly used clinical laboratory test to evaluate the capacity of male fertility. In 2010, the World Health Organization (WHO) guidelines lowered the sperm concentration reference interval from 20

million to 15 million/ml [10]. Osmolality is known as a solution's concentration of osmotically active particles. It is related only to the number of particles per kilogram of solution [11]. Mammalian spermatozoa are mixed with the seminal vesicles, prostate, and bulbourethral gland secretions during ejaculation. Seminal plasma osmolarity has previously been shown to affect sperm motility and activity in invertebrates and vertebrates [12]. The motility of spermatozoa is primarily influenced by changes in the surrounding ionic contents, osmolality, and pH [13, 14]. In sturgeon fish, a negative correlation was found between the osmolality of semen and the percentage of sperm motility [15]. The development of oxidative stress (OS), due to the imbalance between the development of reactive oxygen species (ROS) and antioxidant protection mechanisms [16]. In the male reproductive system, the primary causes of ROS are defective sperm and leukocytes [16, 17]. In the sperm plasma membrane, the high concentration of polyunsaturated fatty acids is vulnerable to ROS, and its attack contributes to lipid peroxidation. Lipid peroxidation takes place in three stages: initiation, progression, and termination. The free radicals combine with fatty acid chains during activation to create the radical lipid peroxyl. Besides, peroxyl radicals bind with fatty acids to create free radicals, and thereby spread the reaction. In closing, the two radicals connect, allowing lipids to break down [18]. Concentrations of seminal MDA are negatively correlated with sperm count and motility [19]. Malondialdehyde is negatively associated with the main sperm parameters [20]. Impaired sperm quality is accompanied by high oxidative stress [21]. Due to poor data worldwide and no data in Erbil city of Iraq about the relationships between semen osmolality and oxidative stress with semen quality and fertility. The present study was done and aimed to evaluate the influence of seminal plasma osmolality and oxidative stress on semen quality and fertility of adult males.

2. Materials Method

2.1. Subjects

The study included 170 healthy males and divided into four groups according to the semen osmolality:

- Semen osmolality is less than 300 mOsm kg^{-1} (50 males).
- Semen osmolality 300-350 mOsm kg^{-1} (45 males).
- Semen osmolality 351-400 mOsm kg^{-1} (40 males).
- Semen osmolality more than 400 mOsm kg^{-1} (35 males).

Also, the subjects were divided into other groups depending on the seminal fluid concentration of the Malondialdehye (indicators to oxidative stress) and as follows:

- Seminal fluid with low normal MDA concentration (Less than 2 µmol/L) (110 males).
- Seminal fluid with high abnormal MDA concentration (More than 2 µmol/L) (60 males).

The study was conducted from September 2018 to November 2019 in the Infertility care and in vitro fertilization center (IVF) and the Biology department of the College of Science at Salahaddin University in Erbil city. The ages of the subjects ranged between 30-40 years.

2.2. Semen collection

Semen samples were collected in plastic containers after 3 days of abstinence via masturbation and after 30 minutes of the liquefaction of semen samples, the following routine

parameters were evaluated according to the methods described in the WHO [22, 23]. The parameters were including; the volume of the semen, osmolality of the semen, sperm (count, motility, and morphology).

2.3. Seminal fluid analysis

A graduated tube was used to measure the volume of the semen. To determine sperm concentration, 10 µL of semen sample was placed in a Makler chamber and covered by a covered glass, and then analyzed at approximately 200 magnifications [23]. Total sperm count= Sperm concentration ×volume. A drop of semen, covered with a cover glass and analyzed under a microscope 400x equipped with heat plate 37ºC was used to determination of sperm motility. Motility % = number of motile spermatozoa/total number of spermatozoa (motile and immotile) ×100. Progressive motility was measured by counting the spermatozoa with straight-line forward movement only in the presence of motile spermatozoa [22]. In each sample, sperm motility is graded to 0, 1, 2, 3, or 4, depending on the degree and activity of the movement. Grade 0 represents xero or no movement and grade 4 represents the excellent forward movement of the spermatozoa [24]. The sperm motility index was calculated by multiplying the grading activity with the percentage of motility [25]. For measurement of sperm viability, two drops of 1 % eosin Y solution were mixed with a drop of liquefied semen, then three drops of nigrosin solution 10 % was added, and mixed after 30 seconds. Within 30 seconds of adding nigrosin, a thin smear of the semen–eosin–nigrosin mixture was made and after air-dried, examined under the microscope (1000×). To determine the percentage of live spermatozoa, one hundred sperm were counted. The live spermatozoa are white and the dead are stained red [22]. Sperm vitality = number of viable sperm/total number of spermatozoa × 100. The normal morphology of spermatozoa was determined by using the hematoxylin and eosin staining procedure [26].

2.4. Seminal fluid Osmolality

Osmometer type (Knauer, D- 14163, Berlin, Germany) and the freezing point depression method was used to measure the seminal plasma osmolality. This method requires samples of semen to be centrifuged free of particulate matter. Before the osmolality of the sample was measured, the osmometer must be calibrated between 0 and 400 mOsm kg^{-1} using distilled water and standard NaCl solution.

2.5. Seminal fluid MDA determination

A procedure described by [27] was used to measure the concentration of the semen MDA. In short; apply the following to 150 µl of semen plasma: 1 ml of trichloroacetic acid 17.5 %, 1 ml of 0.6 % thiobarbituric acid, combined well with vortex, incubated for 15 minutes in a boiling water bath, and then allowed to cool. Then add 1 ml of 70% trichloroacetic acid (TCA), then let the mixture stand at room temperature for 20 minutes, centrifuged for 15 minutes at 2000 rpm, and remove the supernatant for spectrophotometric scanning [28].

The conc. of MDA = absorbance at 532 nm × D / L × $E_{\circ}$

L: light bath (1 cm)

$E_{\circ}$: extinction coefficient $1.56\times105\ M^{-1}.Cm^{-1}$

D: dilution factor = 1 ml volume. used in Ref./0.15=6.7

2.6. Statistical analysis

The data analysis was performed using SPSS version 17. Pearson's correlation (r) was used to founding the relationships between seminal plasma osmolality and oxidative stress (MDA) with semen analysis parameters (volume of semen, sperm concentration, sperm motility, sperm viability, and morphology). A P-value of less than 0.05 was considered to be statistically significant.

3. Results and Discussion

3.1. Osmolality and semen quality

Pearson's correlation (r) between semen osmolality and semen quality parameters are presented in **Table (1).** The volume of semen positively ($r = 0.55$, $p \leq 0.05$) correlated with semen osmolality less than 300 mOsm kg^{-1}. While in the osmolality 300-350, 351- 400, and more than 400 mOsm kg^{-1} it is negatively correlated ($r= -0.46$, $r= -0.48$, and $r= -0.54$ $p \leq 0.05$ respectively). No correlation was found between semen osmolality with sperm concentration, total sperm count, sperm viability, and normal sperm morphology. The correlation between sperm motility kinetics and semen osmolality is mentioned in **Table (2)**. A significant positive correlation was observed between the total sperm motility, grade activity, and sperm motility index with semen osmolality less than 300 mOsm kg^{-1} ($r= 0.62$, $r= 0.64$, and $r= 0.75$ $p \leq 0.01$ respectively) and osmolality 300-350 ($r= 0.53$, $p \leq 0.05$ $r= 0.52$ $p \leq 0.05$, and $r= 0.56$ $p \leq 0.01$ respectively). The increase in the semen osmolality is caused by a decrease in the sperm motility kinetics parameters. Total sperm motility, grade activity, and sperm motility index are negatively correlated with osmolality 351-400 mOsm kg^{-1} ($r = -0.65$ $p \leq 0.05$, $r = -0.56$ $p \leq 0.05$, and $r = -0.67$ $p \leq 0.01$) and more than 400 mOsm kg^{-1} ($r = -0.86$, $r = -0.74$ and $r = -0.88$ $p \leq 0.01$). The seminal plasma is a complex fluid secreted from the testes, epididymis, and accessory sex glands, that acts as a carrier for spermatozoa from the male testicles to the oocyte, their target, and may influence the morphology of sperm, motility, acrosome reaction, and fertility. Several biochemical components are found in seminal plasma, some of which are relatively unique for sperm function control [29, 30]. It is also recognized that there are substances in the seminal plasma that sustain sperm cells. The osmotic balance is formed by sodium and potassium cations in the seminal plasma, while the basic trace elements are the components of several significant enzymes, calcium is also required to stimulate steroidogenesis in the Leydig cells of the testis [31].

Table 1. Pearson's correlation (r) between semen osmolality and semen quality parameters.

Semen quality	Semen osmolality (mOsm kg^{-1})			
	Less than 300	300-350	351-400	More than 400
Volume (ml)	0.55*	- 0.46*	- 0.48*	- 0.54*
Sperm concentration ($\times 10^6$/ml)	0.12	0.18	0.22	0.15
Total sperm count ($\times 10^6$/volume of semen)	0.24	0.18	0.21	0.35
Sperm Viability %	0.35	0.14	0.25	0.32
Normal Sperm morphology %	0.14	0.34	0.36	0.18

*Correlation is significant at $p \leq 0.05$, - the negative correlation was found

Ibn Al-Haitham Journal for Pure and Applied science https://doi.org/10.30526/2021.IHICPAS.2643

Table 2. Pearson's correlation (r) between semen osmolality and sperm motility kinetics parameters.

Sperm motility kinetics	Semen osmolality (mOsm kg^{-1})			
	Less than 300	300-350	351-400	More than 400
Total sperm motility %	0.62**	0.53*	- 0.65*	- 0.86 ***
Grade activity	0.64**	0.52*	- 0.56*	- 0.74**
Sperm motility index	0.75**	0.56**	- 0.67**	- 0.88***

*Correlation is significant at p≤0.05, **Correlation is significant at p≤0.01, ***Correlation is significant at p≤0.001, - the negative correlation was found.

The seminal plasma is a complex fluid secreted from the testes, epididymis, and accessory sex glands, that acts as a carrier for spermatozoa from the male testicles to the oocyte, their target and may influence the morphology of sperm, motility, acrosome reaction, and fertility. Several biochemical components are found in seminal plasma, some of which are relatively unique for sperm function control [29, 30]. It is also recognized that there are substances in the seminal plasma that sustain sperm cells. The osmotic balance is formed by sodium and potassium cations in the seminal plasma, while the basic trace elements are the components of several significant enzymes, calcium is also required to stimulate steroidogenesis in the Leydig cells of the testis [31]. The results of our study are in agreement with the findings of [15] who observed a significant negative correlation (r= -0.893) between semen osmolality and motility percent in sturgeon fish. Also, the study of [12] found that semen osmolality correlates negatively with the kinetic characteristics of sperm motility such as motility percent and grade activity in humans. Besides, when sperm were placed in a solution with an increase in osmolality from 300 to 600 mOsm kg^{-1}, kinetic characteristics of sperm motility were gradually decreased and almost arrest when the osmolarity was 600 mOsm kg^{-1}. These results are in the line with the findings of our study. With the increased osmolality of the activating solution, the percentage of motile spermatozoa drops, osmolality greater than 400 mOsm kg^{-1} should be present in the immobilizing solution in pikeperch [32]. The effect of various osmolalities (240-460 mOsm kg^{-1}) on the sperm quality parameters of Jenynsia multidentata viviparous fish was evaluated by [33]. The results found that semen motility in osmolalities between 280 and 300 mOsm kg^{-1} was higher and the motility observed above 380 mOsm kg^{-1} was 0%.

3.2. Oxidative stress and semen quality

The correlation between oxidative stress and semen quality parameters is presented in **Table (3).** No significant correlation was found between semen MDA concentration with semen volume, sperm concentration, total sperm count, sperm viability, and normal sperm morphology. Regarding the relation between oxidative stress and sperm motility kinetics, total sperm motility, grade activity, and sperm motility index were not significantly correlated with semen MDA concentration less than 2 µmol/L, but is negatively correlated with MDA more than 2 µmol/L (total sperm motility r = - 0.56 p≤0.05, grade activity r = - 0.52 p≤0.05, and sperm motility indexer =- 0.67 p≤0.01), **Table (4)**. As showed in **Table (5)**, no correlation was found between seminal plasma osmolality and oxidative stress. The cellular damage of oxidative stress initiate when the reactive oxygen species (ROS) exceeds the body's natural antioxidant defenses. A common disease seen in nearly half of all infertile men is oxidative stress. ROS, described as comprising oxygen ions, free radicals, and peroxides, is produced

within semen by sperm and seminal leukocytes and produces infertility through two main mechanisms. They damage the sperm membrane first, decreasing the motility of the sperm and its ability to fuse with the oocyte. Secondly, sperm DNA can be changed by ROS, which contributes to the passage of faulty DNA from parents to the fetus [34].

Table 3. Pearson's correlation (r) between oxidative stress and semen quality parameters.

Semen quality	Oxidative stress (Seminal plasma MDA concentration)	
	Less than 2 µmol/L	More than 2 µmol/L
Volume (ml)	0.12	0.18
Sperm concentration ($\times 10^6$/ml)	0.25	0.21
Total sperm count ($\times 10^6$/volume of semen)	0.32	0.34
Sperm Viability %	0.15	0.36
Normal Sperm morphology %	0.14	0.22

No correlation was found between oxidative stress and semen quality

Table 4. Pearson's correlation (r) between oxidative stress and sperm motility kinetics parameters.

Sperm motility kinetics	Oxidative stress (Seminal plasma MDA concentration)	
	Less than 2 µmol/L	More than 2 µmol/L
Total sperm motility %	0.35	- 0.56*
Grade activity	0.32	- 0.52*
Sperm motility index	0.43	- 0.67**

*Correlation is significant at p≤0.05, **Correlation is significant at p≤0.01, − the negative correlation was found.

Table 5. Pearson's correlation (r) between oxidative stress and semen osmolality.

Semen osmolality (mOsm kg^{-1})	Oxidative stress (Seminal plasma MDA concentration)	
	Less than 2 µmol/L	More than 2 µmol/L
Less than 300	0.42	0.25
300-350	0.35	0.34
351-400	0.18	0.22
More than 400	0.38	040

No correlation was found between oxidative stress and semen quality.

Malondialdehyde is one of the lipid peroxidation byproducts. This by-product is a significant marker of oxidative stress, and the degree of lipid peroxidation has been extensively studied for monitoring. Sperm membrane lipid peroxidation can cause changes in sperm and can reduce fertility by affecting sperm motility and sperm-oocyte fusion ability. However, it remains to be determined whether the concentration of MDA seminal fluid influences the consistency or role of sperm [35]. Our results are in agreement in some aspects with the results of [19], who found a negative association between the MDA level of seminal fluid and sperm motility but in contrast with them which record a decrease in sperm count, and sperm morphology. The discovery of a high level of MDA in infertile subjects 'semen suggests that infertile subjects' spermatozoa have been subjected to elevated oxidative stress.

In infertile subjects, the sperm count, sperm morphology, and motility as well as the volume of semen were all found to be significantly lower compared to fertile subjects. It thus means that increased oxidative stress has a detrimental effect on semen quality [36]. Due to ROS-induced peroxidation of lipids in the sperm membrane reduced flexibility has been shown to reduce motility [37]. Mitochondria that produce energy from intracellular ATP stores cover the axosome and related dense fibers of the middle sections of the spermatozoa. ROS is well known to cause axonemal and mitochondrial damage, resulting in the immobilization of spermatozoa [38]. Besides, ROS-induced mitochondrial DNA damage contributes to decreased ATP and energy availability and leads to caspase stimulation and eventually apoptosis, impeding the motility of spermatozoa [39]. Another theory includes a sequence of interrelated events leading to a reduction in ROS motility due to a reduction in phosphorylation of axonemal protein and mitochondrial membrane damage and intracellular enzyme leakage [40].

4. Conclusion

Our results concluded that the total sperm motility, grade activity, and sperm motility index are negatively correlated with osmolality 351-400 and more than 400 $mOsmkg^{-1}$. Seminal plasma MDA concentration of more than 2 µmol/L harms sperm motility kinetics. No significant correlation was found between semen osmolality and MDA concentration with sperm concentration, total sperm count, sperm viability, and normal sperm morphology.

5. Acknowledgement

The authors would like to show sincere gratitude for all patients who participated in the study. The authors are also grateful for the IVF in Erbil city for their help and collection of the samples.

6. Conflict of Interest

The authors declare no conflict of interest.

References

1. Inhorn, M.C.; Patrizio, P. Infertility around the globe: new thinking on gender, reproductive technologies and global movements in the 21st century. *Hum. Reprod. Update*, **2015** ,*21*, 411.
2. Légaré, C.; Droit, A.; Fournier, F.; Bourassa, S.; Force, A.; Cloutier, F.; Tremblay, R.; Sullivan, R. Investigation of male infertility using quantitative comparative proteomics. *J. Proteome Res*. **2014** ,*13*, 5403.
3. Salas-Huetos, A; Bulló,M.; Salas-Salvadó, J. Dietary patterns, foods and nutrients in male fertility parameters and fecundability: a systematic review of observational studies. *Hum. Reprod. Update* **2017**, *23*, 371.
4. Chandra, A.; Martinez, G.M.; Mosher, W.D.; Abma, J.C.; Jones, J. Fertility, family planning, and reproductive health of US women; data from the 2002 National Survey of Family. *Growth Vital Health Statist*. **2002** ,*23*, 1.
5. Hwang, K.; Walters, R.C.; Lipshultz, L.I. Contemporary concepts in the evaluation and management of male infertility. *Nat. Rev. Urol*. **2011** ,*8*, 86.
6. Li, C.J.; Tzeng, C.R.; Chen, R.Y.; Han, B.C.; Yeh, C.Y.; Chien, L.C. Decline in semen quality in men in northern Taiwan between 2001 and 2010. *Chin. J. Physiol*. **2016** ,*59*, 355.

7. Engupta, P.; Nwagha, U.; Dutta, S.; Krajewska-Kulak, E.; Izuka, E. 2017 Evidence for decreasing sperm count in African population from 1965 to 2015. *Afr. Health Sci*. **2017** ,*17*, 418.
8. Radwan, M.; Jurewicz, J.; Polańska, K.; Sobala, W.; Radwan, P.; Hanke, W. Exposure to ambient air pollution-does it affect semen quality and the level of reproductive hormones? *Ann. Hum. Biol*. **2016** ,*43*, 50.
9. Levine, H.; Jørgensen, N.; Martino-Andrade, A.; Mendiola, J.; Weksler-Derri. D.; Mindlis, I.; Pinotti, R.; Swan, S.H. Temporal trends in sperm count: a systematic review and meta-regression analysis. *Hum. Reprod. Update* **2017** ,*23*, 646.
10. Liu, J.; Dai, Y.; Li. Y.; Yuan. E.; Wang, Q.; Wang. X.; Guan. Y.A. A longitudinal study of semen quality among Chinese sperm donor candidates during the past 11 years. *Sci. Rep.* **2020** ,*10*, 1.
11. Holmes, E. On osmolality and sperm function during processing for assisted reproduction PhD Thesis. Karolinska Institutet, Stockholm **,2020**.
12. Rossato, M.; Balercia, G.; Lucarelli, G.; Foresta, C.; Mantero, F. Role of seminal osmolality in the regulation of human sperm motility. *Int. J. Androl*. **2020**, *25*, 230.
13. Alavi, S.M.H.; Rodina, M.; Gela, D.; Linhart, O. Sperm biology and control of reproduction in sturgeon:(I) testicular development, sperm maturation and seminal plasma characteristics. *Rev. Fish Biol. Fisher*. **2012 ,***22*, 695.
14. Dzyuba, B.; Cosson, J.; Boryshpolets, S.; Dzyuba, V.; Rodina, M.; Bondarenko,O.; Shaliutina, A.; Linhart, O. Motility of sturgeon spermatozoa can sustain successive activations episodes. *Anim. Reprod. Sci*. **2013** ,*138*, 305.
15. Baradaran, N.S.; Noori, A.; Bahmani, M.; Sadati, Y.; Akbarzadeh,A. Effects of seminal plasma ionic content, pH and osmolality on spermatozoa motility in bester (Female Huso huso× Male Acipenser ruthenus) sturgeon. *Iran. J. Fisher. Sci*. **2019** ,*18*, 395.
16. Agarwal, A.; Virk, G.; Ong,C.; du Plessis. S.S. Effect of oxidative stress on male reproduction. *World J. Mens. Health* **2014** ,*32*, 1.
17. Leclerc,P.; De Lamirande, E.; Gagnon, C. Regulation of protein-tyrosine phosphorylation and human sperm capacitation by reactive oxygen derivatives. *Free Radic. Biol. Med*. **1997** ,*22*, 643.
18. Ding,G.L.; Liu, Y.; Liu, M.E.; Pan, J.X.; Guo, M.X.; Sheng, J.Z.; Huang, H.F. The effects of diabetes on male fertility and epigenetic regulation during spermatogenesis. *Asian J. Androl.* **2015** ,*17*, 948.
19. Hsieh, Y.Y.; Chang, C.C.; Lin, C.S. Seminal malondialdehyde concentration but not glutathione peroxidase activity is negatively correlated with seminal concentration and motility. *Int. J. Biol. Sci*. **2006** *2*, 23.
20. La Vignera, S.; Condorelli, R.; D'agata, R.; Vicari, E.; Calogero, A.E.; La Vignera, S.; Condorelli, R.A.; Vicari, E.; D'aagata, R.; Salemi, M.; Calogero, A.E. High levels of lipid peroxidation in semen of diabetic patients. *Andrologia* **2012**, *44*, 565.
21. Omu, A.E.; Al-Bader, M.D.; Al-Jassar, W.F.; Al-Azemi, M.K.; Omu, F.E.; Al-Jassar. W.F.; Al-Azemi, M.K.; Omu, F.E.; Mathew, T.C.; Anim, J.T. Antioxidants attenuates the effects of insulin dependent diabetes mellitus on sperm quality. *Bioenergetics* **2014** ,*3*, 1.
22. WHO World Health Organisation. Laboratory manual for the examination of human semen and sperm-cervical mucus interaction Cambridge university press, **2009**.
23. WHO World Health Organization. Laboratory manual for the examination and processing of human semen Fifth edition. Geneva 27 Switzerland ,**2010**.
24. Seaman, E.; Bar-Chama, N.; Fisch, H. Semen analysis in the clinical evaluation of infertility. *Mediguide Urol*. **1994** ,*194*, 7, 1.

25. Makler, A.; Itskovitz, J.; Brandes, J.M.; Paldi, E. Sperm velocity and percentage of motility in 100 normospermic specimens analyzed by the multiple exposure photography (MEP) method. *Fertil. Steril*. **1979** ,*31*, 155.
26. Jequier, A.M.; Crich, J.P. Semen analysis: a practical guide Blackwell Scientific Publications; St. Louis, MO, USA. Distributors, USA, Blackwell Mosby Book Distributors, **1986**.
27. Guidet, B.; Shah, S.V. Enhanced *in vivo* H_2O_2 generation by rat kidney in glycerol-induced renal failure. *Am. J. Physiol. Renal Physiol*. **1989** ,*257*, F440.
28. Muslih, R.; Al-Nimer, O.; Al-Zamely, M. The level of Malondialdehyde after activation with H_2O_2 and $CuSO_4$) and inhibited by Desferoxamine and Molsidomine in the serum of patients with acute myocardial infection. *J. Chem*. **2002** ,*5*, 148.
29. Mann, T.; Lutwak-Mann, C. Epididymis and epididymal semen. Male reproductive function and semen Springer-Verlag New York. **1981**, l39.
30. Asadpour, R. Relationship between mineral composition of seminal plasma and semen quality in various ram breeds. *Acta Sci. Veter*. **2012** ,*40*, 1.
31. Zamiri,M. ;Khodaei, H.R. Seasonal thyroidal activity and reproductive characteristics of Iranian fat-tailed rams. *Anim. Reprod. Sci*. **2005** ,*88*, 245.
32. Dziewulska. K. Effect of pH, osmolality and ion concentration on spermatozoa motility and composition parameters of sperm and seminal plasma in pikeperch (*Sander lucioperca* L.). *Aquaculture* **2020** ,*520*, 735004.
33. Da Silva, J.C.; Junior, A.S.V.; Caldas, J.S.; Da Silva, F.C.; Bothlho,J.G.; Colares, E.P.; Corcini. C.D. The effects of osmolality on sperm quality in *Jenynsia multidentata* (Cyprinodontiformes: Anablepidae). *Fish Physiol. Biochem*. **2016** ,*42*, 93.
34. Tremellen, K. Oxidative stress and male infertility-a clinical perspective. *Hum. Reprod. Update* **2008** ,*14*, 243.
35. Chaudhari, A.; Das, P.; Singh, R. Study of oxidative stress and reduced glutathione levels in seminal plasma of human subjects with different fertility potential. *Biomed. Res*. **2008** ,*19*, 207.
36. Un-Nahar,Z.; Ali, M.; Biswas, S.; Kamrun, N.; Bashar, T.; Arslan, M. Study of seminal MDA level as a oxidative stress marker in infertile male. *J. Sci. Found*. **2011**, *9*, 85.
37. Armstrong, J.S.; Rajasekaran, M.; Chamulitrat, W.; Gatti, P.; Hellstrom, W.J.; Sikka, S.C. Characterization of reactive oxygen species induced effects on human spermatozoa movement and energy metabolism. *Free Radical Biol. Med*. **1999** ,*26*, 869.
38. Peris, S.I.; Bilodeau, J.F.; Dufour, M.; Bailey, J.L. Impact of cryopreservation and reactive oxygen species on DNA integrity, lipid peroxidation, and functional parameters in ram sperm. *Molec. Reprod. Develop*. **2007** ,*74*, 878.
39. Gual-Frau, J.; Abad, C.; Amengual, M.J.; Hannaoui, N.; Checa, M.A.; Ribas-Maynou, J.; Lozano, I.; Nikolaou, A.; Benet, J.; García-Peiró, A.; Prats, J. Oral antioxidant treatment partly improves integrity of human sperm DNA in infertile grade I varicocele patients. *Hum. Fertil*. **2015**,*18*, 225.
40. De Lamirande, E.; Gagnon, C. Reactive oxygen species and human spermatozoa: I. Effects on the motility of intact spermatozoa and on sperm axonemes. *J. Androl*. **1992** ,*13*, 368.

Ibn Al-Haitham Journal for Pure and Applied science https://doi.org/10.30526/2021.IHICPAS.2644

Notes on the ecology and distribution of the annual fern *Anogramma leptophylla* (L.) Link. (Pteridaceae) in Northern districts of Iraq

A.M. Ismail
abbasmurtadeh@yahoo.com
College of Science for Women-
University of Baghdad- Iraq

B. K. Maulood
bahram.Khider@auis.org
Precedency of Kurdistan regional
government- Erbil- Iraq

Abstract

The study involved the description of the environmental characters and distribution of Anogramma *leptophylla* (Annual Maidenhair fern) in Erbil and Garmian districts during May- 2017 in Kurdistan of Iraq. The geographical distribution of the taxa was recorded in Bani Bee region for the first time within the Garmian district but it was recorded before in the Zar Gali region within the Erbil district. The climatic characters of the studied site in Erbil district were: moist, cold and the elevation was up to 560 m above sea level with sandy clay soil texture whereas in the Garmian district: dry, hot, and the elevation was only 330 m above sea level with sandy stone soil. Plant up to 13 cm long, megaphyllous, fronds compound 3-6 cm long, divided into alternate petiolate pinnae. In the present work, some ecological, morphological, and geographical distribution *for A. leptophylla* is described for the first time in the Iraqi Kurdistan region.

Keywords: Anogramma , Pteridaceae, Iraq, Ferns.

1. Introduction

There are over 10,560 species of ferns and 1000 species of fern- allies, recorded in the world so far [1]. Seedless vascular plants have much more diversity over the world in contrast to other plants [2], whereas most previous studies have been carried out on the other vascular plants [3, 4]. Recently many scientific researches on phytochemical, morphological and anatomical features of ferns appeared [2, 5, 6, 7, 8, 9]. Pteridaceae includes over 1000 species which make up almost 10% of ferns [10], the members of this family have a world wide distribution in tropics and arid regions [11]. Anogramma is a genus of Pteridioideae, a subfamily of the Pteridaceae [12], which involves about ten species found in regions with alternating wet and dry seasons [13]. However, A. leptophylla has one of the widest ranges of distribution among all other fern species [14]. In the flora of Iraq, the authors referred to the geographical distribution and habitat of *A. leptophylla* only without any detail of its morphology or ecological features [8, 9, 15, 16] **Figure (1a-b)**. The present study aimed to investigate the ecology and the geographical distribution of the annual fern *Anogramma leptophylla* L. as it is the first attempt in Iraq that deals with pteriodoflora in this respect.

Ibn Al-Haitham Journal for Pure and Applied science https://doi.org/10.30526/2021.IHICPAS.2644

Figure 2. a- Fern in Bani Bee b- Fern in Zar Gali

2. Materials Method

Plant samples (mature sporophyte) have been collected from Erbil district within the Zar Gali region, geographical data were found to be as follows: GPS (36º 37. 490 N, 44º 26. 540 E), elevation up to 560 m above sea level whereas in Garmian district, the station was in Bani Bee region GPS (35º 02. 221 N, 045º 42. 650 E), elevation was only 330m above sea level. Voucher sample under the No. (4, 17, 2, An, le) of the ferns was deposited in the Herbarium of Howler Botanical Garden- Erbil City. Soil samples were collected from studied sites of both regions in plastic bugs and brought back to the laboratory, then the soil properties were estimated according to the standard procedure [17]. In addition, soil texture was also determined. The annual mean of metrological data for the two districts was; (1) in Erbil temperature 36ºC, humidity 65% and rainfall 120 mm, but in (2) Garmian temperature 40.5 ºC, humidity 55% and rainfall 90 mm. The morphological characters of the fern were studied using dissecting and light compound microscope in the advanced environmental postgraduate laboratory in Garmian University-Faculty of Science, Kalar. The classification was performed according to [11].

3. Results and Discussion

3.1. Ecological Study

Results of the present study showed a wide range of variation between soil samples of the two stations, in respect to pH, alkalinity, soil texture, chemical and physical properties of soil, plant nutrients were also estimated and documented in **Tables (1 and 2)**.

Table 1. Some chemical and physical characters of the soil in both studied sites.

Sites	pH	EC µsem./cm	CO_3 ppm	NO_3 ppm	PO_4 ppm	Ca ppm	Mg ppm	K ppm	Na ppm
Zar Gali	7.9	240	200	2.0	0.3	48	42	40	30
Bani Bee	7.8	400	145	0.8	0.13	41	37	28	60

Ibn Al-Haitham Journal for Pure and Applied science https://doi.org/10.30526/2021.IHICPAS.2644

Table 2. Soil color, texture and total organic content of soil samples from the two sites.

Sites	Color	Texture	Total organic content % (TOC)
Zar Gali	Light brown	Sandy clay	14.6
Bani Bee	Light red	Sandy stone	5.4

The result of the present investigation showed a wide range of variation between soil samples of the two stations in respect of both chemical and physical parameters. The outcome results of pH, electrical conductivity, bicarbonate, nitrate, phosphate, and major cations are represented in table (1) whereas **Table (2)** involved the result of soil texture, color, and total organic content of soil samples. It is found that soil color ranged from light brown in Zar Gali to light red in Garmian whereas total organic content in Zar Gali was more than double of that of Bani Bee (14.6% & 5.4%) respectively although soil pH in both sides was weak alkaline the electrical conductivity was almost half of that of Bani bee. Variation and difference between the two sites were quite evident in respect to elevation as it exceeded 560 m in Zar Gali- Rwanduz whereas it did not exceed 360 m in Garmian. However, the variation extended to the difference in metrological data also between the two sites as its shown in **Table (3)** where the amount of rainfall in Zar Gali exceed 120 mm with the temperature only 36ºC whereas in Garmian mean annual rainfall do not exceed 90mm and temperature normally exceed 40ºC.

Table 3. Meterological data in the studied sites.

Sites	Temperature (°C)	Rainfall (mm)	Humidity (%)
Zar Gali	36	120	65
Bani Bee	40.4	90	55

3.2. Morphological Study

The fern morphologically is found to be herbaceous 8.5-13 cm long, petiole up to 4 cm long, brown near the rhizome and green near the blade, blade up to 3 cm long, frond up to 7 cm long, divided into pinnules with a short petiole, pinnule consist of four deltoid segment, smooth ad axial surface, venation is dichotomous, rhizome erect very short up to 0.5 cm long, roots are brown color up to 1-2 cm long, petiole dark brown, with a few small scales near the base, pinna is divided into trilobite pinnules, sori clustered on ab axial surface of pinna along the veins without indicium **Figure (2)**.

Figure 2. *Anogramma leptophylla* (mature sporophyte in the laboratory).

3.3. Habitat and Distribution

The concerned fern is known to be found in moist shaded rocky cliffs which was the case in the current study. In the present investigation, plant was recorded at different elevations (330-560 m) above sea level the habitat was either individual form among other plants or rarely found aggregate in groups. In the Erbil district, the associated taxa were Cheilanthes fragrance in the Zar Gali region. [15] had found the fern in moist and low-temperature climate in Derbendikhan region also they had recorded the fern even in Khanaqin region which is quite hot and regarded as a temperate climate, had also recorded the fern in Rawandoose and Iranian foothills regions which is characterized with low temperature and high humidity at an elevation of 800 m above sea level was recorded by [16]. The climate in the Iraqi Kurdistan districts characterized by Iran toraniane climate [15]. In New Zealand, the plant is normally reported to begin growth in late Winter and early Spring but the maturity has been found in August and September [18], had reported were the fern growth with aggregate form and associated with some bryophytes and grasses which inhabit sandy stone soil and moist environment this agree with present finding in Erbil (Zar Gali) whereas, the results from this work in Bani Bee region disagree with [18] and [19] study because the Garmian district characterized with high temperature and low humidity [8, 9] and the fern was found as individual plants along the area between stones and rocks.

4. Conclusion

The fern *Anogramma leptophylla* have been recorded in a wide range of climatic environments in Kurdistan of Iraq the plant was found to be either a single individual or an aggregation group among the mosses or ferns. Description, habitat, and some ecological factors have been reported for the first time in Iraq in respect to this fern.

References

1. Christenhusz, M.J.; Byng, J.W. The number of know plants species in the world and its annual increase. *Phytotaxa*. **2016**, *45*, 3, 201-217.
2. Murtaza, G.; Asgher. R.; Majed. S.A.; Waheed. A.; Mirza. S.N. Aanatomical and palynological studies on some Fillicales from Neelum Valley, Muzaffarabad, Azad Kishmir. *Pak. J. Botany*. **2006** ,*38*, 4, 921-929.
3. Mir, S.A.; Mishra. A.K.; .Pala. S.A.; Reshi. Z.A.; Sharma. M.P. Ferns and fern allies of district Shopian Kashmir Valley, India. *Biodiversity*. **2015** *16*, 1, 27-43.
4. Javad, S. Sporulation and spore germination in the tissue culture of Cheilanthes fragrans. *J. Appl. Environ. Biol. Sci*. **2015** ,*5*, 2, 225-229.
5. Bercu, R. Anatomy of *Asplenium trichomanes* L. UDK. **2004** ,*582*, 41-48.
6. Chaning, A.; Zamuner, A.; Edwarda, D.; Guido, D. *Equisetum thermal* Nov. (Equisetales) from the Jurassic San Augstin Hot Spring deposit, Patagonia: anatomy, paleoecology, and inferred palieoecophysiology. American J. of Botany. **2011** ,*98*, 4, 680-698.
7. Al-Snafi, A.E. The chemical constituents and pharmacological effects of A. capillus-veneris: A review. *Pharmacologia*, **2015** ,*5*, 5, 106-111.
8. Ismail, A.M. Biological and Molecular Study on the Ferns in Three Districts North of Iraq. Ph. D Thesis Tikrit University. **2018** pp: 211.
9. Ismail, A.M.; Ouaid, T.; Al-Amery, M.; Maulood, B.K. A preliminary syudy of phytochemicals of Equisetum arvense L. & E. ramosissimum Desf. (Equisetaceae) extracts from Northern of Iraq. *Fern Gazzet*. **2020** ,*21*, 3, 125-130.
10. Schuttpelz, E.; Schneider, H.; Huiet, L.; Windham, M.D.; Pryer, K. M. A molecular phylogeny of the fern family Pteridaceae: assessing overall relationships and the affinities of previously un sampled genera. *Mol. Phylogen. Evol*. **2007** ,*44*, 1172- 1181.
11. Smith, A.R.; Pryer, K.M.; Schuettpelz, E.; Korall, P.; Schneider, H.; Wolf, P.G. A classification for extant ferns. *Taxon*. **2006** ,*55*, 705-731.
12. Christenhausz, MJM; Zhang, X.C.; Shcnider, H. 2011 A linear sequences of extant families and genera of lycophytes and ferns. *Phytotaxa*. **2011**, *19*, 7-54.
13. Nakazato, T.; Gastony, G.J. Molecullar phylogeny of *Anograma* species and related genera (Pteridaceae, pteridiodeae). *Syst. Bot*. **2003** ,*28*, 3, 490-502.
14. Christ, H. Die geographic der farne. Verlag von Gostav Fischer, Jena, **1910**.
15. Townsend, C.C.; Guest, E. Flora of Iraq, Ministry of Agriculture-Baghdad. **1966**, *2*, 184.
16. Al-Rawi, A. (1988). Wild plants of Iraq with their distribution . Ministry of Agriculture – Iraq Baghdad **1988**, 232.
17. Goerg, E.R.; Jhon, R. Methods for soil, plants, and water analysis : Manual fore West Asia and North African regions. 3rd Ed **2013**, 244.
18. Brownsey, P.J.; Smith-Dodswerth, J.C. News eland fern and allied plants, Davi Batimas, Auklant, New Seland. 2nd ed Ed. **1989**, 211.
19. Brownsey, P.J.; Perrie, LR. Flora of New Sland Ferns and Lycophytes (Thelypteridaceae). Fascicle 16. Manaaki Whenua Press, Lincoln **2016**, 36.

Ibn Al-Haitham Journal for Pure and Applied science https://doi.org/10.30526/2021.IHICPAS.2645

Gene Expression of *NLRP3* Inflammasome in Celiac Disease of Iraqi Children

Anwar I. S. Al-Assaf
anwar.idrees@yahoo.com
Department of Biology, College of Education for Pure Science (Ibn Al-Haitham), University of Baghdad, Baghdad, Iraq.

Hiba M. Ali
hibamn19921992@gmail.com
Department of Biology, College of Education for Pure Science (Ibn Al-Haitham), University of Baghdad, Baghdad, Iraq.

Ali H. Ad'hiah
dr.ahadhiah@sc.uobaghdad.edu.iq
Tropical-Biological Research Unit, College of Science, University of Baghdad, Baghdad, Iraq

Abstract

Celiac disease (CD) is an autoimmune disorder characterized by chronic inflammation that essentially affects the small intestine and is caused by eating gluten-containing foods. This study sought to determine gene expression of *NLRP3* Inflammasome in peripheral blood of Iraqi CD children using quantitative real-time PCR (qRT-PCR) assay. Thirty children with CD (12 males and 18 females) were enrolled in the study and their age range was 3-15 years. The diagnosis of the disease was confirmed by serological examinations and intestinal endoscopy. A control sample of 20 age-matched healthy children was also included. The children were stratified for age, gender, body max index (BMI), histological findings, and marsh classification. Further, the sera were examined for IgA anti-tissue transglutaminase (tTG) antibody, IgA anti-gliadin antibody, and interleukin-1 beta (IL-1β). Based on Marsh classification, the results revealed that the majority of patients (70%) had partial villous atrophy (Marsh IIІ 3A), while children with subtotal and total villous atrophy (Marsh III: 3B/3C) were presented with a lower frequency (30.0%). Neither Marsh I nor Marsh II has been observed among the patients studied. Serum levels of anti-tTG and anti-gliadin IgA antibodies were significantly higher in CD children than in control children (73.8 and 31.8 vs. 0.8 U//ml, respectively; $p < 0.001$). Conversely, IL-1β serum level was decreased in CD children but the difference was not significant (35.5vs. 53.4 pg/ml; p = 0.285). In the case of *NLRP3* inflammasome, the Relative Fold Change method ($2^{-\Delta\Delta Ct}$) was used to assess the gene expression. The results revealed that the expression of *NLRP3* inflammasome was decreased by 0.594 fold in CD children. In conclusion, the *NLRP3* inflammasome was down-regulated in the present sample of CD children, and it was accompanied by a decreased serum level of IL-1β.

Keywords :Celiac disease; *NLRP3* Inflammasome, IL-1β; Gene expression.

1. Introduction

Celiac disease (CD) is an autoimmune disorder that occurs in genetically predisposed individuals who develop an immune reaction to the ingestion of gluten-containing foods (wheat, barley, and rye) [1]. It is also characterized by chronic inflammation that primarily affects the small intestine and can lead to malabsorption of nutrients, chronic or intermittent diarrhea, growth failure or short stature, weight loss, iron deficiency, and osteopenia [2]. The global prevalence of CD is 1.4%, and it is more common in children than in adults. Further, the prevalence of CD varies with age, gender, and geographical location [3]. In Iraq, the prevalence was found to be 0.25% among healthy blood donors [4]. Human autoimmune

diseases affect 3-5% of the population and arise from complex interactions between genetic and environmental factors, which consequence in immune dysregulation and immune attack to target tissues [5]. The innate immune system works as the first line of defense in protection from pathogenic microbes and host-derived signals of cellular distress. One way in which these "danger" signals trigger inflammation is through activation of inflammasomes, which are multi-protein complexes that assemble in the cytosol after exposure to pathogen-associated molecular patterns (PAMPs) or danger-associated molecular patterns (DAMPs) [6]. They result in activation of caspase-1and subsequent cleavage of the pro-inflammatory cytokines IL-1β and IL-18, and this may be destructive to tissues; however, the specific regulatory mechanisms of *NLRP3* inflammasome activation remain unclear [7]. A role for the *NLRP3* inflammasome in recurrent and chronic inflammation was initially described in a group of rare auto-inflammatory conditions, such as rheumatoid arthritis, multiple sclerosis, and celiac disease [8]. Further, the *NLRP3* inflammasome has been implicated in many common diseases, including cancer, gout, and diabetes [9]. Being able to analyze gene expression patterns is essential for understanding protein function, biological pathways and cellular responses to external and internal stimuli [10]. To elucidate the role of the *NLRP3* inflammasome in celiac disease, this study examined the gene expression of *NLRP3* inflammasome in peripheral blood within the downstream regulatory region of the *NLRP3* gene for association with the expression of *NLRP3* in addition to the pro-inflammatory marker IL-1β.

2. Materials Method

2.1. Children studied

A total of 30 Iraqi children (12 males and 18 females; mean age ± SD: 9.60 ± 0.55 years) with CD attending the consultant clinic at the Central Pediatrics Hospital, Private Nursing Hospital, and Specialist Center for Endocrinology and Diabetes in Iraq-Baghdad during the period August 2018 - March 2019 were enrolled in this study. They were clinically examined and evaluated by the consultant medical staff at these hospitals, and the diagnosis was confirmed through serological and histological tests [11]. Serological diagnosis of CD was based on the presence of IgA antibodies against gliadin and tissue transglutaminase (tTG). This was followed by an examination of an intestinal biopsy. Cases seropositive for the two antibodies but their intestinal biopsy did not confirm the disease were excluded from the study. Children with giardiasis were also excluded. A control sample of 20 healthy children (12 male and 8 females; 9.99 ± 0.77 years) was included. They were randomly selected from healthcare units in Baghdad and had no clinical evidence or family history of CD or other autoimmune diseases.

2.2. Immunological parameters

Serum levels of anti-gliadin and anti-tissue transglutaminase test (anti-tTG) antibodies and IL-1β were measured using ELISA kits (Aeskulisa and Demeditec, respectively; Germany) and instructions of the manufacturer were followed.

2.3. Gene expression of *NLRP3* inflammasome

Gene expression of *NLRP3* inflammasome was determined by the reverse transcription-

Ibn Al-Haitham Journal for Pure and Applied science https://doi.org/10.30526/2021.IHICPAS.2645

quantitative polymerase chain reaction (RT-qPCR) method. Total RNA was isolated from peripheral using ready-to-use reagent (TRIzolTMLS Reagent; Thermo Fischer Scientific; USA). The isolated RNA was reverse-transcribed and the gene expression of NLRP3 inflammasome was assessed using GoTaq®1-Step RT-qPCR System kit (Promega, USA), and instructions of the manufacturer were followed. Forward and reverse primers for NLRP3 inflammasome (5'-AACAGCAGATGGAGAGTGGC-3' and 5'-GGTCGGACTCCTCAAACAGG-3', respectively) and the housekeeping gene GAPDH (5'-AGAAGGCTGGGGCTCATTTG-3' and 5'-AGGGGCCATCCACAGTCTTC-3', respectively) were according to published sequences. The primers were designed using primer design web-based service and validated using the Primer-BLAST-NCBI database. To determine gene expression of NLRP3 inflammasome (expression fold change), the $2^{-\Delta\Delta Ct}$ was calculated (Relative Fold Change). Thus, the expression was expressed as a fold change in the level of the target gene expression, which was normalized to the expression level of the housekeeping gene GAPDH (endogenous control) and relative to the target gene in control subjects (calibrator) [12].

2.4. Statistical analysis

The data was statistically analyzed using the statistical package for social sciences (SPSS version 19.0). Pearson Chi-square test or two-tailed Fisher exact test was used to analyzing categorical variables. For continuous variables and depending on the distribution of data, parametric variables were given as mean ± standard deviation (SD), and significant differences between means were assessed using the Student t-test. For non-parametric variables, median and interquartile range (IQR: 25-75%) were given and a significant difference between medians was assessed using either Mann–Whitney U test (to compare to groups) or Kruskal–Wallis test (to compare more than two groups). Receiver operating characteristic (ROC) analysis was employed to estimate the area under the curve (AUC) and optimum cut-off point that predicts CD. A probability (p) value ≤ 0.05 was considered statistically significant.

3. Results and Discussion

As shown in **Table (1)**, the highest incidence of CD was noticed in children aged 8-12 years (56.7%). This may indicate that the disease is more common in this age range. There is no specific explanation for such age-dependency, but delayed diagnosis and lack of awareness of disease due to the absence of any symptoms may account for underestimation of disease prevalence at a younger age [13]. Delayed onset of CD may also account for the development of disease later in life [14]. Thus, the majority of CD patients are diagnosed during adulthood [15]. The results revealed that female patients outnumbered male patients (60 vs. 40%) but the difference was not significant compared to controls (p = 0.248) **Table (1)**. It is generally agreed that CD is a female-predominant disease, but males had a shorter duration of illness before diagnosis and more severe manifestations of malabsorption [16]. The higher prevalence of CD among females could be explained by multiple factors such as hormones and genetics, the male Y chromosome might have a protective role [17]. Reasons for female predominance have not been well defined, but it has been proposed that females are at greater risk to develop immune-mediated diseases [18]. Regarding growth criteria, most of CD patients were of normal weight (5^{th} to $<85^{th}$; 63.3%) as shown in **Table (1)**. A study in Indian patients indicated that the BMI was significantly lower in CD patients compared to healthy children (17.18 vs. 21.2 kg/cm2; p <0.001), and there was no significant difference between

boys and girls with CD [19]. It has been found that BMI can be increased significantly after a gluten-free diet [20]. Generally, withdrawal of gluten from the diet leads to rapid catch-up growth of body weight within 6-12 months, whereas the height catches up is more gradually [21]. A Swedish study showed that the BMI median was slightly lower among the children with screening-detected CD compared to their healthy children, but most of the CD cases had a normal BMI [22]. In the case of March classification, the majority of patients had partial villous atrophy (Marsh IIIA; 70%), while children with subtotal and total villous atrophy (Marsh III B and III C) were less frequent (30%) **Table (1).** In a previous Iraqi study, different frequencies were found (24% Marsh IIIA, 47.8% Marsh IIIB, and 28.2% Marsh IIIC respectively) [23]. The reason behind the increased frequency of Marsh III A might be related to an early diagnosis of the studied samples. Comparable frequencies have also been presented; 5.3% Marsh III C, 24.2%, 55.3% Marsh III-A, and 15.1% Marsh III B and Marsh III C [24]. In this study, serum concentrations of anti-tTG and anti-gliadin IgA antibodies were significantly elevated in CD children compared to healthy children (73.8 and 31.8 vs. 0.8 U//ml, respectively; $p < 0.001$) **Table (1)**. Consistent with these findings, [25] indicated that an anti-tTG is the marker of choice for CD mass screening and helpful in identifying patients who can benefit from a gluten-free diet and follow-up. Although the gold standard for detecting CD is a duodenal biopsy, it has been shown that anti-tTG antibody together with an anti-gliadin antibody is a sensitive marker for CD [26, 27]. The findings of this study and other studies indicate the diagnostic potential of both antibodies in CD when conducting screening surveys for the disease in children and adolescents [28, 29]. In a study of CD children 5 years old and younger, it has been reached that anti-gliadin IgA is suitable to test for diagnosing the disease, because anti-tTG antibodies may only appear in the elderly [30]. The study also pointed to the role of IL-1β in the pathogenesis of CD. The serum level of this cytokine was decreased in CD children compared to healthy children (35.5 vs. 53.4 pg/mL respectively); however, the difference did not attend a statistical significance ($p = 0.285$) **Table (1)**. Consistent with these findings, it has been demonstrated that serum levels of IL-1β and other cytokines (TNF-α, IL-2, IL-4, and IL-8) showed no significant differences between 3 years old CD children and matched children. The authors also concluded that a gluten-free diet may also influence the serum level of some cytokines [31]. In **Table (1)**, the gene expression of NLRP3 inflammasome was also given as a relative fold changing ($2^{-\Delta\Delta CT}$). The expression was down-regulated by 0.594 in CD children and this may suggest a role for the NLRP3 inflammasome in the immunopathogenesis of CD. To the best knowledge of investigators, this study was the first in Iraqi CD patients. It has been demonstrated that inflammasomes play a significant role in the pathogenesis of autoimmune diseases including CD [8].

Table 1. Anthropometric and laboratory data of celiac disease patients and controls.

Characteristic*	**CD patients (N = 30)**	**Control (N = 20)**	***p***

Ibn Al-Haitham Journal for Pure and Applied science https://doi.org/10.30526/2021.IHICPAS.2645

	Age (year)	9.6 ± 3.0	10.0 ± 3.4	0.666
Age groups (year)	< 8	8 (26.7)	5 (25.0)	0.768
	8 – 12	17 (56.7)	10 (50.0)	
	13 - 15	5 (16.7)	5 (25.0)	
Gender	Male	12 (40.0)	12 (60.0)	0.248
	Female	18 (60.0)	8 (40.0)	
BMI percentiles	< 5th (underweight)	8 (26.7)	1 (5.0)	0.121
	5th to < 85th (normal weight)	19 (63.3)	15 (75.0)	
	≥ 85th (overweight/obese)	3 (10.0)	4 (20.0)	
Marsh classification	Marsh III: 3A	21 (70.0)	NA	
	Marsh III: 3B/3C	9 (30.0)	NA	
IgA anti-tTG antibody (U/mL)		73.8 (26.7-526.1)	0.8 (0.5-1.5)	< 0.001
IgA and anti-gliadin antibody (U/mL)		31.8 (18.0-94.6)	0.8 (0.5-1.2)	< 0.001
IL-1β (pg/mL)		35.5 (28 -47.7)	53.4 (25.7-132)	0.285
NLRP3 gene expression ($2^{-\Delta\Delta Ct}$)		0.594 (0.120-2.018)	NA	

*Values are mean ± SD (standard deviation), number followed by percentage in parentheses or median with the interquartile (IQR) range (25% - 75%); CD: Celiac disease; BMI: Body mass index; tTG: Tissue transglutaminase; NLRP3: Nucleotide-binding oligomerization domain leucine-rich repeat and pyrin domain-containing protein 3; NA: Not applicable; p: Probability; Significant p is bold-marked.

To make a further understanding of the investigated immunological and molecular parameters in the pathogenesis of CD, the patients were distributed into subgroups according to some anthropometric and clinical characteristics **Table (2)**. No significant variations between the medians of anti-tTG and anti-gliadin IgA antibodies, IL-1β, and NLRP3 gene expression between subgroups of CD children were distributed according to age, gender, BMI, and March classification. Two exceptions were encountered. In the first, the decreased level of IL-1β was more pronounced in male patients compared to female patients and the difference was significant (24.7 vs. 37.6 pg/ml; p = 0.050). Although CD patients were children, sex hormones might have a role in deviating serum levels of IL-1β in males and females [32]. The second exception involved a significantly increased concentration of anti-tTG IgA antibody in CD children with Marsh III: 3B/3C classification compared to Marsh III: 3A children (501.6 vs. 36.8 IU; p = 0.022). This may suggest a correlation between anti-tTG IgA antibody and Marsh classification; however, the low sample size of patients may limit such suggestion.

Table 2. IgA anti-tTG antibody, anti-gliadin antibody, IL-1β, and *NLRP3* gene expression ($2^{-\Delta\Delta Ct}$) distributed according to anthropometric and clinical characteristics of celiac disease patients.

Ibn Al-Haitham Journal for Pure and Applied science https://doi.org/10.30526/2021.IHICPAS.2645

Characteristic	Median with the interquartile (IQR) range (25% - 75%)			
	IgA anti-tTG antibody (U/mL)	**IgA and anti-gliadin antibody (U/mL)**	**IL-1β (pg/mL)**	***NLRP3* gene expression ($2^{-\Delta\Delta Ct}$)**
Age groups (year)				
< 8	7.0 (35.4 - 70.8)	35.4 (7.0 - 70.8)	36.9 (31.4 - 49.6)	1.214 (0.305 - 3.807)
8 – 12	29.0 (56.0 - 147.4)	56.0 (29.0 - 147.4)	36.2 (31.3 - 40.9)	0.300 (0.182 - 1.774)
13 - 15	17.2 (19.4 - 22.4)	19.4 (17.2 - 22.4)	24.4 (15.1 - 25.0)	0.051 (0.029 - 2.954)
p-value	0.537	0.088	0.155	0.353
Gender				
Male	39.2 (24.5 - 73.4)	22.4 (14.3 - 38.8)	24.7 (19.5 - 36.3)	0.191 (0.058 - 3.043)
Female	220.6 (29.9 - 529.2)	51.8 (25.9 - 123.7)	37.6 (31.4 - 49.6)	0.725 (0.246 - 1.657)
p-value	0.204	0.086	0.050	0.703
BMI percentiles				
$< 5^{th}$ (underweight)	28.3 (1.5 - 377.9)	29.6 (22.4 - 244.5)	37.6 (28.7 - 40.9)	0.422 (0.246 - 1.207)
5^{th} to $< 85^{th}$ (normal weight)	183.7 (41.5 - 801.8)	31.0 (15.0 - 93.0)	32.6 (24.1 - 37.4)	0.508 (0.065 - 3.132)
$\geq 85^{th}$ (overweight/obese)	15.5 (14.5 - 16.4)	73.8 (47.5 - 100.0)	38.4 (29.0 - 47.8)	1.214 (0.887 - 1.540)
p-value	0.061	0.562	0.591	0.562
Marsh classification				
Marsh III: 3A	36.8 (18.1 - 226.5)	28.8 (15.0 - 48.6)	36.3 (29.0 - 40.9)	0.592 (0.176 - 2.010)
Marsh III: 3B/3C	501.6 (152.8 - 992.0)	93.4 (56.0 - 95.5)	33.1 (24.1 - 40.9)	0.775 (0.120 - 1.774)
p-value	0.022	0.110	0.635	0.839

CD: Celiac disease; BMI: Body mass index; tTG: Tissue transglutaminase; NLRP3: Nucleotide-binding oligomerization domain leucine rich repeat and pyrin domain-containing protein 3; p: Probability; Significant p is bold-marked.

Receiver operating characteristic (ROC) curve analysis was performed to determine whether there was an additional advantage of using the study parameters for predicting CD. Both antibodies (anti-gliadin and anti-tTG IgA antibodies) occupied a significant area under the curve (AUC). It was 0.999 for the former antibody, while it was lower in the latter antibody (AUC = 0.956) with sensitivity and specificity of 100 and 95% and 91.7 and 90%, respectively. Whereas, IL-1β and NLRP3 gene expression did not occupy a significant AUC (0.398 and 0.627, respectively); therefore, their diagnostic performance in CD was limited **Table (3)** and **Figure (1)**.

Table 3. ROC curve analysis of IgA anti-tTG, IgA antibody, anti-gliadin antibody, IL-1β and NLRP3 gene expression in celiac disease patients.

Variable	AUC	95% CI	*p*-value	Sensitivity (%)	Specificity (%)	Cut-off value
IgA and anti-gliadin antibody (U/mL)	0.999	0.995-1.000	< 0.001	100.0	95.0	1.7
IgA anti-tTG antibody (U/mL)	0.956	0.896-1.000	< 0.001	91.7	90.0	1.8
IL-1β (pg/mL)	0.398	0.219-0.576	0.248	55.0	50.0	56.4
NLRP3 gene expression (dCT)	0.627	0.461-0.793	0.150	65.0	58.0	0.800

Ibn Al-Haitham Journal for Pure and Applied science https://doi.org/10.30526/2021.IHICPAS.2645

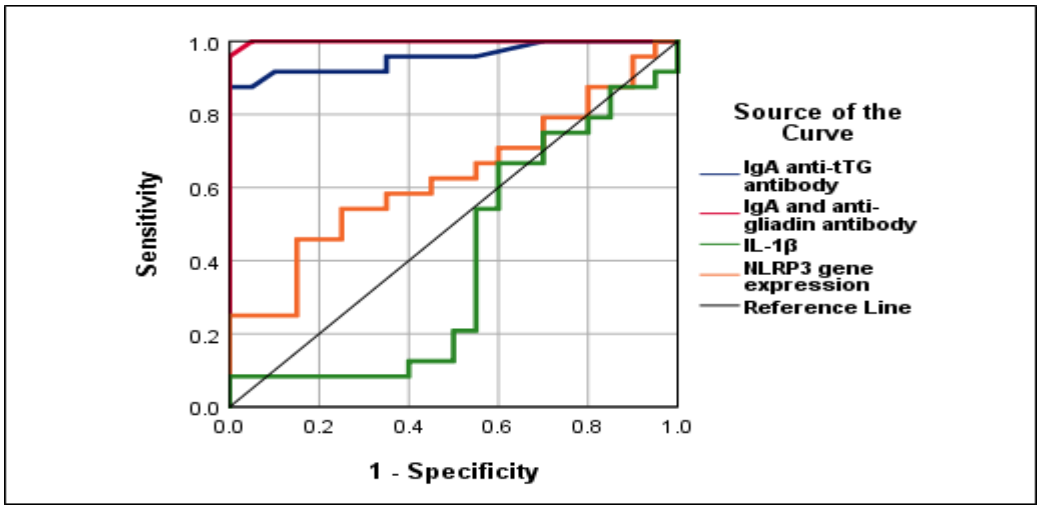

Figure 2. ROC curve analysis of IgA anti-tTG, IgA antibody, anti-gliadin antibody, IL-1β and *NLRP3* gene expression in celiac disease patients showing area under the curve.

4. Conclusion

In conclusion, the *NLRP3* inflammasome was down-regulated in the present sample of CD children, and it was accompanied by a decreased serum level of IL-1β. The diagnostic significance of anti-tTG and anti-gliadin IgA antibodies was reinforced by the present study.

References

1. Lebwohl, B.; Sanders, D.S.; Green, P.H. Coeliac disease. *Lancet* **2018** ,*391*, 70.
2. Mearin, M.L.; Montoro-Huguet, M.; Polanco, I.; Ribes-Köninckx, C.; Santolaria, S. Clinical Manifestations of Celiac Disease and Diagnostic Criteria: Differences Among Children, Adolescents and Adults In: Arranz. E.; Fernández-Bañares. F.; Rosell. C.M.; Rodrig, L.; Peña, A.S. (eds.). Advances in the Understanding of Gluten Related Pathology and the Evolution of Gluten-Free Foods. Omnia Science.Barcelona, Spain. **2015**, 291.
3. Singh, P.; Arora,A.; Strand, T.A.; Leffler, D.A.; Catassi, C.; Green, P.H.; Kelly, C.P.; Ahuja. V.; Makharia. G.K. Global prevalence of celiac disease: systematic review and meta-analysis. *Clin. Gastroenterol. Hepatol*. **2018** ,*16*, 823.
4. Toma, M.; Fayadh, M.H.; Al-Nasseri, S. *Broad look on Celiac disease in Iraq*. M.Sc. thesis submitted to College of Medicine Baghdad University, **2004**.
5. Aune, T.M.; Maas, K.; Parker, J.; Moore, J.H.; Olsen, N.J. Profiles of gene expression in human autoimmune disease. *Cell Biochem. Biophys*. **2004** ,*40*, 81.
6. Horai, R.; Saijo. S.; Tanioka, H.; Nakae, S.; Sudo, K.; Okahara, A.; Ikuse, T.; Asano,M.; Iwakura, Y. Development of chronic inflammatory arthropathy resembling rheumatoid arthritis in interleukin 1 receptor antagonist-deficient mice. *J. Exp. Med*. **2000** *191*, 313.
7. Yang, Y.; Wang, H.; Kouadir,M.; Song, H.; Shi, F. Recent advances in the mechanisms of *NLRP3* inflammasome activation and its inhibitors. *Cell Death Dis*. **2019** *10*, 128.
8. Shaw, P.J.; McDermott, M.F.; Kanneganti, T.D. Inflammasomes and autoimmunity. *Trends Mol. Med*. **2011** ,*17*, 57.
9. Cook, G.P.; Savic, S.; Wittmann, M.; McDermott, M.F. The *NLRP3* inflammasome, a target for therapy in diverse disease states. *Eur. J. Immunol*. **2010**, *40*, 631.
10. Aslam, B.; Basit, M.; Nisar, M.A.; Khurshid, M.; Rasool, M.H. Proteomics: technologies and their applications. *J. Chromatogr. Sci*. **2017** ,*55*, 182.
11. Volta, U.; Villanacci, V. Celiac disease: diagnostic criteria in progress. *Cell Mol Immunol*. **2011**, *8*, 96.
12. Livak, K.G.; Schmittgen, T.D. Analysis of relative gene expression data using real-time quantitative PCR and the 2-Delta, Delta C (T). *Methods* **2001** ,*25*, 402.

13. Ludvigsson, J.F.; Montgomery, S.M.; Ekbom, A.; Brandt, L.; Granath, F. Small-intestinal histopathology and mortality risk in celiac disease. *JAMA* **2009** ,*302*, 1171.
14. Vilppula, A.; Kaukinen, K.; Luostarinen, L.; Krekelä, I.; Patrikainen, H.; Valve. R.; Mäki. M.; Collin, P. Increasing prevalence and high incidence of celiac disease in elderly people: a population-based study. *BMC Gastroenterol*. **2009** ,*29*, 49.
15. Van Gils, T.; Nijeboer, P.; Hein, G.; Waesberghe, T.V. Splenic volume differentiates complicated and non-complicated celiac disease **2016** https://doi.org/10.1177% 2F2050640 616663571.
16. Bai, D. Effect of gender on the manifestations of celiac disease: Evidence for greater malabsorption in men Scandinavian. *J. Gastroenterol*. **2005** ,*40*, 183.
17. Quintero, O.L. Author's personal copy autoimmune disease and gender: Plausible mechanisms for the female predominance of autoimmunity. *J. Autoimmun*. **2012** ,*38*, J109.
18. Tajuddin, T.; Razif, S.; Thorne, J.; Murray, F.E. Clinical presentation of adult coeliac disease. *Irish Med. J.* **2011** ,*18*, 30.
19. Siddh, L.; Sengar, G.S.; Nagraj, N.; Shyam, R.; Garg, P. Body mass index in celiac disease and effect of a gluten-free diet on body mass index. *Home* **2016** ,*4*, 20.
20. Dehghani, S.M. Prevalence of celiac disease in healthy Iranian school children. *Ann. Saudi Med.* **2018** ,*33*, 159.
21. Meazza, C.; Pagani, S.; Diletta, G.; Laarej., K. Growth Retardation in Children with Celiac Disease. *Curr.Ped. Rev*. **2008** ,*4*, 174.
22. Van der Pals, M.; Myléus, A.; Norström, F.; Hammarroth, S.; Högberg, L.; Rosén, A.; Ivarsson, A.; Carlsson, A. Body mass index is not a reliable tool in predicting celiac disease in children. *BMC Pediatr.* **2014** ,*14*, 165.
23. Osman, M.; Taha, B.; Al-Duboni, G. Assessment of the response to gluten-free diet in an Iraqi population with coeliac disease. A histological and serological follow-up study. *Arch. Med Sci.* **2014** ,*10*, 294.
24. Bekdas, M. Investigation of celiac disease according to Marsh classification in childhood. *Bangladesh J. Med. Sci*. **2017**, *16*, 259.
25. Dipper, C.; Maitra, S.; Andrew, C.; Thomas, L.R. Anti-tissue transglutaminase antibodies in the follow-up of adult coeliac disease. *Aliment. Pharmacol. Therap*. **2009** ,*30*, 236.
26. Hopper, A.D.; Hadjivassiliou, M.; Hurlstone, D.P. Lobo, A.G.; McAlindon, M.E.; Egner. W.; Wild, G.; Sanders. D.S. What is the role of serologic testing in celiac disease? A prospective, biopsy-confirmed study with economic analysis. *Clin. Gastroenterol. Hepatol*. **2008** ,*6*, 314.
27. Al-Kazraji, K. Celiac disease: presentation with clinical and serological response. *Med. J. Tikrit University* **2009** ,*2*, 145.
28. Benson, B.C.; Mulder, C.J.; Laczek, J.T. Anti-Gliadin Antibodies Identify Celiac Patients Overlooked by Tissue Transglutaminase Antibodies Hawaii. *J. Med. Public Health* **2013** ,*72*, 14.
29. Aldaghi, M.A. Evaluation of the Correlation Between tTG-IgA Titer and Duodenal Biopsy Findings in Children with Suspected Celiac Disease. *Iranian J. Pediatr*. **2016** ,*26*, 1.
30. Bizzaro, N.; Tonutti, E. Anti-gliadin antibodies in Autoantibodies 2nd Elsevier **2007** 451pp.
31. Björck, S.; Lindehammer, S.R.; Fex, M.; Agardh, D. Serum cytokine pattern in young children with screening detected coeliac disease. *Clin. Exp. Immunol*. **2015** ,*179*, 230.
32. Oertelt-Prigione, S The influence of sex and gender on the immune response. *Autoimmun. Rev*. **2011,** *11*, A479.

Ibn Al-Haitham Journal for Pure and Applied science https://doi.org/ 10.30526/2021.IHICPAS.2646

Estimation of Some Biomarkers and Cholesterol / HDL Ratio to Predict the Risk of Cardiovascular Disease in Rheumatoid Arthritis patients

Enas Abdul Kareem Jabbar
enaskareemjj0@gmail.com
Department of Basic Medical Science, College of Nursing, University of Thi Qar, Iraq.

Shaymaa Z. Al-Rumaidh
shaymaaalrumaidh@gmail.com
College of Science,University of Thi-Qar, Iraq.

Jamela Jouda
jamela.jouda@uomustansiriyaha.idu.iq
Department of Biology, College of Science, Mustansiriyiah University, Bagdad, Iraq.

Abstract

Rheumatoid arthritis (AR) is one of the chronic diseases resulting in many complications such as cardiovascular disease (CVD). Any change in the lipid profiles and myocardial markers indicates cardiovascular disease risk, so this study is designed to monitor the pattern of lipid profiles and myocardial markers in newly diagnosed RA patients. Blood samples were collected from 70 Iraqi patients newly diagnosed with rheumatoid arthritis (male and female) and 30 healthy served as control. These individuals were aged 35-65 years. The serum samples were obtained to determine myocardial markers; included troponin, creatinine kinase (CK), lactate dehydrogenase (LDH), and glutamic oxaloacetic transaminase GOT; and lipid profiles; such as cholesterol, triglyceride, high-density lipoprotein (HDL), low-density lipoprotein (LDL), and very-low-density lipoprotein (VLDL); using a kit from Roch (Germany), measured automatically with Minividas, Biomerieux (France). No differences between levels of all lipid profiles and myocardial markers in newly diagnosed RA patients compared with the healthy group were found as well as they were within the normal values, but interestingly, the cholesterol/HDL ratio increased significantly in RA patients comparing with healthy, so it could conclude that the risk of CVD could be increase also among the newly diagnosed of RA patients. Moreover, the cholesterol/HDL ratio should be probably included in a model to predict the risk of cardiovascular disease for RA in addition to the gender, age at the disease onset, and severity markers of disease.

Keywords: Cardiovascular disease risk, myocardial biomarkers, lipid profile, rheumatoid arthritis disease, TC/HDL ratio.

1. Introduction

One of the multiple systemic chronic diseases is rheumatoid arthritis (RA) which is usually characterized as heterogeneous symptoms, variable disease progression, and extracurricular manifestations [1]. One of the complications of this disease is the risk of developing cardiovascular disease (CVD), where studies indicate that the risk of accidental cardiovascular disease has increased by 48% in previously diagnosed patients with rheumatoid arthritis compared to the individuals without RA [2].

Clinical reports define many markers that could detect the transaminases released from dying myocytes, help diagnosis of myocardial infarction, prognosis, and risk stratification of

patients with the potential cardiovascular disease. These markers included troponin, creatinine kinase (CK), glutamic oxaloacetic transaminase GOT, and Lactate dehydrogenase (LDH). All these enzymes are released in different quantities by the death of muscle cells, but the research continued since the sensitivity and specificity for myocardial necrosis fuels are lacking [3].

Many studies have reported lipid abnormalities in previously diagnosed RA patients [4, 5, 6] one of the traditional cardiovascular risk factors [7]. Dyslipidemia is observed in these patients differently than in the general population, including total cholesterol and HDL [8, 9]. Since the ratio of disproportionate between TC and HDL levels increases the index of atherogenic, it is an important predictive sign of CVD [1].

These pieces of evidence proved that the previously diagnosed patients with RD could have lipid and myocardial markers abnormalities while to our knowledge there is no research study on these markers in newly diagnosed patients with RD, so this study is designed to monitor the pattern of lipid profiles and myocardial markers in newly diagnosed RA patients.

2. Materials Method

Seventy newly diagnosed Iraqi patients with rheumatoid arthritis and thirty healthy (male and female) are recruited from the al-Husain hospital in Thi-Qar city at age of 35-65 years. Five ml blood was collected from the antecubital vein of each of the patients and healthy and put in dry sterilized test tubes. The blood samples were centrifuged for 5min at 3000rpm to obtain the serum that used to determine myocardial markers; included troponin, CK, LDH, and GOT; and lipid profiles; included cholesterol, triglyceride, HDL, LDL, and VLDL; using a kit from Roch (Germany), measured automatically with Minividas, Biomerieux (France). The results were computed as the mean ± standard error. In all statistical analyses, only $p \leq 0.05$ was considered significant. Differences among groups were analyzed by variance one-way analysis ANOVA followed by Fisher's test for multiple comparisons, using Statview version 5.0. Differences were considered significant when $p<0.05$. Regression analysis was performed by analysis of covariance (ANCOVA) also using Stat view version 5.0.

3. Results and Discussion

There are no differences between levels of myocardial markers in RA patients comparing with the healthy group included troponin, creatinine kinase, GOT, and Lactate dehydrogenase. Moreover, there are no differences between these enzyme levels in male and female groups. However, they were within normal values which are as following: (troponin=0-0.4ng/ml, CK=22-198U/L, GOT=8-45U/L, and LDH=140-280U/L) (**Figure 1**).

Ibn Al-Haitham Journal for Pure and Applied science https://doi.org/ 10.30526/2021.IHICPAS.2646

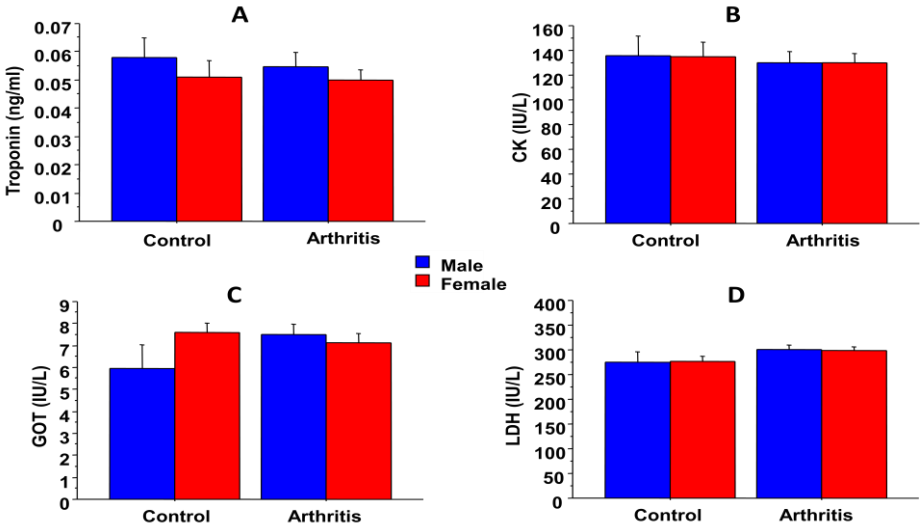

Figure 1. Myocardial markers levels in rheumatoid arthritis patients and control groups. (A) troponin, (B) creatinine kinase (CK), (C) glutamic oxaloacetic transaminas GOT, (D) Lactate dehydrogenase (LDH).

Figure 2 shows lipid profile levels in both RA patients and healthy groups (male and female). There were no differences in all lipid profiles levels of control and RA patients groups however they were within normal values which are as following: (cholestrol<150mg/dl, triglyceride<150mg/dl, HDL=40-59mg/dl, VLDL=2-30mg/dl, and LDL<100mg/dl). Moreover, there are no differences between these enzyme levels in male and female groups. Interestingly, the cholesterol / HDL ratio was also calculated. It increased significantly from (2.53±0.027) in control to (3.78±0.26) in RA patients.

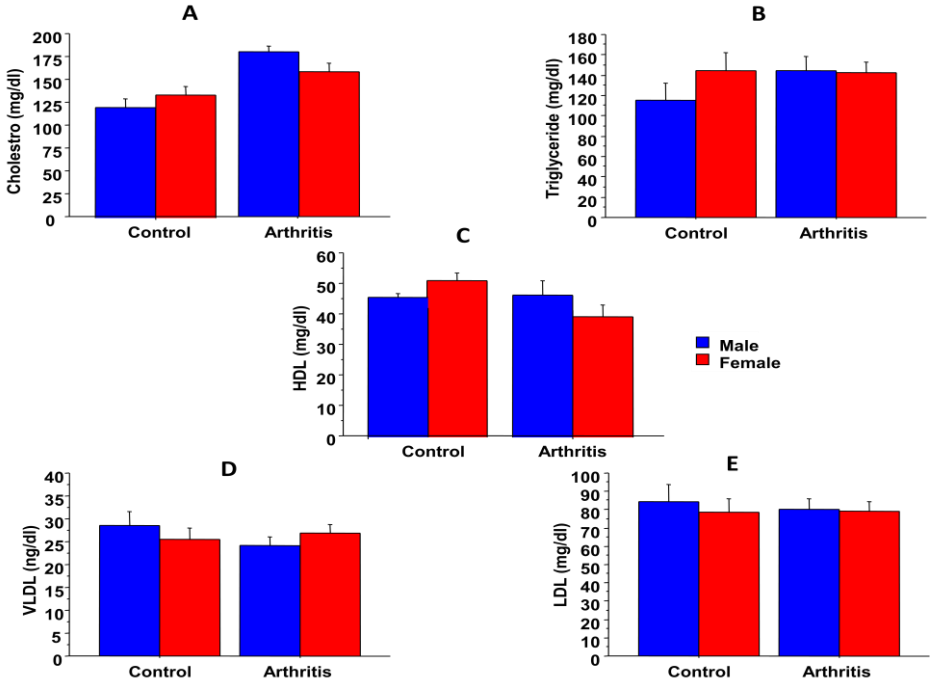

Figure 2. Lipid profiles levels in rheumatoid arthritis patients and control groups. (A) cholestrol, (B) triglyceridle, (C) high-density lipoprotein (HDL), (D) very-low-density lipoprotein (VLDL), (E) low-density lipoprotein (LDL).

The correlation between all these markers and age was also calculated. There were only significantly positive correlations between cholesterol and triglyceride with age whereas there

Ibn Al-Haitham Journal for Pure and Applied science https://doi.org/ 10.30526/2021.IHICPAS.2646

was no correlation between other markers and age (**Table 1**).

Table 1. the correlation between lipid profiles and myocardial markers.

Parameters		Age	
		R	P. value
Myocardial Markers	Troponin	0.134	0.198
	CK	0.077	0.455
	GOT	0.01	0.890
	LDH	0.122	0.247
Lipid Profils	Cholestrol	0.219	0.049
	Triglyceride	0.305	0.002
	HDL	0.01	0.946
	LDL	0.055	0.687
	VLDL	0.045	0.687

4. Discussion

Since RA patients have a higher rate of cardiovascular disease risk compared to individuals without autoimmune diseases [10], Periodic examination of cardiovascular risk according to the national guidelines used for the care of RA patients [11]. However, the general risk calculators used do not succeed in capturing the increased risks in these patients [12, 13].

Cardiovascular disease risk is associated with Many mechanisms, for example, the adverse effects of pharmacological RA, RA treatment, and accelerated atherosclerosis due to inflammatory processes associated with long-term RA [14-17]. In our work, all patients were newly diagnosed with rheumatoid arthritis, so this could be the reason why there wasn't a difference between cardiac parameters levels in RA patients compared with healthy groups. Kremers et al and Lindhardsen et al also stated that the cardiovascular disease risk in RA patients was similar to that of people without rheumatoid arthritis [7, 18]. But this result does not exclude the possibility of an increase in cardiovascular disease risk after 5–10 years of rheumatoid arthritis, although intensive treatment aimed at controlling inflammation in recent years is likely to decrease the cardiovascular disease risk rate that increases during the period of rheumatoid arthritis [19].

It is known that the lipid profile is one of the signs of cardiovascular disease because it makes rheumatoid arthritis patients triple cardiovascular disease risk. After all, this disease itself caused atherosclerosis (1). Lipid levels seem to change due to rheumatoid arthritis activity. Data of total cholesterol and low-density cholesterol concentrations differ in RA patients. Some works show similar levels [20] or less [21] of total cholesterol, however other researches indicated high concentration of total cholesterol and LDL cholesterol in early RA patients [22] or indicate decreased total cholesterol, LDL, and HDL inactive untreated RA patients [6, 21, 23]. In our results, there was no difference in all lipid profiles between RA patients and the health group.

Regardless of the changes in total cholesterol and HDL in RA patients, several studies support the calculating importance of total cholesterol to HDL ratio in RA patients, which leads to a more fatty arteriosclerosis profile and is associated with disease activity and

improves after treatment with antirheumatic drugs [20, 21, 22, 24]. In our results, the cholesterol/HDL ratio increased significantly in the RA patients than in the control group.

A similar gender-based pattern of cardiovascular disease risk observed in this study was reported by [25] and [7], who also found no general difference in cardiovascular disease risk between genders whereas there weren't differences in lipid profile and myocardial markers between women and men with RA in this study.

4. Conclusion

In conclusion, the cardiovascular disease risk could be increase also in the patient with newly diagnostic rheumatoid arthritis so other patient characteristics, such as gender, age at the onset of the disease, disease severity markers, and TC / HDL ratio should be probably included in a model to predict the cardiovascular disease risk for RA, developing such a model, validating it and assessing its primary and secondary prevention strategies for cardiovascular disease in rheumatoid arthritis patients.

References

1. Erum, U.; Ahsan, T; Khowaja, D. Lipid abnormalities in patients with Rheumatoid Arthritis. *Pak. J. Med. Sci*. **2017**, *33*, 1, 227-230.
2. Avina-Zubieta, J.A.; Thomas, J.; Sadatsafavi, M.; Lehman, A.J.; Lacaille, D. Risk of incident cardiovascular events in patients with rheumatoid arthritis: a meta-analysis of observational studies. *Ann. Rheum. Dis*. **2012** ,*71*, 9, 1524-1529.
3. Pant, S.; Deshmukh, A.; Neupane, P.; Kumar, M.P.K.; Vijayashankar, C.S. cardiac Biomarkers. In: Lakshmandoss U, editor. Noval strategies in ischemic heart disease. India: Mercy Health **2012**, 17-42.
4. Gabriel, S.E.; Crowson, C.S. Risk factors for cardiovascular disease in rheumatoid arthritis. *Curr. Opin. Rheumatol*. **2012** ,*24*, 2, 171-176.
5. Boyer, J.F.; Gourraud, P.A.; Cantagrel, A.; Davignon, J.L.; Constantin, A. Traditional cardiovascular risk factors in rheumatoid arthritis: a meta-analysis. *Joint Bone Spine*. **2011** *78*, 2, 179-183.
6. Choy, E.; Sattar, N. Interpreting lipid levels in the context of high-grade inflammatory states with a focus on rheumatoid arthritis: a challenge to conventional cardiovascular risk actions. *Ann. Rheum. Dis*. **2009**, *68*, 4, 460-469.
7. Lindhardsen, J.; Ahlehoff, O.; Gislason, G.H.; Madsen, O.R.; Olesen, J.B.; Torp-Pedersen. C. The risk of myocardial infarction in rheumatoid arthritis and diabetes mellitus: a Danish nationwide cohort study. *Ann. Rheum. Dis*. **2011** ,*70*, 6, 929-934.
8. Steiner, G.; Urowitz. M.B. Lipid profiles in patients with rheumatoid arthritis: mechanisms and the impact of treatment. *Semin Arthritis Rheum*. **2009** ,*38*, 5, 372-381.
9. Amezaga-Urruela, M.; Suarez-Almazor, M.E. Lipid paradox in rheumatoid arthritis: changes with rheumatoid arthritis therapies. *Curr Rheumatol Rep*. **2012** ,*14*, 5, 428-437.
10. Naranjo, A.; Sokka, T.; Descalzo, M.A.; Calvo-Alen, J.; Horslev-Petersen, K.; Luukkainen. R.K. Cardiovascular disease in patients with rheumatoid arthritis: results from the QUEST-RA study. *Arthritis Res. Ther.* **2008** ,*10*, 2, R30.
11. Agca, R.; Heslinga, S.C.; Rollefstad, S.; Heslinga, M.; McInnes, I.B.; Peters, M.J. EULAR recommendations for cardiovascular disease risk management in patients with rheumatoid arthritis and other forms of inflammatory joint disorders: 2015/2016 update. *Ann Rheum Dis*. **2017** ,*76*, *1*, 17-28.

12. Crowson, C.S.; Matteson, E.L.; Roger, V.L.; Therneau, T.M.; Gabriel, SE. Usefulness of risk scores to estimate the risk of cardiovascular disease in patients with rheumatoid arthritis. *Am J Cardiol*. **2012** ,*110*, 3, 420-424.
13. Siontis, G.C.; Tzoulaki, I.; Siontis, K.C.; Ioannidis, J.P. Comparisons of established risk prediction models for cardiovascular disease: systematic review. *Bmj*. **2012** ,*344*, e3318.
14. Gonzalez, A.; Maradit-Kremers. H.; Crowson. C.S.; Ballman. K.V.; Roger. V.L.; Jacobsen, S.J. Do cardiovascular risk factors confer the same risk for cardiovascular outcomes in rheumatoid arthritis patients as in non-rheumatoid arthritis patients? *Ann Rheum Dis*. **2008** ,*67*, 1, 64-69.
15. Solomon, D.H.; Curhan, G.C.; Rimm, E.B.; Cannuscio, C.C.; Karlson, E.W. Cardiovascular risk factors in women with and without rheumatoid arthritis. *Arthritis Rheum*. **2004** ,*50*, 11, 3444-3449.
16. Toms, T.E.; Symmons, D.P.; Kitas, G.D. Dyslipidaemia in rheumatoid arthritis: the role of inflammation, drugs, lifestyle and genetic factors. *Curr Vasc Pharmacol*. **2010**, *8*, *3*, 301-326.
17. Solomon, D.H.; Kremer, J.; Curtis, J.R.; Hochberg, M.C.; Reed, G.; Tsao, P. Explaining the cardiovascular risk associated with rheumatoid arthritis: traditional risk factors versus markers of rheumatoid arthritis severity. *Ann Rheum Dis*. **2010** ,*69*, *11*, 1920-1925.
18. Kremers, H.M.; Crowson, C.S.; Therneau, T.M.; Roger, V.L.; Gabriel, S.E. High ten-year risk of cardiovascular disease in newly diagnosed rheumatoid arthritis patients: a population-based cohort study. *Arthritis Rheum*. **2008** ,*58*, 8, 2268-2274.
19. Avina-Zubieta, J.A.; Choi, H.K.; Sadatsafavi, M.; Etminan, M.; Esdaile, J.M.; Lacaille, D. Risk of cardiovascular mortality in patients with rheumatoid arthritis: a meta-analysis of observational studies. *Arthritis Rheum*. **2008** *59*, *12*, 1690-1697.
20. Park, Y.B.; Lee, S.K.; Lee, W.K.; Suh, C.H.; Lee, C.W.; Lee, C.H,. Lipid profiles in untreated patients with rheumatoid arthritis. *J. Rheumatol*. **1999** ,*26*, *8*, 1701-1704.
21. Boers, M.; Nurmohamed, M.T.; Doelman, C.J.; Lard, L.R.; Verhoeven, A.C.; Voskuyl. A.E. Influence of glucocorticoids and disease activity on total and high density lipoprotein cholesterol in patients with rheumatoid arthritis. *Ann Rheum Dis*. **2003,** *62*, *9*, 842-845.
22. Georgiadis, A.N.; Papavasiliou, E.C.; Lourida, E.S.; Alamanos, Y.; Kostara, C.; Tselepis. A.D. Atherogenic lipid profile is a feature characteristic of patients with early rheumatoid arthritis: effect of early treatment--a prospective, controlled study. *Arthritis Res. Ther*. **2006** ,*8*, *3*, R82.
23. Myasoedova, E.; Crowson, C.S.; Kremers, H.M.; Roger, V.L.; Fitz-Gibbon. P.D.; Therneau. T.M. Lipid paradox in rheumatoid arthritis: the impact of serum lipid measures and systemic inflammation on the risk of cardiovascular disease. *Ann Rheum Dis*. **2011** ,*70*, *3*, 482-487.
24. van Halm, V.P.; Nielen, M.M.; Nurmohamed, M.T.; van Schaardenburg, D.; Reesink. H.W.; Voskuyl, A.E. Lipids and inflammation: serial measurements of the lipid profile of blood donors who later developed rheumatoid arthritis. *Ann Rheum Dis*. **2007**, *66*, *2*, 184-188.
25. Solomon, D.H.; Goodson, N.J.; Katz, J.N.; Weinblatt, M.E.; Avorn, J.; Setoguchi, S. Patterns of cardiovascular risk in rheumatoid arthritis. *Ann Rheum Dis*. **2006**,*65*, *12*, 1608-1612.

Ibn Al-Haitham Journal for Pure and Applied science https://doi.org/10.30526/2021.IHICPAS.2647

A Study of Chemical Content in Some Species of Tribe Apieae / Apiace

Zahra B. Muhammad
zahrabiology@gmail.com
Biology Deptment,College of Education, Al-Haweja, University of Kirkuk, Iraq

Talib O. Al-Khesraji
profdr.taliboh@tu.edu.iq
University of Tikrit, Iraq

Abstract

In this study, the flavonoid and alkaloid content in the alcoholic extract of the shoots and flowers were identified in four species of the tribe Apieae / Apiacese *: Ammi majus, Ammi visgana, Anethum graveolens* and *Foeniculum vulgaris*, and the flavonoids that were detected are (Apigenin, Coumarin, Kaempferol and Quercetin). The species *Foeniculum vulgaris* has recorded the highest concentration of total flavonoid content (Shoots and Flowers) among the studied species, reaching 4139.2 µg / ml. The total alkaloids are estimated for these species, and the *Foeniculum vulgaris* has recorded the highest concentration of the total alkaloid content as well.

Keywords: Apiaceae, *Ammi*, Apigenin, Coumarin, Alkaloid.

1. Introduction

The Apiaceae family is considered one of the most important families of flowering plants at the academic and practical levels, as its inflorescences had a great role in diagnosing them long before they are described scientifically for the first time [1] (Heywood,1976). Researchers disagreed about the number of genera and species belonging to this family, as [2] Lawrence (1951) indicated that it includes (200) genera and (2900) species. [3] Judd et. al (1999) indicated that this family is widespread and spreads in tropical to temperate regions and that it includes (400) genera and (4250) species.

In Iraq, this family is represented wildly by about (60) genera and (143) species [4] (Al-Mousawi, 1987), while Al-Katib [5] (1988) indicated that there are (130) wild species and (9) cultivated species. [6] Ghazanfar and McDaniel (2016) also mentioned that this family is the fifth-largest plant family in Iraq and that it is represented by approximately (67) genera and (155) species.

The plants of this family contain many important chemical compounds that have contributed to strengthening their role as medicinal plants and a source of treatment for diseases, and the most important of these compounds are flavonoids [7] (Trovato et. al, 1996). This family is considered to be one of the most economically important families, as many of its species are used as food or flavorings such as the Foeniculum vulgare Mill. , And Anethum graveolens L. In addition, many of the species are medicinal plants that have been used in the treatment of several medical conditions due to their containment of very important effective compounds such as essential oils, volatile oils, flavonoids, and alkaloids [8, 9] (Mutlag , 2007 and Al-Mayah, 2013). This family is considered to be a source of gum and perfumes, and a few of its species are used for decoration [4] (Al-Mousawi, 1987).

Ibn Al-Haitham Journal for Pure and Applied science https://doi.org/10.30526/2021.IHICPAS.2647

A review of the available scientific sources revealed that the current study is the first local study in which the flavonoid and alkaloid contents of the four studied species are identified.

2. Materials Method

2.1. Collection of Plant Specimens

Fresh plant specimens are collected during the flowering stage and then marked with the necessary herbal information such as (place of collection, collector's name, the common name of the plant, and date of collection). These samples are dried and pressed with the aforementioned herbal information recorded. The taxonomic keys and the Iraqi flora / fifth volume are used for the diagnosis of the samples, and it is confirmed by comparing the collected samples with the herbal samples kept in the Kurdistan Botanical Foundation herbarium in Sulaymaniyah and the Iraqi national herbarium in Abu Ghraib.

2.2. Chemical Study

2.2.1. Extraction of plant samples

Liquid-liquid and solid-liquid extraction are the most commonly used procedures before analysis of Polyphenols and simple phenolic in natural plants. They are still the most widely used techniques, mainly because of their ease of use, efficiency, and wide-ranging applicability. Commonly used extraction solvents are alcohols (methanol, ethanol), acetone, diethyl ether, and ethyl acetate. The first steps of a preparation procedure are milling and homogenization. Extraction is the main step for the recovery and isolation of bioactive phytochemicals from plant materials, before analysis. It is influenced by their chemical nature, the extraction method employed, sample particle size, as well as the presence of interfering substances. Additional steps may be called for if the removal of unwanted phenolic and non-phenolic substances such as waxes, fats, terpenes, and chlorophylls is of interest. Thirty grams of plant powdered was extracted using 15 ml chloroform with constant stirring for 24 hours at the ambient temperature. The extract was placed in an ultrasonic device for 15 minutes. Then 100 ml of butanol was added and then transferred to the separation funnel. The polar organic layer (butanol) is collected and transferred to the rotary evaporator device to obtain a dry extractor. The operation is repeated (3) times to obtain an adequate amount before analysis.

2.2.2. HPLC Condition for Analyzed Phenolic and Flavonoid Compounds

Samples are analyzed by high-performance liquid chromatography HPLC model (SYKAM) Germany. Pump model: S 2100 Quaternary Gradient Pump, Autosampler model: S 5200, Detector: UV (S 2340), and Column Oven model: S 4115. The mobile phase was = (Methanol: D.W : acetic acid) (85 : 13 : 2), the column is C18-ODS (25 cm * 4.6 mm) and detector UV – 360 nm at flow rate 1ml/min.

2.2.3. Total Alkaloid Content

The 20 gm of each plant material was ground and then extracted with methanol for 24 hours in a continuous extraction (Soxholet) apparatus. The extract was filtered and methanol was evaporated on a rotary evaporator under vacuum at a temperature of 45°C to dryness.

Ibn Al-Haitham Journal for Pure and Applied science https://doi.org/10.30526/2021.IHICPAS.2647

2.2.4. Qualitative Estimation (Test for Alkaloids)

The presence of alkaloid was confirmed by Dragendroff's method. A part of the extract was dissolved in dilute HCL and 2 drops of Dragon drops are added, a crystalline precipitate indicates the presence of alkaloid. The sample which has shown positive alkaloid is then subjected to further quantitative evaluation.

2.2.5. Separation of Alkaloid

A part of the extract residue is dissolved in 2N HCL and then faltered. 1 ml of this solution is transferred to a reparatory funnel and washed with 10 ml chloroform. The pH of this solution is adjusted to neutral with 0.1 N NaOH. Then 5 ml of Bromocresol Green (BCG) solution and 5 ml of phosphate buffer are added to this solution.

2.2.6. Standard Carve

Accurately measured aliquots (0.4, 0.6, 0.8, 1, and 1.2 ml) of Atropine standard solution were transferred to different reparatory funnels. Then 5 ml of pH 4.7 phosphate buffer and 5 ml of BCG solution is taken and the mixture is shaken with extract with 1, 2, 3, and 4 ml of chloroform. The extracts are then collected in a 10 ml volumetric flask and then have diluted to adjust the solution with chloroform. The absorbance of the complex in chloroform is measured at a spectrum of 470 nm in UV-Spectrophotometer (SHIMADZU UV-1800) against the blank prepared as above but without Atropine.

3. Results and Discussion

The results of the chemical study (**Table 1**) have shown the presence of four types of flavonoid compounds in the alcoholic extract of the shoots. These compounds are Coumarin, Catchine, Kaempferol, and Quercetin. The results of the chemical analysis have shown that the shoots are free of the flavonoid compound Apigenin.

The highest concentration of Coumarin in the shoots is 632.7 µg / ml in *F.vulgare*, and the lowest concentration of this compound reached 402.0 µg/ ml in *A. visgana*. As for the compound Catchine, the highest concentration reached 145.0 g/ ml in the type *A. majus*, while the species *A.visgana* recorded the lowest concentration of this compound, which is 105.4 µg / ml. It should be noted that the concentrations of Kaempferol are similar in the four studied species, and its highest concentration is 39.7 g/ml in species *A.visgana*, while the lowest concentration is 37.7 µg / ml in species *A.majus*, and the rest of the species has ranged between these values mentioned (**Table 1**). Regarding Quercetin, the highest concentration is 156.2 µg/ ml in *F. vulgare*, and the lowest concentration is 51.7 µg/ ml in *A.visgana* .

It is found from this study also that the flavonoid compound Coumarin is the highest concentration compound in the alcoholic extract of the shoot of all the studied species (**Table 1**). As for the total content of flavonoids in the alcoholic extract of the shoots in the studied species, the highest value of it is in the *F.vulgare* and reached 944.8 µg / ml, while the lowest value for the total number of flavonoids is 598.8 \g / ml in the type *A.visgana* (**Table 1**).

Concerning the total content of flavonoids in the alcoholic extract of flowering inflorescences in the studied species (**Table 2**), the highest value of this total is recorded in *F.vulgare* as it is 3194.4 µg / ml, while the lowest total value is 418.6 µg / ml in *A.visgana*. It is revealed through this study that only Apigenin and Coumarin are present in the alcoholic extract of the inflorescences (**Table 2**).

The species *F.vulgare* have shown the highest concentration of these two compounds

Ibn Al-Haitham Journal for Pure and Applied science https://doi.org/10.30526/2021.IHICPAS.2647

(395.7 and 2798.7) µg / ml, respectively. The flavonoid compound Apigenin is absent from the flowers of *A. majus*. The lowest concentration of Coumarin is 313.2 µg / ml in *A.visgana*.

It should be noted that the species *F.vulgare* has recorded the highest concentration of compounds Apigenin, Catchine, Coumarin, and Quercetin for the whole plant (both the vegetative and flowering parts). Also, the species *F.vulgare* has the highest concentration of flavonoids in the vegetative and flowering parts, as it reaches 4139.2 g / ml, while *A.visgana* has the lowest concentration and reaches 1017.4 µg / ml (**Table 3**).

It is worth noting that coumarins are the most abundant flavonoids in the studied species, and this is in agreement with [3] (Judd *et.al*, 1999) who have indicated that coumarins are among the compounds most present in the plants of the Apiaceae family.

Table 1. Flavonoid concentrations measured in µg / ml in the shoot parts of the studied species.

no.	Flavonoides Sp.	Apigenin	Coumarin	Catchine	Kaempferol	Quercetin	total
1	*A.majus*	0	568.2	145.0	37.7	114.8	865.7
2	*A.visgana*	0	402.0	105.4	39.7	51.7	598.8
3	*A.graveolens*	0	468.4	130.5	38.2	98.7	735.8
4	*F. vulgare*	0	632.7	116.5	39.4	156.2	944.8
Total		0	2071.3	497.4	155	421.4	3145.1

Table 2. Flavonoid concentrations measured in µg / ml in the flowering parts of the studied species.

no.	Flavonoides Sp.	Apigenin	Coumarin	Catchine	Kaempferol	Quercetin	total
1	*A.majus*	0	527.7	0	0	0	527.7
2	*A.visgana*	105.4	313.2	0	0	0	418.6
3	*A.graveolens*	328.6	1482.7	0	0	0	1811.3
4	*F. vulgare*	395.7	2798.7	0	0	0	3194.4
total		829.7	5122.3	0	0	0	5952

Table 3. Total group of flavonoids (vegetative and flowering parts) measured in µg / ml in each of the studied species.

no.	Flavonoides Sp.	Apigenin	Coumarine	Catchine	Kaempferol	Quercetin	total
1	*A.majus*	0	1095.9	145	37.7	114.8	1393.4
2	*A.visgana*	105.4	715.2	105.4	39.7	51.7	1017.4
3	*A.graveolens*	328.6	1951.1	130.5	38.2	98.7	2547.1
4	*F. vulgare*	395.7	3431.4	116.5	39.4	156.2	4139.2
total		829.7	7193.6	497.4	155	421.4	9097.1

Regarding the total alkaloids, it is found from this study that the highest percentage of alkaloids in the shoot system is 7.2% in *A.visgana*, while *A. majus* recorded the lowest percentage, reaching 5.6% (**Table 4**).

The highest percentage of alkaliod content recorded in the flowering system is in *F.vulgare* and is 16.2%, while the lowest percentage recorded is 13.4% in *A.visgana*. It is evident from the observation of **Table (4)** that the species *F.vulgare* possesses the highest percentage of total alkaloid in the vegetative and flowering systems and of the studied species, which reaches 22.4%, while the two species *A.majus* and *A.visgana* recorded the lowest total percentage, which is 20.6% for each.

The flowering system is higher in its total alkaloid content than the shoots of the species

Ibn Al-Haitham Journal for Pure and Applied science https://doi.org/10.30526/2021.IHICPAS.2647

under study, and the percentages are close in the studied species, which are few percentages and do not exceed 30% in one species, and perhaps these few percentages are the reason for the lack of interest of researchers in studying these important chemical compounds.

Table 4. Percentages of total alkaloids in shoots and inflorescents of the studied species.

No	Sp.	Shoots %	Inflorescents %	Total %
1	*A.majus*	5.6	15	20.6
2	*A.visgana*	7.2	13.4	20.6
3	*A.graveolens*	5.7	16	21.7
4	*F. vulgare*	6.2	16.2	22.4
Total		24.7	60.6	85.3

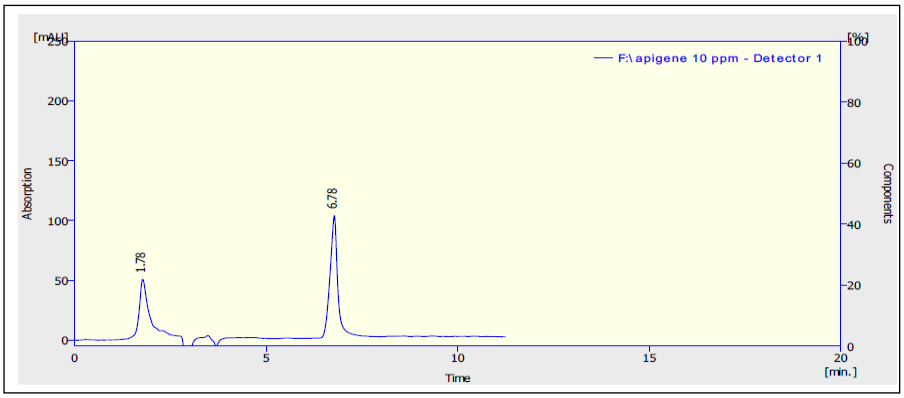

1

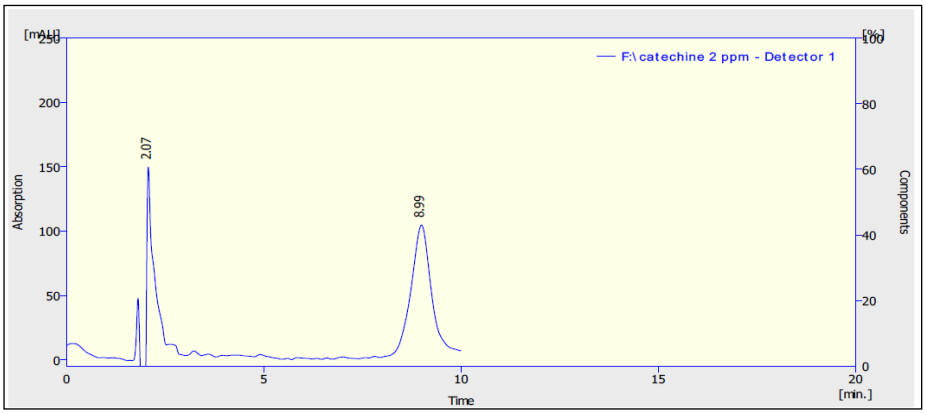

2

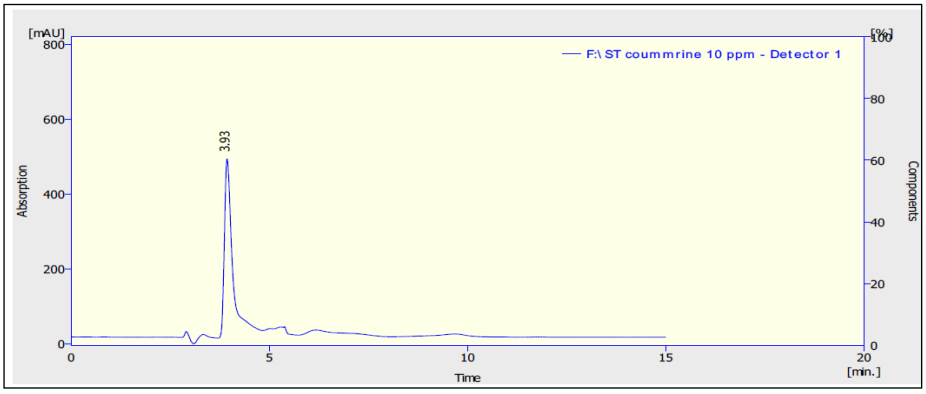

3

Ibn Al-Haitham Journal for Pure and Applied science https://doi.org/10.30526/2021.IHICPAS.2647

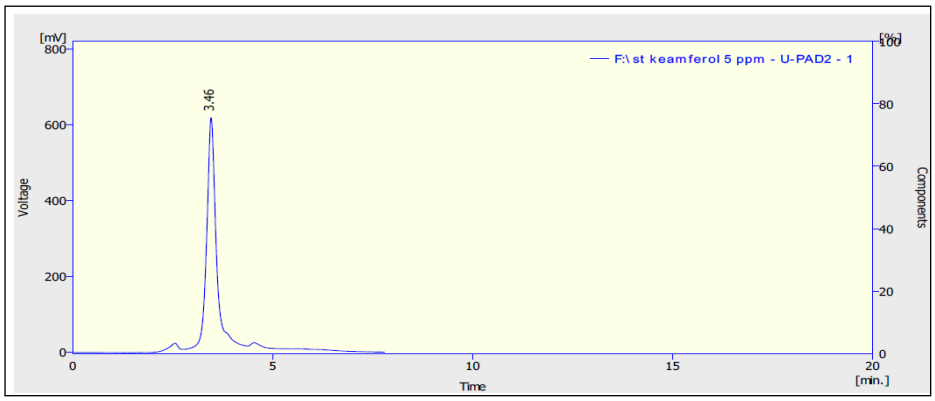

4

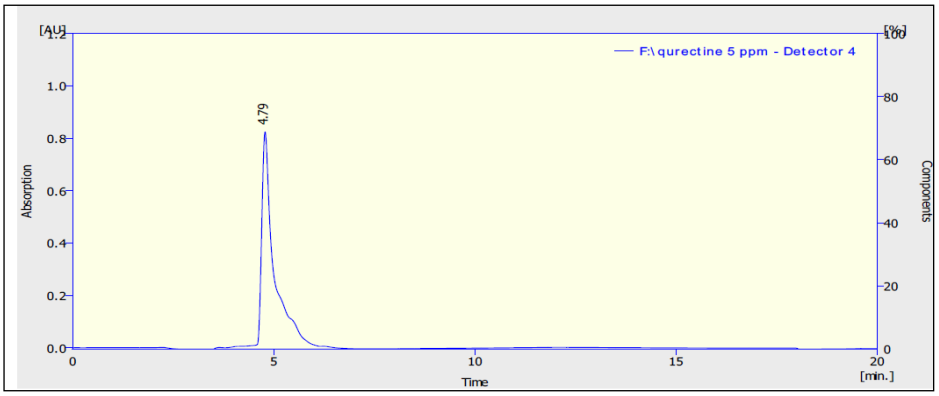

5

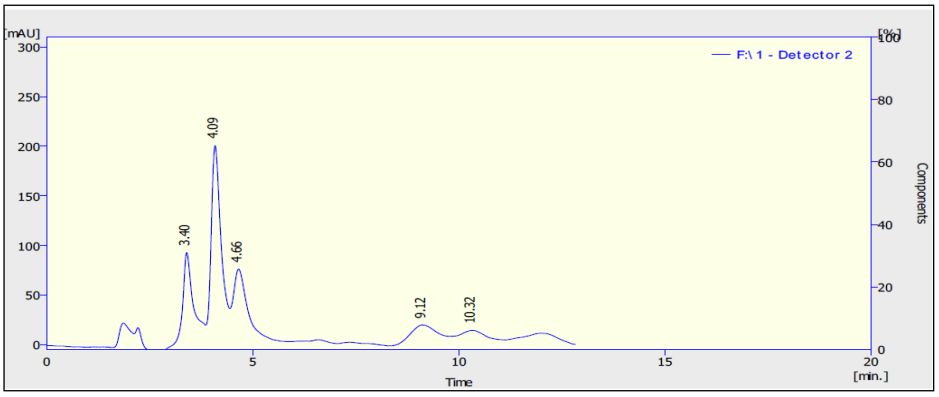

6a

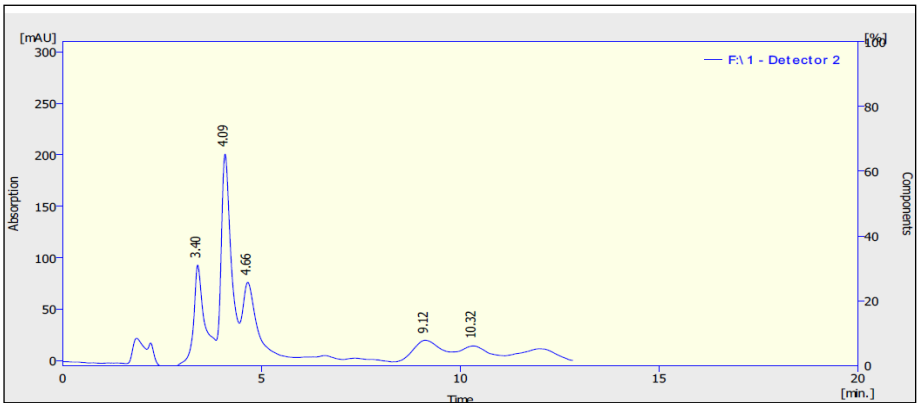

6b

Ibn Al-Haitham Journal for Pure and Applied science https://doi.org/10.30526/2021.IHICPAS.2647

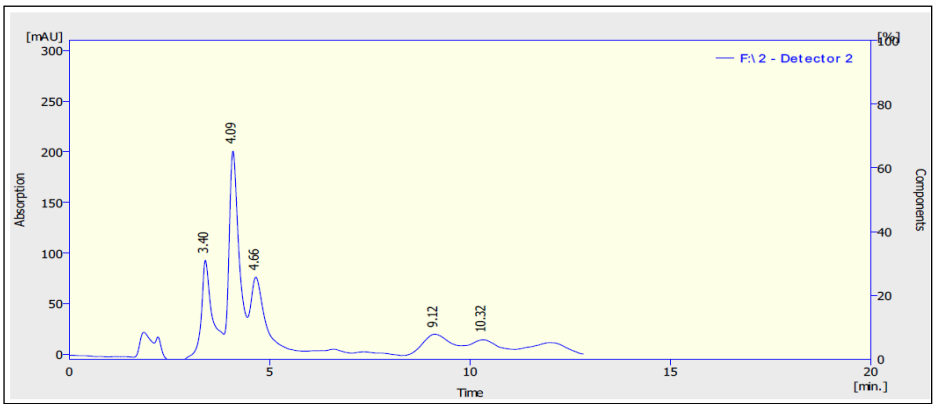

7a

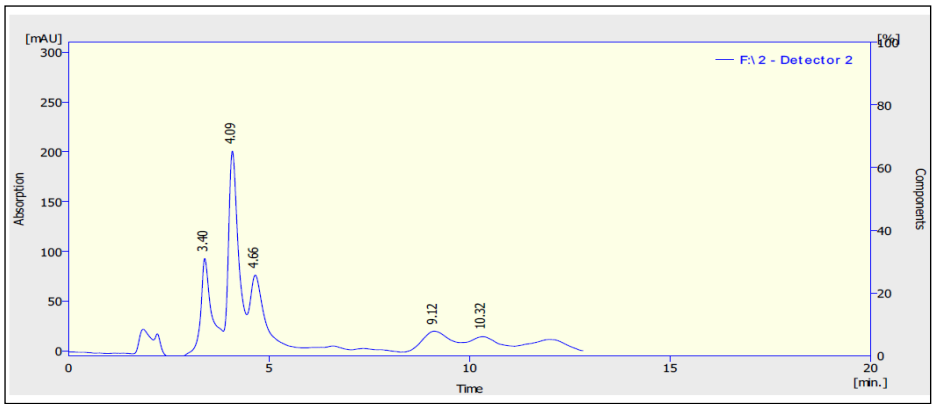

7b

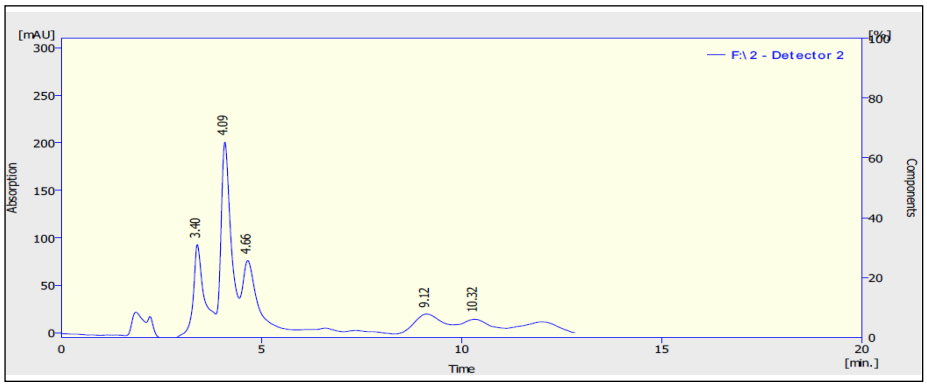

8a

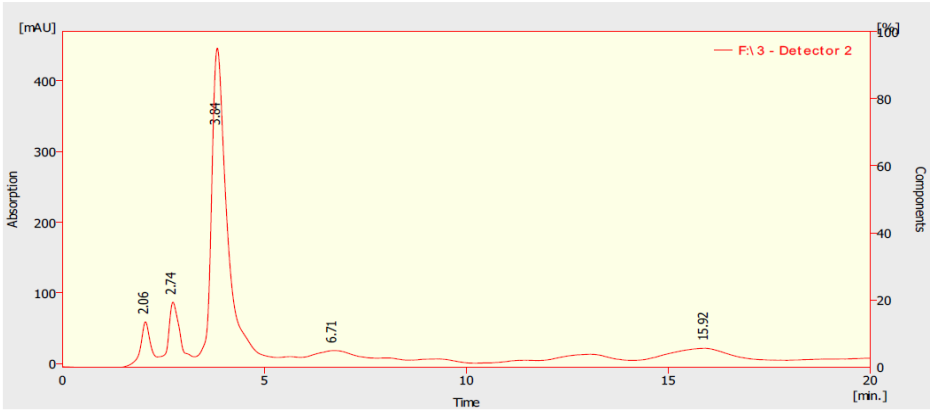

8b

Ibn Al-Haitham Journal for Pure and Applied science https://doi.org/10.30526/2021.IHICPAS.2647

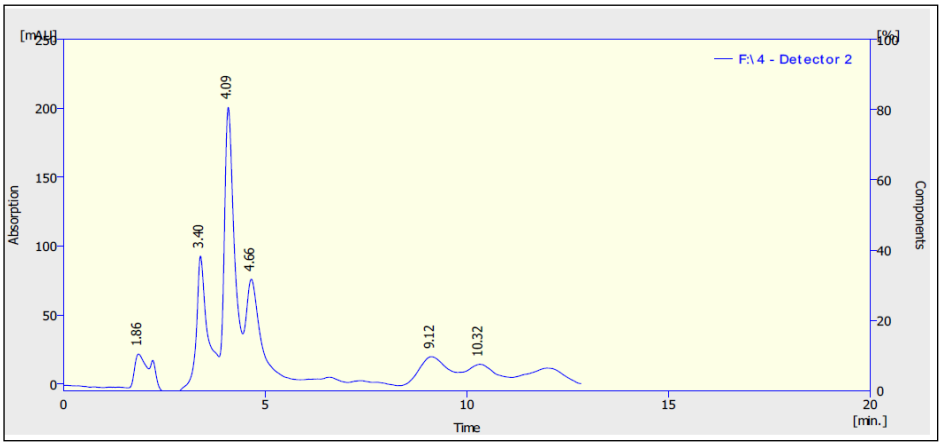

9a

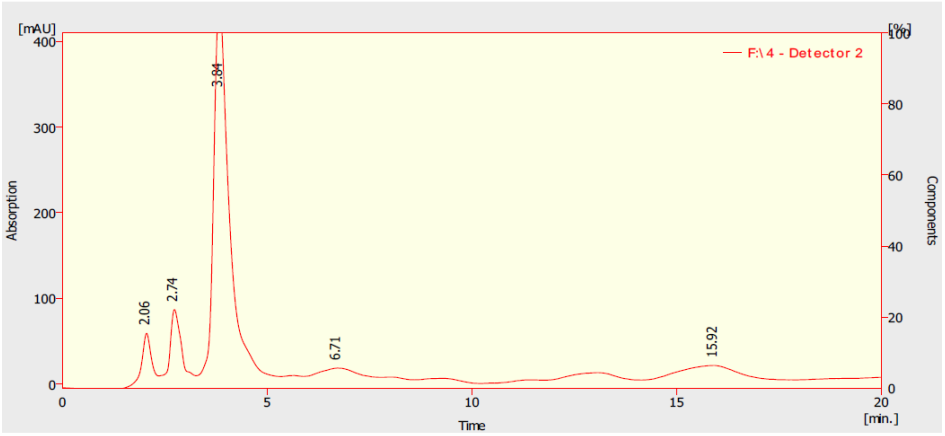

9b

Figure 1. Standard curves of shoots and flowers extract of the studied species. (Standards: 1. Apigenin, 2. Catchine, 3. Coumarin, 4. Kaempferol, 5. Quercetine) (Species: a. shoot, b.flowers, 6. *A.majus*, 7. *A.visgana*, 8. *A.graveolens*, 9. *F.vulgare*).

1 **2**

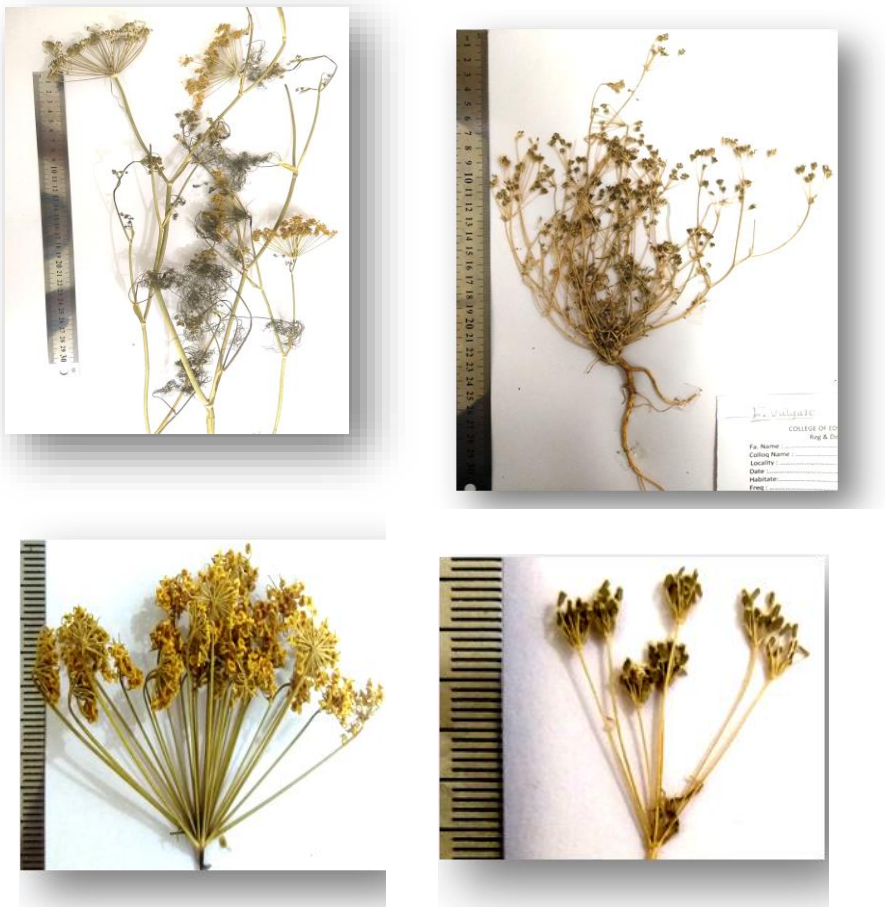

3 4

Figure 2. Studied species with their flowers: (1. *A.majus* , 2. *A.visgana* , 3.*A.graveolens*, 4.*F.vulgare*).

References

1. Heywood, V.H. Plant Taxonomy. 2nd Ed. Edward Arnold **1976**, London.
2. Lawrence, G.H.M. Taxonomy of vascular plants. The Macmillan Company. New York. **1951**, 823.
3. Judd, W.S.; Campbell, C.S. Kellogg, E.A. ; Stevens, P.F. Plant systematics. Sinauer associates, Inc., Sunderland, Massachusetts, U. S. A. **1999**, 464 .
4. Al-Mousawi, A.H. Plant Taxonomy. Books House for Printing and Publishing. University of Al Mosul **1987**, 379.
5. Al-Katib. Y.M. Classification of seed plants. Baghdad University. Ministry of Higher Education and Scientific Research. Iraq **1988**, p. 243 .
6. Ghazanfar. S.A. and McDaniel. T. (2016) . Flora of the middle east : quantitative analysis biogeography of the flora of Iraq. *Edinburgh J. Bot.* **2016** ,*73*, 1, 1–24 .
7. Trovato. A.; Monforte. M.T.; Rossito. A.; Forestieri. A.M. *In vitro* cytotoxic effect of some medicinal plants containing flavonoids. *Boll. Chim. Farm*. **1996** ,*135*, 263-266.
8. Mutlag. S.H. Study of the Hepatoprotective effect of *Ammi majus* seeds extract in CCL4-induced liver toxicity in rats.MSc.Thesis.University of Baghdad- College of pharmacy **2007**, 90.
9. Al-Mayah. A.A. Medicinal plants and herbal remedies. Al-basaer Press. Beirut, Lebanon. **2013**,358.

Ibn Al-Haitham Journal for Pure and Applied science https://doi.org/ 10.30526/2021.IHICPAS.2649

Genomics and Molecular Phylogenetics Tree Analysis of *Actinopolyspora Iraqiensis*

Talal Sabhan Salih
talal.salih@uomosul.edu.iqn
Department of Biophysics,
College of Science, University of Mosul, Iraq

Raghad Riyadh Shafeek
raghad.riyadh@uomosul.edu.iq
College of Science,
University of Mosul, Iraq

Abstarct

Actinopolyspora iraqiensis IQ-H1 is a novel strain of actinobacteria isolated from extremely halophilic soil samples in Iraq. The whole-genome sequence of this strain is deposited in the National Center for Biotechnology Information (NCBI) GenBank under the accession number NZ_AICW01000000. In this study, the genome features and the molecular phylogenetic tree of *Act. iraqiensis* IQ-H1are analyzed. The RAST tool was used for genome annotation. The genomic features were elucidated using QUAST tool. The circular genome map, and the core and pan-genome map of *Act. iraqiensis* IQ-H1 was generated using CGView and the GView tools respectively. The JSpeciesWS server was used for the tetranucleotide signature analysis and the REALPHY server was utilized for the construction of the whole genome sequence based phylogenetic tree. The genome size of the strain was around 4.0 Mpb and the number of contigs was 110 with a GC content of 70.46%. The core genome of *Act. iraqiensis* IQ-H1 was estimated to be 2.2 Mpb. Based on z-scores of the tetranucleotide signature analysis, *Act. halophila* DSM 43834, *Act. mortivallis* DSM 44261 and *Act. saharensis* DSM 45459 were the most relative strains to *Act. iraqiensis* IQ-H1with z-scores 0.99784, 0.98943 and 0.99789 respectively. Based on the phylogenetic tree constructed from the whole genome sequences, *Act. iraqiensis* IQ-H1 was the most closely related to Act. saharensis DSM 45459, *Act. halophila* DSM 43834 and Act. mortivallis DSM 44261. The results suggest that the web-based bioinformatics tools such as QUAST, CGView, GView, JSpeciesWS and REALPHY can be utilized for the analysis of the genomic features of *Act. iraqiensis* IQ-H1 and other species of the genus *Actinopolyspora*.

Keyword:*Actinopolyspora iraqiensis,* Phylogenetics Tree, Genomic Features, Tetranucleotide Signature.

1. Introduction

The genus of Actinopolyspora was proposed for the first time in 1975 by Gochnauer and his colleagues [1]. The genus currently encompasses 13 species with validly published names *Act. halophila, Act. mortivallis, Act. iraqiensis, Act. alba, Act. erythraea, Act. xinjiangensis, Act. algeriensis, Act. lacussalsi, Act. mzabensis, Act. saharensis, Act. righensis, Act. biskrensis* and *Act. salinaria* [2, 3]. Species belong to the genus *Actinopolyspora* are extremely halophilic which can grow in saturated NaCl up to 20% [4]. The strains of this genus are Gram positive bacteria that belong to the phylum Actinobacteria with high GC content (67-70%) of the DNA [2]. Like other members of Actinobacteria which are well-

known for producing bioactive compounds [5, 6], some Actinopolyspora has been reported to produce antibacterial bioactive compounds [7, 8].

In our study, the whole genome sequence of *Act. iraqiensis* strain IQ-H1, which isolated from extremely saline soil samples in Iraq [9], along with eight *Actinopolyspora* strains whose whole genome sequences are available in the National Center for Biotechnology Information (NCBI) were utilized. The genomics and molecular phylogenetics analyses utilizing genomic comparative programs and tools showed that *Act. iraqiensis* IQ-H1 has unique genomic features and has different genomic characteristics at the strain level than other related *Actinopolyspora* species.

2. Materials Method

2.1. Whole genome sequences of *Actinopolyspora*

As the main objective of this research is to genomics analysis of *Act. iraqiensis* IQ-H1. The genomic reference sequences of *Actinopolyspora* genus as well as the whole genome sequence of *Act. iraqiensis* were utilised. The genome sequences of *Act. halophila* DSM 43834, *Act. mortivallis* DSM 4426, *Act. erythraea* YIM 90600, *Act. righensis* DSM 4550, *Act. alba* DSM 45004, *Act. saharensis* DSM 45459, *Act. mzabensis* DSM 45460 and *Act. xinjiangensis* DSM 46732 were obtained from the National Center for Biotechnology Information (NCBI) Genbank database as of March 2020. Genome sequences along with their accession numbers, genome sizes, number of contigs, and GC contents are listed in **Table 1**. The whole-genome sequences were downloaded and stored in a fasta format for further analyses.

Table 1. *Actinopolyspora* reference whole genome sequences used in this study.

Genome	Accession Number	Size (Mbp)	Number of Contigs	GC(%)
Act. halophila DSM 43834	AQUI00000000	5.25	1	68.0
Act. mortivallis DSM 44261	NZ_AQZN00000000	4.23	18	68.8
Act. erythraea YIM 90600	NZ_CP022752	5.24	1	68.8
Act. righensis DSM 45501	NZ_FPAT00000000	4.92	23	67.5
Act. alba DSM 45004	NZ_FOMZ00000000	5.23	42	67.6
Act. saharensis DSM 45459	NZ_FNKO00000000	4.68	2	69.5
Act. mzabensis DSM 45460	NZ_FNFM00000000	5.00	25	67.7
Act. xinjiangensis DSM 46732	NZ_FNJR00000000	5.03	34	68.4

2.2. Genome features of *Act. iraqiensis* IQ-H1

To study the genome features of *Act. iraqiensis* IQ-H1, the whole genome sequence of this strain was first uploaded to the Rapid Annotation using Subsystem Technology tool (RAST) [10] for annotation. The annotated genome was then sent to QUAST tool [11] to elucidate the unique features. rRNA annotation was done using tRNAscan -SE v2 .0 program [12]. The circular genome map of *Act. iraqiensis* IQ-H1 was performed using CGView Comparison Tool [13] as the annotated files produced by RAST were in the GeneBank (.gbk) and Gene-Finding (.gff) formats *utilized*.

2.3. Core and Pan-Genome Comparative Analysis

For the generation of the core and pan-genome map, the GView tool [14] was used. The *Act. iraqiensis* IQ-H1 genome along with all the reference genome sequences in GenBank format were uploaded to the server. The *Act. erythraea* YIM 90600 was selected as a seed genome and the other genomes were compared to the seed to locate the unique regions. The seed is incrementally built up with the unique features of the queries to become the pan-genome. A BLAST atlas was created to display the presence or absence of features within the query genomes compared to the pan-genome.

2.4. Tetranucleotide Signature Analysis

The tetranucleotide signature analysis computes correlation coefficients between tetranucleotide usage patterns of DNA sequences, which can be used as an indicator of bacterial genome sequences relatedness. The calculation of tetranucleotide frequencies for each genome sequence was performed according to [15] through the JSpeciesWS server [16]. In brief, a fragment of DNA sequence with 4 bases can be transformed to an array of 256 possible tetranucleotide patterns and their corresponding expected frequencies are computed. The differences between frequencies and expected values are transformed into Z-scores for each tetranucleotide.

2.5. Whole Genome Sequence Based Phylogenetic Tree

For construction of a maximum likelihood phylogenetic tree based on whole genome sequences, the REALPHY version 1.12 method was used [17]. The whole genome of all *Actionopolyspora* sequences was submitted to the program in the Genbank format. *Salinispora tropica* was introduced as an outgroup species. The provided sequences were mapped to each other via bowtie2 aligning tool [18]. The sequence alignments of phylogeny were performed using PhyML. The phylogenetic tree was edited using MEGA-6 program [19].

3. Results and Discussion

A detailed summary of the genome features of *Act. iraqiensis* IQ-H1is shown in **Table 2**. From the results, it can be seen that the genome size of *Act. iraqiensis* IQ-H1was around 4.0 Mpb and the number of contigs was 110 with the largest one 217989 pb. The data obtained from the whole genome sequences have shown that the genome sizes of *Actinopolyspora* genus ranges from 4.23 Mpb as in the case of *Act. mortivallis* to 5.25 Mpb as in case of *Act. halophila* [20, 21]. The results have also shown that the GC content of *Act. iraqiensis* IQ-H1was 70.46%. Previous studies found that Gram-positive bacteria have high GC content than Gram-negative bacteria [22]; also found that GC content is positively correlated with the genome size in bacteria [23]. Although *Act. iraqiensis* IQ-H1has the smallest genome size compared to the other species of *Actinopolyspora* that are included in this study (**Table 1**), it can be seen that *Act. iraqiensis* IQ-H1has the highest GC content. However, this is clearly because that the whole genome of *Act. iraqiensis* IQ-H1 was not sequenced completely as the genome sequence of this strain was deposited as a draft genome with 110 contigs and many regions from the genome might be missing. However, only the Act. erythraea YIM 90600 genome of the genus *Actinopolyspora* was sequenced completely [21]. Other genome features, including protein coding genes (CDS), tRNA genes, rRNA genes, open reading frames (ORF) and GC skew as well as GC content, are shown in **Figure 1**.

Ibn Al-Haitham Journal for Pure and Applied science https://doi.org/ 10.30526/2021.IHICPAS.2649

Table 2. . Genome features of *Act. iraqiensis IQ-H1* draft genome.

Attribute	Value
Genome total length	3827684
Contigs	110
G+C content (%)	70.46
Largest contig	217989
Protein coding genes (CDS)	4039
tRNA genes	53
rRNA genes (23S, 16S, 5S)	5
N50	87719
L50	146

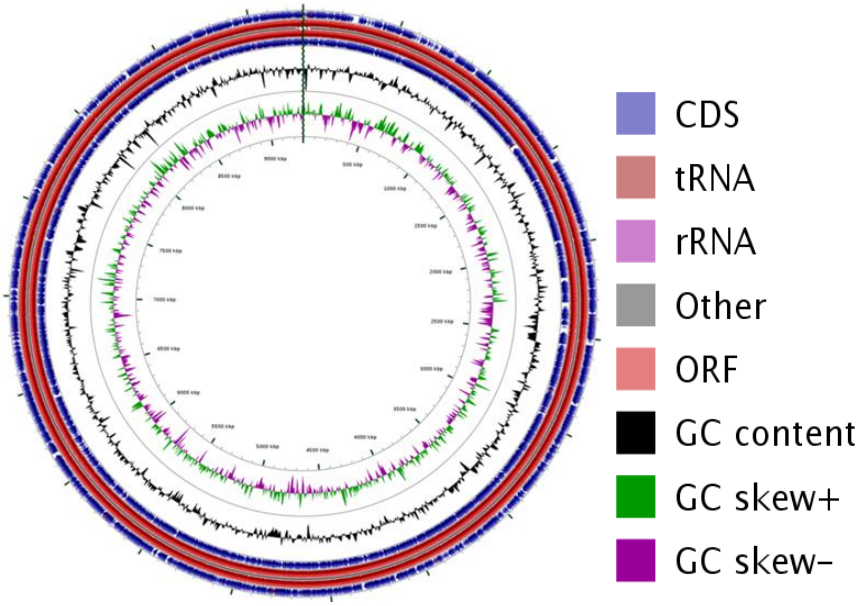

Figure 1. Circular genome representation of *Act. iraqiensis* IQ-H1 draft genome. The inner most ring represents chromosome position megabase pairs. The next rings represent the feature regions which are indicated in different colors..

It was necessary for determining the core and the pan-genome of the candidate *Actinopolyspora* species to identify genomic features common to all and to distinguish those that are unique to *Act. iraqiensis* IQ-H1.The results from the core and pan-genome analysis reveal that the pan-genome size of the nine strains of *Actinopolyspora* comprises of 15 Mpb (**Figure 2**). However, studies have shown that adding more bacterial genome sequences result in an expansion in the pan-genome size of a bacterial species which is known as open pan-genome [24, 25]. The outer-most slot (red) represents the core genome of *Act. iraqiensis* IQ-H. The core genome of *Act. iraqiensis* IQ-H1 is estimated to be 2.2 Mpb (from 12.8-15 Mpb, **Figure 2**). The core genome slot shows regions, where a BLAST hit, was present between the reference sequence, *Act. erythraea* YIM 90600 in this case, and all of the other genome sequences. Moreover, rapid advances in whole-genome sequencing methodologies have led to an enormous increase in the number of bacterial genomes deposited Genbank databases [26].

Ibn Al-Haitham Journal for Pure and Applied science https://doi.org/ 10.30526/2021.IHICPAS.2649

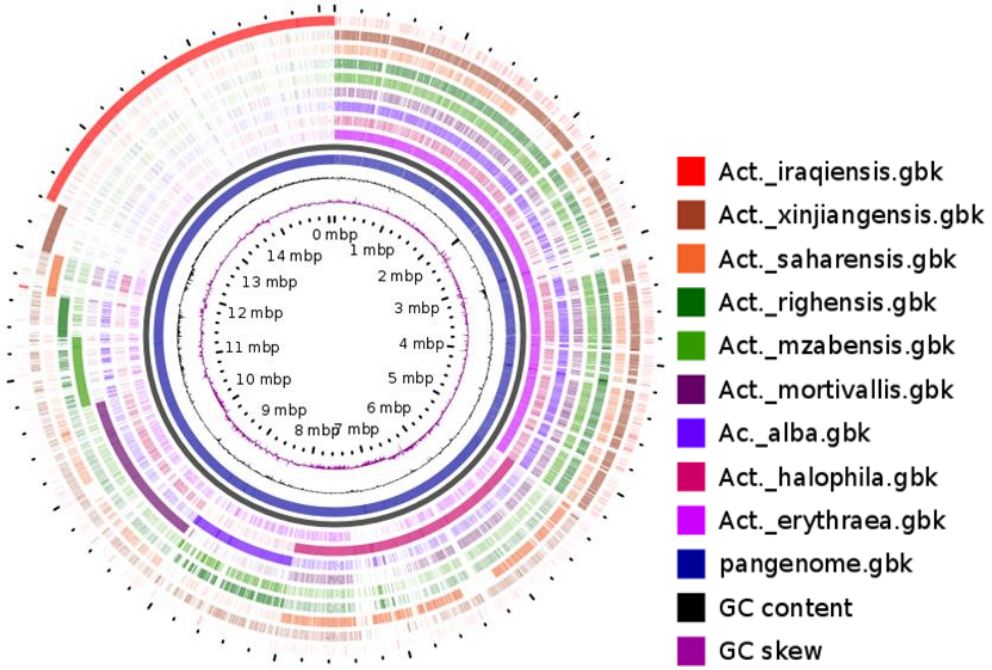

Figure 2. Core and pan-genome analysis map using the nine *Actinopolyspora* genomes. The inner-most slot (blue) shows the constructed pan-genome using all uploaded genome sequences. The next slots show regions where there were BLAST hits between the constructed pan-genome and the other uploaded genomes. The large gaps show regions missing from the seed genome (*Act. erythraea* YIM 90600) but found in one of the other genomes. These regions were appended onto the reference pangenome and are thus visible as gaps in the BLAST results for the seed genome slot (*Act. erythraea* YIM 90600).

In the era of genome sequencing and bioinformatics, it is now generally accepted that genome sequencing has the potential to be a routine approach of measuring genetic relatedness between closely related species. It has been demonstrated in many studies, the analysis of tetranucleotide usage patterns is often as a much more reliable measure of sequence relatedness than the GC content the traditional method of DNA-DNA hybridisation [15, 27, 28]. The threshold value > 0.999 (Above cut-off) indicates that the two genomes are the same species while the threshold value > 0.989 (Below cut-off) indicates that the two genomes are distinctly different [15]. Based on these values, the results have shown that *Act. iraqiensis* IQ-H1 is a new distinct species in the genus of *Actinopolyspora* (**Table 3**). However, *Act. halophila* DSM 43834, *Act. mortivallis* DSM 44261 and *Act. saharensis* DSM 45459 seem to be the most relative strains to *Act. iraqiensis* IQ-H1with z-scores 0.99784, 0.98943 and 0.99789 respectively. Remarkably, it was noticed that when two genomes are closely related the distinction between the z-scores values will decrease while when the relatedness between two genomes decreased, the disparity between the z-scores values will increased [29]. According to this, *Act. iraqiensis* is the most related species to *Act. saharensis* DSM 45459 and *Act. iraqiensis* is the most distinct species to *Act. righensis* DSM 45501 with z-scores 0.99789 and 0.89345 respectively (**Table 3**).

Table 3. Tetranucleotide signature results for the relatedness between *Act. iraqiensis* IQ-H1genome and the related species in the genus *Actinopolyspora* based on whole/draft genome sequences.

Genome sequences		**Z-Score**		
Query Genome	Reference Genomes	*Above cut-off* (> 0.999)	*In range* (> 0.989)	*Below cut-off* (< 0.989)
Act. iraqiensis IQ-H1	*Act. halophila* DSM 43834		0.99784	
	Act. mortivallis DSM 44261		0.98943	
	Act. erythraea YIM 90600			0.92642
	Act. righensis DSM 45501			0.89345
	Act. alba DSM 45004			0.89534
	Act. saharensis DSM 45459		0.99789	
	Act. mzabensis DSM 45460			0.89651
	Act. xinjiangensis DSM 46732			0.9182

It was observed that using the whole genome sequence for phylogenetic analysis is quite complicated and that the phylogenetic trees based on whole-genome analysis are not similar [30]. In our study, we utilized a REALPHY bioinformatics program [17] to infer a phylogenetic tree of *Act. iraqiensis* IQ-H1 with those of closely related *Actinopolyspora* strains based on whole genome sequences. From the results, it is very obvious that *Act. iraqiensis* IQ-H1 is the most closely related to *Act. saharensis* DSM 45459, *Act. halophila* DSM 43834 and *Act. mortivallis* DSM 44261 (**Figure 3**).

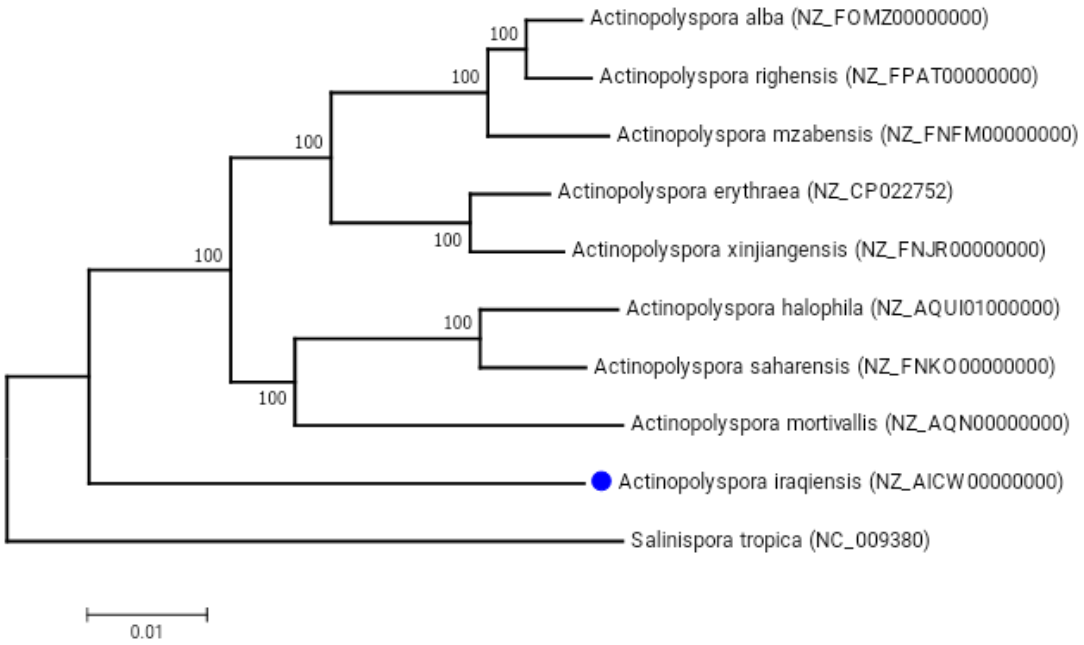

Figure 3. A maximum likelihood phylogenetic tree constructed from the nine whole genome sequences in the GenBank format using the REALPHY method [17] via bowtie2 aligning tool [18]. *Salinispora tropica* was introduced as an outgroup species. The phylogenetic tree was edited using MEGA-6 program [19]. The

phylogeny was tested by 1000 of bootstrap replications.

Figure 3. A maximum-likelihood phylogenetic tree constructed from the nine whole genome sequences in the GenBank format using the REALPHY method [17] via bowtie2 aligning tool [18]. *Salinispora tropica* was introduced as an outgroup species. The phylogenetic tree was edited using MEGA-6 program [19]. The phylogeny was tested by 1000 of bootstrap replications.

4. Conclusion

This study has shown that *Actinopolyspora iraqiensis* IQ-H1 is an Iraqi novel strain of actinobacteria. *Act. iraqiensis* IQ-H1 was closely related strain to *Act. halophila* DSM 43834, *Act. mortivallis* DSM 44261 and *Act. saharensis* DSM 45459 based on z-scores; and most related strain to *Act. saharensis* DSM 45459, *Act. halophila* DSM 43834 and *Act. mortivallis* DSM 44261based on whole genome sequences phylogenetic tree. The findings indicate that the biological information in the form of whole genome sequences stored at the National Center for Biotechnology Information (NCBI) database along with the bioinformatics tools used in the study can be utilized for the molecular phylogenetics and genomic features analyses of *Act. iraqiensis* IQ-H1 and related species of the genus *Actinopolyspora*.

References

1. Gochnauer, M.; Leppard, G.; Komaratat, P.; Kates, M.; Novitsky, T.; Kushner, D. Isolation and characterization of *Actinopolyspora halophila*, gen. et sp. nov., an extremely halophilic actinomycete. *Can. J. Microbiol.* **1975**, *21*, 1500-1511, doi: 10.1139/m75-222.
2. Zhi, X.Y.; Li, W.J.; Stackebrandt, E. An update of the structure and 16S rRNA gene sequence-based definition of higher ranks of the class Actinobacteria, with the proposal of two new suborders and four new families and emended descriptions of the existing higher taxa. *Int. J. Syst. Evolut. Microbiol.* **2009**, *59*, 589-608, doi: 10.1099/ijs.0.65780-0.
3. Parte, A.C. LPSN-List of Prokaryotic names with Standing in Nomenclature (bacterio.net), 20 years on. *Int. J. Syst. Evol. Microbiol.* **2018**, *68*, 1825-1829, doi: 10.1093/nar/gkt1111.
4. Zhi, X.; Yang, L.; Wu, J.; Tang, S.; Li, W. Multiplex specific PCR for identification of the genera Actinopolyspora and Streptomonospora, two groups of strictly halophilic filamentous actinomycetes. *Extremophiles.* **2007**, *11*, 543-548, doi.org/10.1007/s00792-007-0066-1
5. Newman, D.J.; Cragg, G.M.; Snader, K.M. Natural products as sources of new drugs over the period 1981− 2002. *J. Nat. Prod.* **2003**, *66*, 1022-1037, doi.org/10.1021/np030096l.
6. Benhadj, M.; Gacemi-Kirane, D.; Menasria, T.; Guebla, K.; Ahmane, Z. Screening of rare actinomycetes isolated from natural wetland ecosystem (Fetzara Lake, northeastern Algeria) for hydrolytic enzymes and antimicrobial activities. *J. King Saud University-Sci.* **2019**, *31*, 706-712, doi.org/10.1016/j.jksus.2018.03.008.
7. Johnson, K. G.; Lanthier, P.H. β-Lactamases from Actinopolyspora halophila, an extremely halophilic actinomycete. *Arch. Microbiol.* **1986**, 1*43*, 379-386, doi.org/10.1007/BF00412806.
8. Yoshida, M.; Matsubara, K.; Kudo, T.; Horikoshi, K. Actinopolyspora mortivallis sp. nov., a moderately halophilic actinomycete. *Int. J. Syst. Evol. Microbiol.* **1991**, *41*, 15-20, doi.org/10.1099/00207713-41-1-15.
9. Ruan, J.S.; Al-Tai, A.M.; Zhou, Z.H.; Qu, L.H. Actinopolyspora iraqiensis sp. nov., a new halophilic actinomycete isolated from soil. *Int. J. Syst. Evol. Microbiol.* **1994**, *44*, 759-763, doi.org/10.1099/00207713-44-4-759.

10. Aziz, R.K.; Bartels, D.; Best, A.A.; DeJongh, M.; Disz. T.; Edwards. R. A.; Formsma. K.; Gerdes. S.; Glass. E. M.; Kubal. M.; Meyer. F. The RAST Server: rapid annotations using subsystems technology. *BMC genomics.* **2008**, *9*, 75, doi.org/10.1186/1471-2164-9-75.
11. Gurevich, A.; Saveliev, V.; Vyahhi, N.; Tesler, G. QUAST: quality assessment tool for genome assemblies. *Bioinformatics.* **2013**, *29*, 1072-1075, doi: 10.1093/bioinformatics/btt086.
12. Lowe, T. M.; Chan, P. P. tRNAscan-SE On-line: Search and Contextual Analysis of Transfer RNA Genes. *Nucl. Acids Res.* **2016**, *44*, W54-57, doi: 10.1093/nar/gkw413.
13. Stothard, P.; Grant, J. R.; Van Domselaar, G. Visualizing and comparing circular genomes using the CGView family of tools. *Briefings Bioinform.* **2019,** *20*, 1576-1582, doi: 10.1093/bib/bbx081.
14. Petkau, A.; Stuart-Edwards, M.; Stothard, P.; Van Domselaar, G. Interactive microbial genome visualization with GView. *Bioinformatics.* **2010**, *26*, 3125-3126, doi: 10.1093/bioinformatics/btq588.
15. Teeling, H.; Meyerdierks, A.; Bauer, M.; Amann, R.; Glöckner, F.O. Application of tetranucleotide frequencies for the assignment of genomic fragments. *Environ. Microbiol.* **2004**, *6*, 938-947, doi: 10.1111/j.1462-2920.2004.00624.x
16. Richter, M.; Rosselló-Móra, R.; Oliver, F.; Peplies, J.J. SpeciesWS: a web server for prokaryotic species circumscription based on pairwise genome comparison. *Bioinformatics.* **2016**, *32*, 929-931, doi: 10.1093/bioinformatics/btv681.
17. Bertels, F.; Silander, O.K.; Pachkov, M.; Rainey, P.B.; van Nimwegen, E. Automated reconstruction of whole-genome phylogenies from short-sequence reads. *Mol. Biol. Evol.* **2014**, *31*, 1077-1088, doi: 10.1093/molbev/msu088.
18. Langmead, B.; Salzberg, S.L. Fast gapped-read alignment with Bowtie 2. *Nature methods.* **2012**, *9*, 357, doi.org/10.1038/nmeth.1923.
19. Tamura, K.; Stecher, G.; Peterson, D.; Filipski, A. Kumar, S. MEGA6: molecular evolutionary genetics analysis version 6.0. *Mol. Biol. Evol.* **2013**, *30*, 2725-2729, doi: 10.1093/molbev/mst197.
20. Tang, S.K.; Wang, Y.; Klenk, H.P.; Shi, R.; Lou, K.; Zhang, Y. J.; Chen, C.; Ruan, J. S.; Li, W.J. Actinopolyspora alba sp. nov. and Actinopolyspora erythraea sp. nov., isolated from a salt field, and reclassification of Actinopolyspora iraqiensis Ruan et al. 1994 as a heterotypic synonym of Saccharomonospora halophila. *Int. J. Syst. Evol. Microbiol.* **2011**, *61*, 1693-1698, doi.org/10.1099/ijs.0.022319-0.
21. Chen, D.; Feng, J.; Huang, L.; Zhang, Q.; Wu, J.; Zhu, X.; Duan, Y.; Xu, Z. Identification and characterization of a new erythromycin biosynthetic gene cluster in Actinopolyspora erythraea YIM90600, a novel erythronolide-producing halophilic actinomycete isolated from salt field. *PloS one.* **2014**, *9*, e108129, doi: 10.1371/journal.pone.0108129.
22. Li, X. Q.; Du, D. Variation, evolution, and correlation analysis of C+ G content and genome or chromosome size in different kingdoms and phyla. *PLoS One.* **2014**, *9*, e88339, doi.org/10.1371/journal.pone.0088339.
23. Nishida, H. Evolution of genome base composition and genome size in bacteria. *Front. Microbiol.* **2012**, *3*, 420, doi: 10.3389/fmicb.2012.00420.
24. Livingstone, P.G.; Morphew, R.M.; Whitworth, D.E. Genome sequencing and pan-Genome analysis of 23 Corallococcus spp. strains reveal unexpected diversity, with particular plasticity of predatory gene sets. *Front. Microbiol.* **2018**, *9*, 3187, doi.org/10.3389/fmicb.2018.03187.
25. Blaustein, R.A.; McFarland, A.G.; Maamar, S.B.; Lopez, A.; Castro-Wallace. S.; Hartmann, E.M. Pangenomic approach to understanding microbial adaptations within a model built environment, the International Space Station, relative to human hosts and soil. *Systems.* **2019**, *4*, e00281-18, doi: 10.1128/mSystems.00281-18.

26. Brockhurst, M.A.; Harrison, E.; Hall, J.P.; Richards, T.; McNally, A.; MacLean, C. The ecology and evolution of pangenomes. *Curr. Biol.* **2019**, *29*, R1094-R1103, doi.org/10.1016/j.cub.2019.08.012.
27. Liu, Y.; Yang, D.; Zhang, N.; Chen, L.; Cui, Z.; Shen, Q.; Zhang, R. Characterization of uncultured genome fragment from soil metagenomic library exposed rare mismatch of internal tetranucleotide frequency. *Front. Microbiol.* **2016**, *7*, 2081, doi.org/10.3389/fmicb.2016.02081.
28. Siranosian, B.; Perera, S.; Williams, E.; Ye, C.; de Graffenried, C.; Shank, P. Tetranucleotide usage highlights genomic heterogeneity among mycobacteriophages. *F1000Research.* **2015**, *4*, doi: 10.12688/f1000research.6077.2.
29. Richter, M.; Rosselló-Móra, R. Shifting the genomic gold standard for the prokaryotic species definition. *Proc. Nat. Acad. Sci.* **2009,** *106*, 19126-19131, doi.org/10.1073/pnas.0906412106.
30. Dutilh, B.E.; Huynen, M.A.; Bruno, W.J.; Snel, B. The consistent phylogenetic signal in genome trees revealed by reducing the impact of noise. *J. Mol. Evol.* **2004**, *58*, 527-539, doi.org/10.1007/s00239-003-2575-6.
31. Auch, A.; von Jan, M.; Klenk, H.P.; Göker, M. Digital DNA-DNA hybridization for microbial species delineation by means of genome-to-genome sequence comparison. *Standards in Genomic Sciences.* **2010,** *2*, 117-134, doi: 10.4056/sigs.531120
32. Konstantinidis, K.; Tiedje, M. Genomic insights that advance the species definition for prokaryotes. *Proc. Nat. Acad. Sci. United States Am.* **2005,** *102*, 2567–2572, doi: 10.1073/pnas.0409727102.
33. Varghese, N.; Mukherjee, S.; Ivanova, N.; Konstantinidis, K.T.; Mavrommatis, K.; Kyrpides. N.C.; Pati. A. Microbial species delineation using whole genome sequences. *Nucl. Acids Res.* **2015**, *43*, 6761–6771, doi: 10.1093/nar/gkv657.
34. Jain, C.; Rodriguez-R, L.M.; Phillippy, A.M.; Konstantinidis, K.T.; Aluru, S. High throughput ANI analysis of 90K prokaryotic genomes reveals clear species boundaries. *Nat. Commun.* **2018**, *9*, 5114, doi.org/10.1038/s41467-018-07641-9.

Ibn Al-Haitham Journal for Pure and Applied science https://doi.org/10.30526/2021.IHICPAS.2650

Physiological Changes of Thyroid Hormones in Women with Osteoporosis in Iraq / Basra Province

Mustafa A Almajeed
abdalmajeed46@yahoo.com
Department of Physiology, Basrah Medical College, Basrah University, Iraq.

Sami J Kathim
sami.kadhim@uobasrah.edu.iq
Department of Biology, College of Education Pure Sciences, Basrah University , Iraq.

Abstract

Osteoporosis is described as sickness due to fading bone mass and microarchitecture spoilage of bone tissue leads to consolidation bone fragility and increase risk of fracture. The relationship between osteoporosis and thyroid is important by of the skeleton bones in turnout of circulating physical thyroid hormone and TSH condensation to reduced bone mineral loss in osteoporosis patients, also researcher derives that hormone thyroid and TSH scale increased bone resorption, by increase bone mineral deposition. (110) patients female transfer from provincial and civilian habitation, their ages between (55-75) years old, they pay a visit to DEXA station to measure the density. The samples of blood after diagnosis of disease were taken, then the thyroid hormones were gauged by the modern VIDAS automated quantitative device according to the methods which assay serum or plasma. The outcome appeared to decrease significantly ($p \leq 0.05$) in TSH, T3, and T4 in osteoporosis women compared with healthy women, also no significant changes occur between housing status. Thyroid hormones have significant changes in osteoporosis women matched with good health women in Iraq / Basra province.

Keywords: Thyroid hormones, Osteoporosis, Low mineral density.

1. Introduction

Osteoporosis is an important disease associated with increased mortality after fractures [1]. Osteoporosis will be defined as a sickness in bone specialized with bone mass deformity and microarchitecture analysis of tissue bone lead to enhance fragility of bone and rise a percent of the risk of fracture [2]. The percent of high fractures risk in people have decreased in bone mineral density, the fractures majority will be found in patients with decrease density of bone rather than osteoporosis because the individuals with bone mass in this range are a high number [3]. Thyroid hormones excess the rate of basal metabolic, affect the synthesis of protein, assist to long bone growth regulation (growth hormone synergy with it), uptight maturation, and increase the sensitivity of the body to catecholamine's, these hormones also arrange fat, protein, and metabolism of carbohydrate [4]. Thyroid problems are significantly more common in women, in the time leading up to menopause, estrogen levels fall significantly, which would undoubtedly affect thyroid levels [5]. The osteoporosis associated with thyroid function for immediate effects of TSH on both components of osteoblastic bone formation, osteoclastic bone resorption, and skeletal remodeling, with move a role for TSH as

Ibn Al-Haitham Journal for Pure and Applied science https://doi.org/10.30526/2021.IHICPAS.2650

a molecular single switch in the independent control of both bone resorption and formation [6]. The relationship between osteoporosis and thyroid is important by of the skeleton bones in the existence of normal thyroid hormone circulating and concentration of TSH to reduced bone mineral loss in osteoporosis patients, also researcher derives that thyroid hormone standard and TSH increased bone resorption, with rising mineral bone deposition [7].

2. Materials Method

This study was conducted between February 2019 to November 2019 in Basra province / Iraq to include (110) women referring from rural and urban placing, (68) of them considered osteoporosis women while (42) determined as healthy. The age between (55-75) years old and weighing between (50-70 kg) while the length of this patient about (145-165 cm). Those patients visited al Zahraa clinic in Ibnalbetar private hospital to quantum the density of bone mineral by measure the hips and lumbar spine density using Lunar Prodigy (version 16) a dual-energy x-ray absorptiometry (DEXA) from (USA). According to the WHO criteria the patients are divided into normal, osteopenia, and osteoporosis, also the main outcome measure is low bone mineral density (T-score).

2.1. Human Models

The women are divided into two groups according to age and residing of housing status:

- (43) Women age between (55-75) years old residing in urban and this category are subdivided into two categories: (15) Healthy patients, (28) Osteoporosis patients.
- (67) Women age between (55-75) years old residing in rural, also subdivided into two subgroups: (31) Healthy patients, (36) Osteoporosis patients.

2.2. Dual Energy X-ray Absorptiometry

The technique of choice to diagnose osteoporosis and to monitor the response to treatment is called (DXA, DEXA) Dual-energy X-ray absorptiometry **Figure (1)**. It is considered a useful for also body composition measuring. The (WHO) known as World Health Organization has assign criteria for assessing the risk of fracture after diagnosis of osteoporosis by employ DXA screening, bone mineral density value at the hip or spine that is above 2.5 SDs under the optimal average health young people of the same perspiration and genus clarifies individuals have osteoporosis (T- score $\leq$ -2.5) [8].

Figure 1. Dual-energy X-ray absorptiometry.

2.3. Sample Collection

Ibn Al-Haitham Journal for Pure and Applied science https://doi.org/10.30526/2021.IHICPAS.2650

After diagnosing the disease by using a DEXA machine, four milliliters of venous blood sample was drawing from each patient. Also, blood samples were collected from healthy persons. Blood transfused into a disposable gelatin tube, left at room temperature for at least 30 minutes for clotting, centrifuged (3500 r/m for 10 minutes) then the produced serum was removal into the special tube and stored at (– 20 ºC) unless used directly.

2.4. Measurement of Thyroid Hormone

For the determination of thyroid hormone (TSH, T3, T4) the modern VIDAS automated quantitative device, these trials were examined in a specialist laboratory according to the methods which assay by using the Enzyme-Linked Fluorescent Assay (ELFA) technique to plasma or serum [9].

2.5. Statistical Analysis

According to SPSS16 program in the computer, the Analysis of variance table (ANOVA) was used in this study, and then the Least Significant Differences test (L.S.D) was used to determine the significant differences among the categories at a significant level ($p \leq 0.05$).

3. Results

Thyroid hormones in healthy and osteoporosis women aged between (55-75) years old. The results in **Table (1)** clarify a decrease ($p \leq 0.05$) in thyroid hormones TSH, T3, T4 in women who suffers from osteoporosis disease compared with healthy women.

Table 1. Thyroid and growth hormone in healthy and osteoporosis women (mean ± SD).

Hormones	Healthy women (n=46)	Osteoporosis women (n=64)
TSH (mic. IU/ml)	3.43 ± 1.33	*2.02 ± 0.38
T3 (nmol/L)	1.89 ± 0.64	*0.48 ± 0.42
T4 (nmol/L)	81 ± 5.31	*62 ± 6.08

*Indicates significant changes at the level of probability ($p \leq 0.05$) compared with healthy women

3.1. Thyroid hormones in healthy and osteoporosis women aged between (55-75) years old living in (urban).

The results in **Table (2)** show the changes in thyroid hormones which include a significant decreased ($p \leq 0.05$) in all criteria for women with osteoporosis disease compared to women from the healthy group and residents in the urban.

Table 2. Thyroid hormones in healthy and osteoporosis women living in (urban) (mean ± SD).

Hormones	Healthy women (n=15)	Osteoporosis women (n=28)
TSH (mic. IU/ml)	3.38 ± 1.37	*1.95 ± 0.44
T3 (nmol/L)	1.85 ± 0.64	*0.43 ± 0.36
T4 (nmol/L)	80 ± 5.79	*61 ± 4.35

* Indicates significant changes at the level of probability ($p \leq 0.05$) compared with healthy women.

3.2. Thyroid hormones in healthy and osteoporosis women aged between (55-75) years old and living in (rural).

The results in **Table (3)** show a decrease ($p \leq 0.05$) in thyroid hormones (TSH, T3, T4) in women with osteoporosis disease who is living in the rural areas compared with healthy women living in the same area.

Table 3. Thyroid hormones in healthy and osteoporosis women living in (rural) (mean ± SD).

Hormones	Healthy women (n=31)	Osteoporosis women (n=36)
TSH (mic. IU/ml)	3.48 ± 1.30	*2.10 ± 0.42
T3 (nmol/L)	1.93 ± 0.64	*0.53 ± 0.43
T4 (nmol/L)	81 ± 5.02	*63 ± 4.79

*Indicates significant changes at the level of probability ($p \leq 0.05$) compared with healthy women.

4. Discussion

Data of our study suggested a significant decrease in thyroid hormonal levels in osteoporosis women which include TSH, T3, T4 compared with healthy women in the same age. Also, results showed changes but not significant between housing status of osteoporosis women compared with control women in the same area. The functions of the thyroid have prevalent systemic semblance include effect metabolism of bone mineral contain a clinical disease have received enormous solicitude from scientist through the bygone century with be the paramount cause of secondary osteoporosis [10]. Thyroid hormone is required for regulates bone turnover and mineralization in adults, these results suggested that osteoporosis women have decreased in thyroid hormones may be due to that mechanism of T3-action in bone include receptors of T3 which expressed in growth plate chondrocytes and osteoblasts, that represent T3 primary target cells of the skeleton and increase the resorption of osteoclast-mediated bone leading to loss of bone density [11, 12]. Furthermore, (TSH) act a significant role in the metabolism of bone by rising bone bulk and recover microarchitecture for bone and intensity at least partially by osteoclastogenesis restrain [13]. The hormones of the thyroid include catabolic direct effect on homeostasis mineral bone, the inhibition in these hormones due to excess resorption of mineral bone, and calcium deprivation through kidneys which consider a basic reason for cause major abnormality in mineral bone density of osteoporosis patients [14, 15]. In addition, TSH, T3, T4 restrain bone lack and catalyze the formation of bone by preventing osteoclast activity, also TSH has stimulated the formation of bone osteoblast target receptors by motivating osteoblastogenesis, likewise, animate osteoblasts to make osteoprotegerin (OPG) production that reduces osteoclastic resorption for maintaining the health of bone [16]. The results of our study found that thyroid hormones are associated with abnormalities in the markers of bone turnover and density of mineral bone, osteoporosis women have a decrease in TSH, T3, T4 hormones with effect in bone turnover by a role in the maintenance of osteoblast cell and prevent loss bone density [17]. On the other hand, the role of estrogen levels affects thyroid receptors, these receptors are the molecules that allow thyroid hormones to enter cells when estrogen levels decrease they might affect this receptor and lead to a decrease in thyroid hormones [18].

5. Conclusion

The osteoporosis women have significant changes in thyroid hormones compared with healthy women in Iraq / Basra province.

References

1. Nguyen, J.R.; Schneider, D.; Sambrook, P.N., Eisman, J.A. Mortality after all major types of osteoporotic fractures in men and women: an observational study. *Lancet* **2009**, *353*, 878.

2. Kanis,J.A. Assessment of fracture risk and its application to screening for postmenopausal osteoporosis: synopsis of a WHO report. *Osteoporosis Int*. **2013** ,*4*, 368.
3. Johnell, O.; Kanis, J.A. An estimate of the worldwide prevalence and disability associated with osteoporotic fractures. *Osteoporosis Int*. **2016** ,*17*, 1726.
4. Grozinsky, S.; Fraser, A.; Nahshoni, E.; Weizman, A .; Leibovici, L. Thyroxine-triiodothyronine combination therapy versus thyroxine monotherapy for clinical hypothyroidism: meta-analysis of randomized controlled trials. *J. Clin. Endocrinol. Metab*. **2016** ,*91*, 2592.
5. Jacobson, M.H.; Howards, P.P.; Darrow, L.A. Thyroid hormones and menstrual cycle function in a longitudinal cohort of premenopausal women. *Paediatr. Perinat. Epidemiol*. **2018** ,*32*, 225.
6. Marians, R.C.; Yu, W.; Wu, X.B.; Ando, T.; Li. Y.; Zaidi, M. TSH is a negative regulator of skeletal remodeling. *Cell* **2013** ,*115*, 151.
7. Bassett, J.H.; Oshea, P.J.; Rabier, B.; Boyde, A.; Howell, P.G.; Weiss, E. Thyroid hormone excess rather than thyrotropin deficiency induces osteoporosis in hyperthyroidism. *Mol. Endocrinol.* **2015** ,*21*, 1095.
8. Vondracek, S.F.; Linnebur, S.A. Diagnosis and management of osteoporosis in the older senior. *Clin. Interv. Aging*. **2009** ,*4*, 121.
9. Freidberg, A.; Baldach, C.; Mestre, B.; Smadja., V.; Morel, F. Vidas TSH3 (bioMerieux): Approche analytic performance diagnostic thyroid panel Immuno-anal. *Biol. Specialisee* **2001** ,*14*, 339.
10. Dinesh, K. Thyroid disorders and bone mineral metabolism. *Indian J. Endocrinol. Metab*. **2011** ,*15*, 107.
11. Williams, G.R. Thyroid hormone actions on bone and growth. *Endocr. J.* **2002** ,*4*, 51.
12. Tsai, K.S.; Lai, S.M.; Huang, K.M.; Chieng, P.U.; Su, C.T.; Chen, F.W. Decreased bone mineral density in patients with prolonged thyrotoxicosis before and after treatment. *J. Formos Med. Assoc*. **2015** ,*90*, 250.
13. Zhang, W.; Zhang, Y.; Liu, Y.; Wang. J. Thyroid-stimulating hormone maintains bone mass and strength by suppressing osteoclast differentiation. *J. Biomech*. **2014** ,*47*, 1307.
14. Dhanwal, D.K.; Kochupillai, N.; Gupta, N.; Cooper, C. Dennison, E.M. Bone mineral metabolism and bone density in hypothyroidism. *J. Clin. Densitom*. **2010** ,*13*, 462.
15. Mosekilde, L.; Christensen, M.S. Relationship between serum parathyroid hormone, calcium phosphorus metabolism and thyroid function. *Acta Endocrinol. (Copenh)* **2016** ,*84*, 566.
16. Baliram, R.; Latif, R.; Berkowitz, J.; Frid, S.; Colaianni, G.; Sun, L. TSH acts directly on osteoblasts to increase bone production. *J. Bone Key Rep*. **2012** ,*1*, 16.
17. Fairfield, W.P.; Sesmilo, G.; Katznelson, L.; Pulaski, K.; Freda, P.U. Effects of a thyroid hormones and growth hormone receptor antagonist on bone markers. *Clin. Endocrinol. (Oxf)*. **2012**, *57*, 385.
18. Mochizuki, Y.; Shacha, N.; Aborey, Y.; Mollen, T. Correlation between thyroid hormone and biomarkers of bone metabolism in postmenopausal women. *Hormone Res*. **2016** ,*66*, 236.

Ibn Al-Haitham Journal for Pure and Applied science https://doi.org/10.30526/2021.IHICPAS.2651

The Effect of Cigarette Smoking on Serum Liver Enzymes in Baghdad

Wasan Qasim Turki
wasan.turki@almustafafauniversity.edu.iq
Department of Medical Laboratory Techniques, Al-Mustafa University College, Baghdad, Iraq.

Abstract

Smoking is the most noticeably horrible human conduct; it is rehearsed by individuals dependent on nicotine numerous hurtful sicknesses, for example, cancer and liver disorder are brought about by smoking cigarettes. So this study aimed to study some of the liver function represented by the enzymes aspartate aminotransferase (AST or GOT) and alanine aminotransferase (ALT or GPT) in smokers and non-smokers for 50 persons in a group consists of 25 smokers and 25 non-smokers of different ages and to study the effectiveness of cigarette smoking on liver enzymes by checking the secretion of (AST) (35.84± 4.1)U/ 1 (ALT)(51.08±7.286) U/1($p<0.05$) relative to non-smokers were significantly correlated with heavy cigarette smoking.

Keywords: Smokers, Liver enzyme, Cigarette, Tobacco.

1. Introduction

Many diseases are caused by Smoking, and because of the risk of smoking, one person dies in the world per six minutes [1]. More than 4000 chemicals are present in tobacco smoke [2] and various hazardous substances like nicotine, free extremists, carbon monoxide, and other gaseous materials are submitted to a cigarette smoker [3]. That can lead to various degenerative pulmonary cardiovascular diseases and cancer. Cigarette smoking has been embroiled as a huge danger factor for the tobacco smoke contains various mixes, huge numbers of which are oxidants and favorable to oxidants fit for creating free extremists and improving the oxidative stress in vivo [4] (Preston, 1991). The liver, which has several duties, is an essential organ. The liver is responsible, among other things, for removing narcotics, alcohol, and other toxins from the body to remove them. The liver is one of the organs that are not directly affected by smoking so Heavy smoking creates toxins that stimulate necroinflammation and rise the dangerousness of hepatic lesions (fibrosis and activity scores) that related to hepatitis C virus (HCV) or hepatitis B virus (HBV) infection [5, 6]. Three main adverse effects on the liver are caused by smoking: direct or indirect harmful impact, immunological effects, and tumorigenesis effects. Smoking can cause a Direct toxic effect when produced chemicals with the potential for cytotoxicity [7]. Some Chemicals caused by smoking lead to oxidative stress linked to lipid peroxidation [8, 9]. Where it stimulates the production of stellar cells and the growth of fibrosis. Cigarette smoke also helps in the production of pro-inflammatory cytokines that are related to liver cell damage (IL-1, IL-6, and TNF-alpha) [10]. Heavy cigarettes are related to carboxyhaemoglobin and lowered ability of red blood cells (RBC) to carrying oxygen, contributing to tissue hypoxia. Hypoxia promotes the development of erythropoietin, which causes bone marrow hyperplasia. This leads to the production of secondary polycythemia, which in turn increases the mass and turnover of red cells. This enhances catabolic iron resulting from both old red blood cells and iron produced

from elevated red cell destruction associated with polycythemia [11, 12]. In addition, erythropoietin promotes iron absorption from the intestine. Both elevated catabolic iron and high iron absorption lead to its concentration in macrophages over time and then in hepatocytes, inducing oxidative stress in hepatocytes [13]. Subsequently, the reason for this examination is to inspect the differences of liver enzymes among smokers than non-smokers in males and clarify the negative impacts of tobacco when smoking for long periods and the extent of its impact on the liver.

2. Materials Method

Blood samples are taken during February from (50) healthy male subjects in Baghdad, Al-Rusafa whose ages ranged from 20 to 55 years of age and divided into two groups, with 25 smoking persons and 25 non-smoking persons with varying smoking durations in the second group. We had to make sure that the volunteer had no illness before taking the sample to prevent cases that could rise liver enzyme secretion and interfere with the results of our study. The two groups (smoking persons and non-smoking persons) were chosen at close ages to be appropriate for the statistical study. People under the test are divided into smokers (who are smoking more than (20) cigarette daily) (n=25) and non-smokers (n=25). 5.0 ml of blood were taken from each participant, and this 5.0 ml of venous blood were drowning by venipuncture using antiseptic for the skin (70%alcohol), and then the samples placed in a heparinized tube, after that we made centrifugation to the blood samples at about three thousand, then the enzymes AST and ALT were estimated. In current experiments used ABBOTT C4000 Chemistry Analyzer to detect AST and ALT. To determine substantial differences and all the differences, the statistical assessment was carried out by statistical package for social sciences (spss) 26.0 and found the significant differences between the values (Mean± SEM) of the test and the control groups, t-test (at $p<0.05$) was applied.

3. Results and Discussion

The results showed that high concentrations of aspartate aminotransferase (AST or GOT) and alanine aminotransferase (ALT or GPT) compared to non-smokers $p<0.05$ (**Table 1**) were significantly associated with heavy cigarette smoking (ALT).

Table 1. Concentrations AST and ALT enzymes of smokers compared with non-smoker.

Parameters	Smoking N= 25	Non-smoking N= 25	P-value	Significant p<0.05
AST or GOT (U/I)	35.84±4.1	19.20±1.534	0.006	S*
ALT or GPT (U/I)	51.08±7.286	25.72±1.837	0.001	S*

*S= Significant

Figure (1) and **Figure (2)** show that both AST and ALT have a higher level in smokers if we compare them with non-smokers where ($p<0.05$). According to the results in **Figure (1)**. Height of the concentrations of aspartate aminotransferase (AST or GOT) and alanine aminotransferase (ALT or GPT) because of the intensity of tobacco smoke and its harmful substance affected on liver cells, prompting the emission of liver enzyme (AST) and (ALT) through inflammatory pathways or exacerbating the pathogenic effects of other compounds on

Ibn Al-Haitham Journal for Pure and Applied science https://doi.org/10.30526/2021.IHICPAS.2651

the liver [14]. Furthermore, that may occur due to nitrosative stress, which is a disorder that arises when the processing of chemicals containing highly reactive, such as nitrous oxide, exceeds the human body`s capacity to neutralize and remove them. Nitrosative stress able to run the reactions that convert the structure of proteins so interfere with normal body functions [15, 16]. Cigarette smoke contains a large number of hepatotoxic chemicals, like nicotine [7].

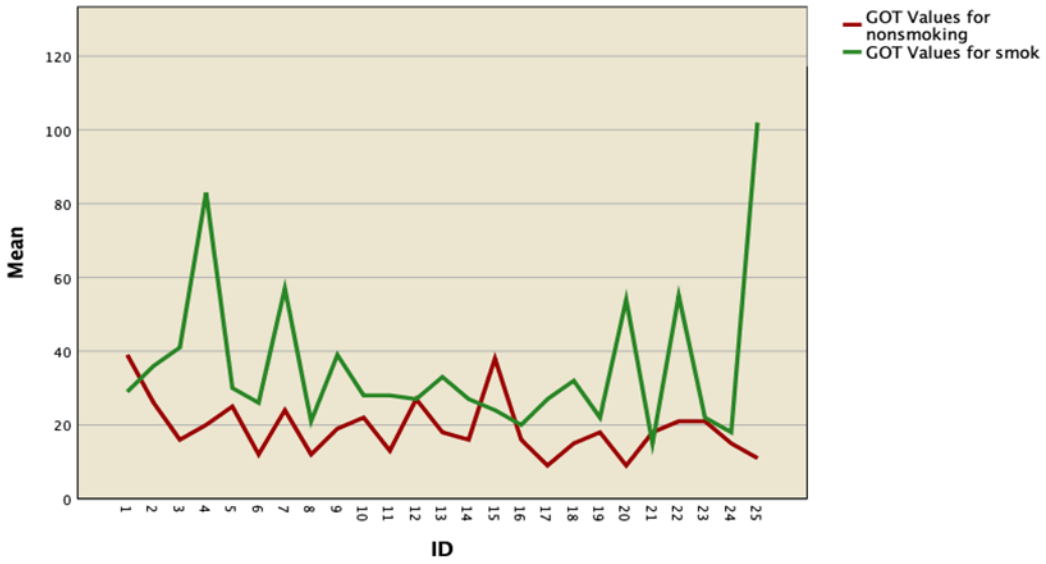

Figure 1. Concentrations (AST or GOT) enzymes of smokers compared with non-smoker.

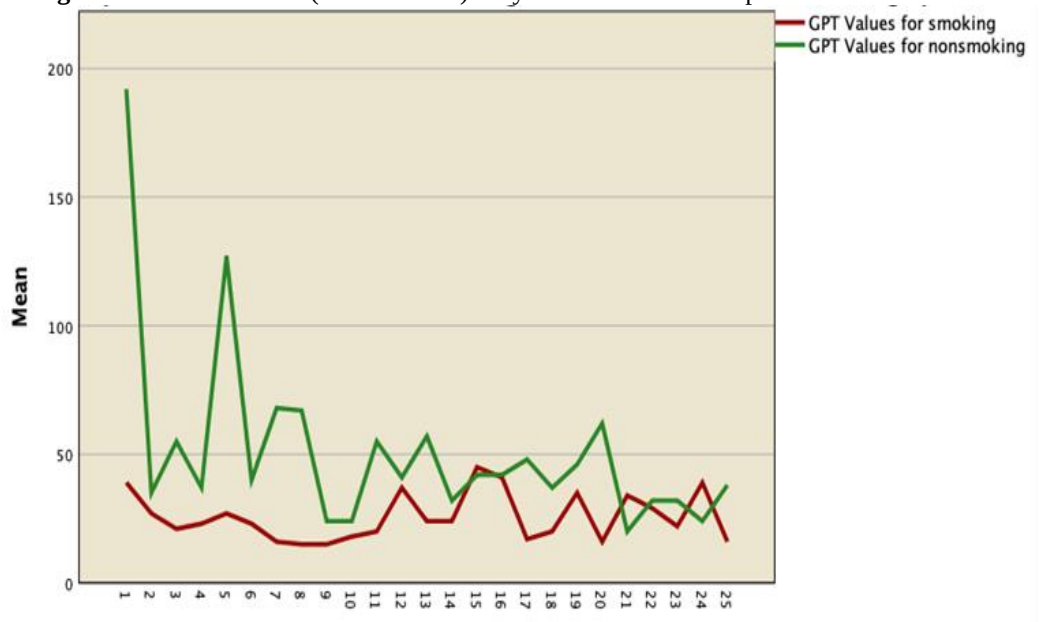

Figure 2. Concentrations (ALT or GPT) enzymes of smokers compared with a non-smoker.

Important changes in the activity concentrations of AST and ALT liver enzymes in smokers relative to non-smokers, and increases in proportion to the duration of smoking. So the liver enzymes AST and ALT in which increased due to exposure to smoke or duo to release a high level of the cellular oxidative radicals as reported in [17, 18]. The enzyme that is important for producing energy is alanine aminotransferase (ALT or GPT), this enzyme is found in the liver and other tissues besides the liver but in fewer concentrations than its

concentration in the liver, it is found for example in the heart and the skeletal muscles. In comparison to other liver enzymes can be used to diagnose liver diseases, such as in the diagnosis of hepatitis and cirrhosis [19].

4. Conclusion

The results show that cigarette smoking has an effect on the liver function that is expressed in the amount of liver enzyme secretion in the blood serum, so smoking can affect liver functions by affecting the secretion of AST and ALT liver enzymes, causing liver injury in the community of smokers compared to non-smokers. shows that the level of AST and ALT enzymes are higher in cigarette smokers when we compare them with non-smokers, and this may be related to the effect of smoking on the liver.

References

1. Mathers, C.D.; Loncar, D. 2006 Projections of global mortality and burden of disease from 2002 to 2030. *PLoS Med*. **2006**, *3*, e442.
2. Yeh, C.C.; Barr, R.G.; Powell, C.A.; Mesia-Vela, S.; Wang, Y.; Hamade, N.K.; Austin, J.H.; Santella. R.M. No effect of cigarette smoking dose on oxidized plasma proteins. *Environ. Res*. **2008** *106*, 219.
3. Aula, F.A.; Qadir, F.A. Effects of cigarette smoking on some immunological and hematological parameters in male smokers in Erbil city Jordan. *J. Biol. Sci*. **2013**, *147*, 1.
4. Preston. A. 1991. Cigarette smoking-nutritional implications. *Progr. Food Nut. Sci*. **1991** *15*, 183.
5. Pessione, F.; Ramond, M.J.; Njapoum, C.; Duchatelle, V.; Degott, C.; Erlinger, S.; Rueff, B.; Valla, D.C.; Degos, F. Cigarette smoking and hepatic lesions in patients with chronic hepatitis C. *Hepatology*, **2001,** *34*, 121.
6. Yu, M.-W.; Hsu, F.-C.; Sheen, I.-S.; Chu, C.-M.; Lin, D.-Y.; Chen, C.-J.; Liaw. Y.-F. Prospective study of hepatocellular carcinoma and liver cirrhosis in asymptomatic chronic hepatitis B virus carriers. *Am. J. Epidemiol*. **1997,** *145*, 1039-1047.
7. Yuen, S.T.; Gogo, Jr. A.R.; Luk, I.S.; Cho, C.H.; Ho, J.C.; Loh, T.T. The effect of nicotine and its interaction with carbon tetrachloride in the rat liver. *Pharmacol. Toxicol*. **1995**, *77*, 225.
8. Husain, K.; Scott, B.R.; Reddy, S.K.; Somani, S.M. Chronic ethanol and nicotine interaction on rat tissue antioxidant defense system. *Alcohol* ,**2001,** *25*, 89.
9. Watanabe, K.; Eto, K.; Furuno, K.; Mori, T.; Kawasaki, H.; Gomita, Y. 1995 Effect of cigarette smoke on lipid peroxidation and liver function tests in rats. *Acta Medica Okayama*, **1995,** *49*, 271.
10. El-Zayadi, A.R. Heavy smoking and liver. *World J. Gastroenterol.* WJG 2006, *12*, 6098.
11. Young, C.J.; Moss. J.Smoke inhalation: diagnosis and treatment. *J. Clinical Anesth*. **1989** *1*, 377.
12. Heimbach, D.M.; Waeckerle, J.F. Inhalation injuries. *Ann. Emerg.Med*. **1988**, *17*, 1316.
13. Gutteridge, J.M.; Halliwell, B. Iron toxicity and oxygen radicals Bailliere's. *Clin. Haematol*. **1989,** *2*, 195.
14. Farsalinos, K.E.; Romagna,G.; Allifranchini, E.; Ripamonti, E.; Bocchietto, E.; Todeschi, S.; Tsiapras. D.; Kyrzopoulos. S.; Voudris. V. 2013 Comparison of the cytotoxic potential of cigarette smoke and electronic cigarette vapour extract on cultured myocardial cells. Int. J. Environ. *Res. Public Health* **2013** *10*, 5146.
15. Chakraborty, A.; Selvaraj, S. Differential modulation of xenobiotic metabolizing enzymes by vanadium during diethylnitrosamine-induced hepatocarcinogenesis in Sprague-Dawley rats. *Neoplasma* ,**2000,** *47*, 81.

16. Padmavathi, P.; Reddy, V.D.; Varadacharyulu, N. Influence of chronic cigarette smoking on serum biochemical profile in male human volunteers. *J. Health Sci*. **2009,** *55*, 265.
17. Abdul-Razaq, S.N.; Ahmed, B.M. Effect of cigarette smoking on liver function test and some other related parameters Zanco. *J. Med. Sci*. **2013,** *17*, 556.
18. Dhahir, N. K.; Noaman, A. A. 2017. Study effect of cigarette smoking on the liver functions and electrolytes. *Iraqi J. Sci*. **2017** ,*58*, 211-215.
19. Aubin, H.J.; Rollema, H.; Svensson, T.H.; Winterer, G. Smoking, quitting, and psychiatric disease: a review Neurosci. *Biobehav. Rev.* **2012** ,*36*, 271.

Ibn Al-Haitham Journal for Pure and Applied science https://doi.org/10.30526/2021.IHICPAS.2652

Gene Expression of MicroRNA-370 in Some Iraqi Women with Breast Cancer

Wafaa Sabri Mahood
wafa.sabry@yahoo.com
Department of Biology, College of Education for Pure Science, University of Baghdad, Baghdad, Iraq

Maryam Jasim Hasan
meryamej526@yahoo.com
Department of Biology, College of Education for Pure Science, University of Baghdad, Baghdad,

Mohammed Jasim Mohammed
mohamed.jasim.mj@gmail.com
Kindy Hospital, Baghdad, Iraq

Abstract

Breast cancer becomes a major threat to female health, many reports refer to a high incidence of breast cancer in Iraq; especially, in the last years. The micro RNA-370 molecules have not been reported in Iraqi cancer patients. Our objective in this study was to identify the expression of micro RNA-370 molecules in breast cancer patients as an early detection biomarker of breast tumors and detect its relation with clinicopathological characters of breast cancer patients. Fifty fresh tissue samples were collected from benign and malignant breast patients in addition to ten normal tissue samples collected as a control group, the age ranged was(19 - 77) years for patients. The miR-370 gene expression level was measured by the quantitative real-time reaction (qRT-PCR). Our results demonstrate a high expression of-miR370 in benign and malignant tissues. The miR-370 expression level was inversely correlated with the age of the patients. It was a significant relation of miR-370 gene expression on the left side of breast malignant (p- 0.05). In conclusion, significantly associated with high miR-370 expression were found depending on age, tumor location, tumor type, and stage of differentiation. The upregulation of miR-370 gene expression in benign lesions and breast cancer tissue can be applied as a biomarker for early breast cancer detection.

Keywords: Gene Expression, microRNA-370, Breast Cancer, Benign, Iraq, qRT-PCR.

1. Introduction

Breast cancer is the second leading cause of death among women worldwide. It is the most common tumor in the United States, accounting for 14% (1.68 million) of all newly diagnosed cancers, about 40.290% of all deaths from cancer [1]. It is the most prevalent tumor among females in Iraq and it is diagnosed at advanced stages among young women causing short survival, making it a great challenge facing public health in Iraq and the world [2]. Breast tumors are a heterogeneity disease, and its diagnostic and clinical findings are widely divergent and biomarkers or diagnostic methods that are used to predict breast tumors may be of limited use [3]. The microRNAs are small uncoded molecules of RNAs consisting of 18-25 nucleotides. They regulate gene expression by partial matching with untranslated region 3 '(UTR), form RNA Induced Silencing Complexes (RISCs) to lyses the target mRNAs or inhibit their translation respectively. They also provide a rapid mechanism to regulate the gene expression of a large number of genes [4,5]. Previous studies have suggested that microRNAs play a vital role in the growth and development of breast cancer. The miRNAs

may act as diagnostic biomarkers for early detection [6,7]. Different level of several miRNA expressions between normal and malignant tissues was observed in different tumor subtypes of breast cancer and age groups in Tsai et al., study. They are found down-regulated of miR-335 and miR-145 while up-regulated expression was detected in miR-21, miR-200a, miR-200c, and miR-141 for all patients [8]. Quan et al. also reported up-regulated miR-206 and down-regulated miR-145 in breast cancer tissues, which may indicate the prognosis effect of miRNA in patients [9]. A recent study showed that measured miRNA profiles in blood facilitate early detection and less-invasive diagnosis of aggressive type triple-negative breast cancer [10]. One of the rare studies that investigated the miRNA370 in breast cancer is the Iranian study and which was performed by Mollainezhad and his colleagues. They refer to up-regulation (six-fold higher) of miR-370 in breast cancer tissue compared with the normal adjacent tissue. Patient characteristics like stage III, larger tumor size, invasive ductal type, and other features showed a significantly high level of expression in miR-370, suggesting that miR-370 may have an onco-miRNA role. It may be helpful as a diagnostic biomarker and therapeutic if detect its action targets [11]. Another study suggests that miR-370 is associated with gastric carcinoma progression by down-regulating of transforming growth factor -β receptor II(TGFβ-RII) and it may be considered as onco-miRNA [12]. Although it has different targets, miR370 - could have an essential role in the reduction of colorectal cancer tumorigenesis by independently targeting epidermal growth factor receptor (EGFR) and PIK3CA via overexpression of miR-370. They cause suppression of the important molecules of the PI3K/AKT/mTOR pathway which is important in most cancer cell characteristics as proliferation, migration, and invasion [13]. The tumor suppressor role of miR-370 also was found in osteosarcoma cells and human prostate cancer as miR-370 could directly target the 3' UTR of FOXM1and FOXO1 genes [14.15]. The protein encoded by these genes is a member of the FOX family of transcription factors [16].miR-370 enhanced endometrioid ovarian cancer cell chemosensitivity tocisplatin (CDDP) as well as acts as a tumor suppressor in endometrioid ovarian cancer cells [17]. In a recent study (published in 2018) the miR-370 encoded gene stimulated apoptosis in the colon cells with a direct effect on mouse double minute-4 (MDM4). The miR-370 expression was low in the tumor tissue and the expression of miR-370 was linked conversely to the stages of the disease. The higher progression of the disease, the lower level of miR-370 expression. These results suggest a new biomarker in the diagnosis and treatment of colorectal tumors based on the miR-370 molecules [18]. The current study was aimed to identify miR-370 expression as a biomarker in some patients of Iraqi women with breast cancer and its relation with clinicopathological characters.

2. Materials Method

2.1. Patient tissue specimens

The samples were obtained from breast tumor patients who underwent to the Medicine city Hospital in Baghdad and private laboratories from October 2017 to April 2018. All received chemotherapy or radiotherapy patients were excluded. Fifty tissue samples were collected, including 25 tissue samples from each benign and malignant breast cancer patient, besides ten samples from normal tissue were used as a control group. The age range of patients and control group (19-77) years and (22-76) years respectively. The samples were stored in the

deep freeze until RNA extraction. The approval by the Ethics Committee of the Ministry of Health in Iraq and Baghdad University was obtained to conduct the research.

2.2. The miR-370 Expression Analyses

Total RNA was extracted from tissue samples using (miRNeasy Mini Kit) (QIAgen, Germany) (Cat No. /ID: 217004) according to the manufacturer's procedure. The miScript II RT kit and HiSpec buffer (QIAgen Germany) (Cat No. /ID: 218161), were used to syntheses for total RNA reverses transcribed. The total volume of reaction was 10 µl including (2µl 5x miScript HiSpec Buffer, 1µl of 10x miScript Nucleics Mix, 4µl of RNase-free water RNase, 1µl of miScript Reverse Transcriptase Mix and 2µl of Template). Final cDNA samples were stored at a -20°C. The expression level of miR-370 gene was detected by RT-qPCR technique using the master mix miScript SYBR Green PCR (QIAgen) kit (Cat No. /ID: 218073). The relative amount of miR-370 was normalized against U6 small nuclear (sn) RNA (as an internal control). The primers used for qRT-PCR reactions as described by Saberi et al., for U6 [19] and Mollainezhad et al., for miR-370 [11] (**Table 1**). All primers were purchased from (Alpha DNA Company, Canada). The total volume of qRT-PCR reaction was 10 µl and it contained 5µl master mix, 1 µl for each forward and reverse primers, 2 µl RNase free water, and 1 µl of cDNA template. The PCR condition was 95°C for 10 minutes, followed by 40 cycles at 95°C for 15 seconds for denaturation then 20 seconds at 55°C for annealing, finally 30 seconds at 72°C. The threshold cycle (Ct) is described as the cycle number at which the fluorescence level will pass into the assumed threshold. To analyze miR-370 expression, the fold-change of gene expression between cancer tissues and normal breast tissue control was calculated by the $2^{-\Delta\Delta Ct}$ method, in which $\Delta\Delta Ct = (Ct miR\text{-}370 - Ct U6\ snRNA)$ mean tumor-(CtmiR-370 – CtU6 snRNA) means normal. The relative expression levels of miRNAs in cancer compared to normal tissue (control group) were selected and calculated using the method of $2^{-\Delta\Delta Ct}$ [20].

Table 1. Sequence-specific primers of qRT-PCR reactions.

Molecule	Sequences
MicRNA-370 (Forward)	5'-GCCTGCTGGGGTGGAACCTGGTAA-3'
MicRNA-370 (Reverse)	5'- GCGAGCACAGAATTAATACGAC-3'
U6snRNA (Forward)	5'-CTCGCTTCGGCAGCACA-3'
U6snRNA (Reverse)	5'-AACGCTTCACGAATTTGCGT-3'

2.3. Statistical analysis

Differences in the mean between miR-370 expression in the sample of the breast (benign and malignant) and control group. As well as the relation of miR-370 expression with clinical parameters was analyzed using χ^2 and Student's t-test. All tests were performed using SPSS 16 and a $P<0.05$ was supposed to be statistically significant.

3. Results and Discussion

3.1. Patients clinical characteristics

Clinical characteristics of breast cancer patients such as tumor type, grade, differentiation, and tumor site are shown in (**Table 2**). The study group consists of 50 patients including 25 breast benign lesion patients with an average age of 34 years range (19-57) years and 25 breast cancer patients with an average age of 50 years, range (35-77) years. Also, ten normal samples with 38 years of age means were used as the control group. Depending on

Ibn Al-Haitham Journal for Pure and Applied science https://doi.org/10.30526/2021.IHICPAS.2652

age, 52% (13/25) of females less than fifty years, no significant difference was identified between the groups regarding ages (P=0.325). There was a high rate of (80% (20/25) of patients enrolled in this study with invasive carcinoma. According to tumor grade, 48% and 36% were grade 1 and grade 2 respectively. While 84% of patients were recorded with a moderately differentiated tumor.

Table 2. Clinical characteristics of patients with breast malignancies.

Characteristics of patients with cancer	Number	Percentage%
Total number of patients	25	100
Average age 50		
<50	13	52
> 50	12	48
Type of tumor		
Lobular carcinomas	2	8
Ductal carcinomas	3	12
Invasive carcinomas	20	80
Grade		
Grade I	12	48
Grade II	9	36
Grade III	4	16
Differentiation		
Moderately	21	84
Well	4	16
Poorly	0	0
Tumor site		
Left	10	40
Right	10	40
Un known	5	20

3.2. The miR-370 expression level in breast benign lesions

The study was conducted to investigate the miR370 expression levels in breast benign and malignant tumors compared with normal breast tissues. The PCR products were pure and homogeneous; indicating by melting curves of miR-370, they are showed as sharply defined melting curves with narrow peaks (**Figure 1**). Expression of miR-370 in 25 breast benign patients (breast lesion) was detected, the results showed an increase of fold miR-370 expression in those patients. The mean of fold expression was 8.2 in comparison with 1.6 means for normal tissue with standard error (Mean±SE- 9.38±4.32) with significant differences were found depending on age (P=0.047) in breast lesion. There was a high expression level of miR-370 in the right site, the mean of fold expression was 11.38 (SE 1.6±0.805) while no significant differences depending on the site of breast benign were found (P=0.2).

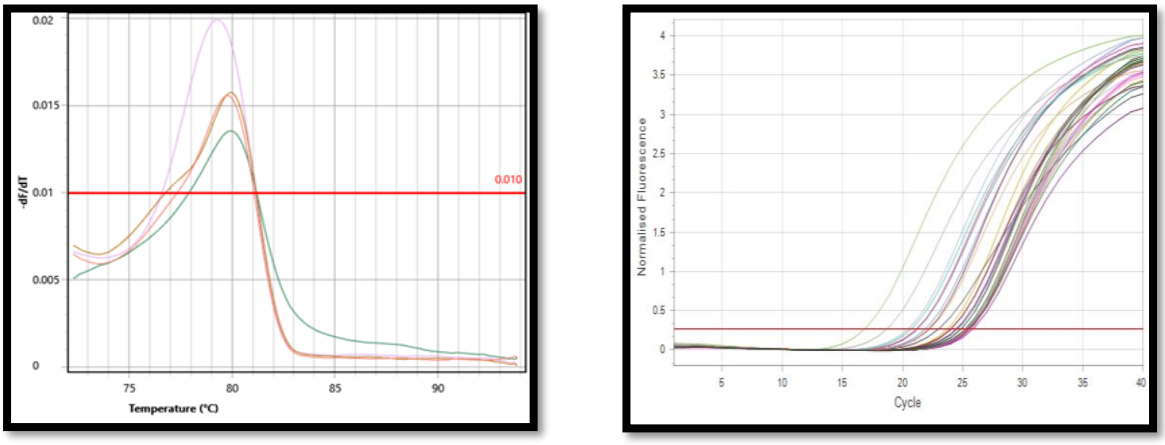

A **B**

Figure 1. (A) Melting Curves (B) Cycling Curves of miR-370.

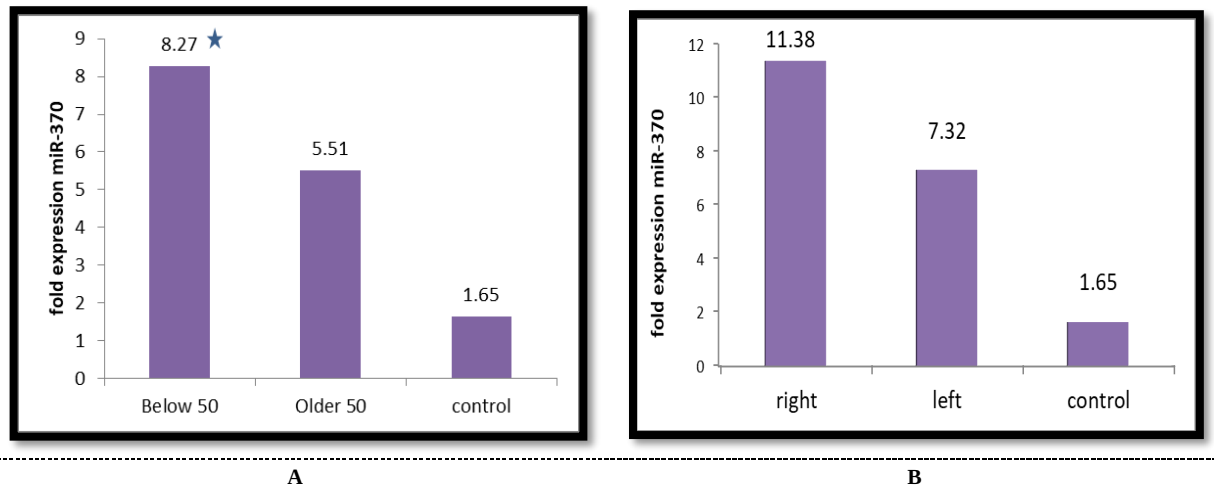

A **B**

Figure 2. Gene expression of miR-370 in benign tumors (A) High level of miR-370 expression in age below 50 years depending on age (*) significant difference ($p \leq 0.05$), (B): High level of miR-370 expression in right and left site depending on location compared with control group.

3.3. The miR-370 expression level in breast cancer patients

The fold expression level was increased by 8.56 in less than fifty years old patients. In the older 50 years of patients, the fold expression level was 2.61 compared with the fold expression level of control samples at 1.65. It was observed that the significant difference between the control group and patients with age of fewer than 50 years (P= 0.03) was (SE -6.91± 2.92). Whilst the significant difference between the younger and older ages of 50 years (P = 0.05), it was (SE 5.01± 2.45) compared to (1.61±0.805) for the control group, **(Figure 3. A)**. Concerning the tumor site, the fold expression level of the miR-370 was 5.46 and 3.81 on the left and right side respectively compared to the fold expression of the control samples by 1.65. There was a significant difference between the left group and the control group (P = 0.05) (-4.53±2.12) **(Figure 3. B)**. Other tumor characteristics like tumor type and tumor grade are summarized in **(Figures 3. C and D)**. A high rate of invasive carcinoma as tumor type 80% (20/25) in breast patients showed up-regulated expression of miR-370 gene expression (Mean SE± 8.57 ±2.099) more than a control group. No significant association of miR-370 expression with tumor type, (P= 0.2) although high levels of fold expression (7.53 and 6.09). Up-regulated gene expression of miR-370, also was showed (SE 7.46±3.39) comparable with the control group in tumor grade II. Results showed no significant association was observed in miR-370 expression with tumor grade (P= 0.5) despite a high level of fold expression (8.67 and 6.59) in grades 1 and 2 respectively compared to the control group. No significant differences of the miRNA370 expression depending on differentiation were observed. Despite the increasing level of miRNA370 fold expression 7.8 (SE 9.96±4.04), (P=0.4) in moderately differentiated in comparison to the control group (SE 1.68± 0.77) (Fig. 3. E).

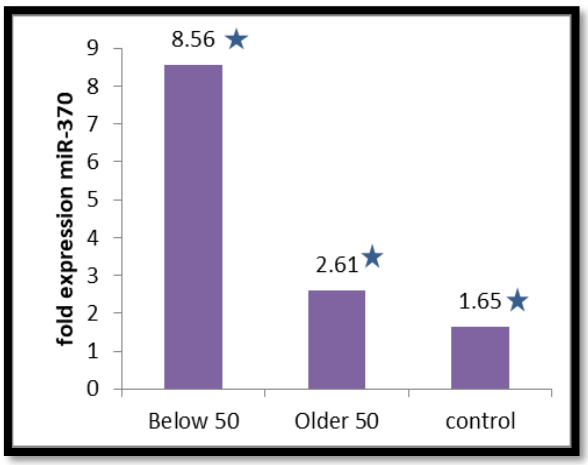

Age
A

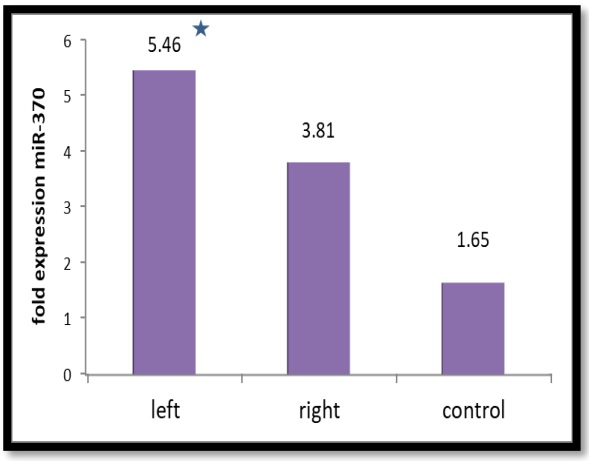

Tumor site
B

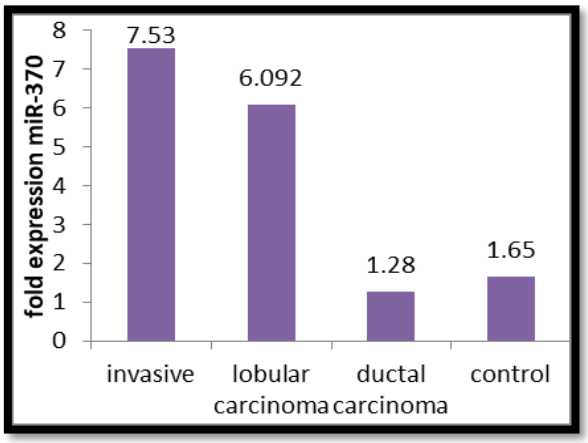

Type of tumor
C

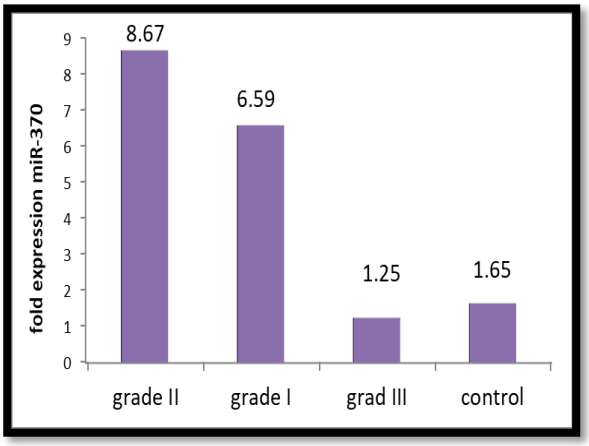

Grade of tumor
D

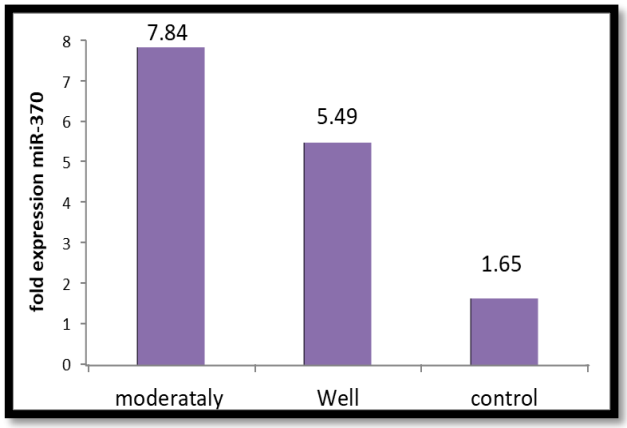

Differentiation
E

Figure 3. Gene expression of miR-370 in tumor patients: Depending on (A) Age; (B) Tumor location; (C) Type of tumor; (*) Significant differences. (D) Grade of tumor; (E) Differentiation. There were no significant differences in the miRNA370 expression depend on differentiation, tumor type, and grad.

3.4. Comparison between the miR-370 expressions in benign and tumor breast tissues

The miR-370 expression was up-regulated in 60 % (30/50) of benign and malignant breast patients tissue compared with normal tissue, with an average increase of 7.2 fold ex-

pression with significant differences P=0.03 **(Figure 4)**.

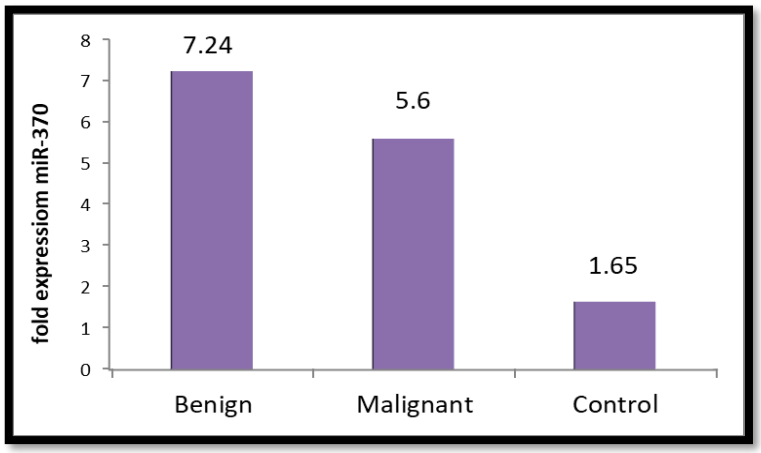

A **B**

Figure 4. Comparison of miR-370 gene expression between benign, malignant and normal tissues, significant differences, P=0.03.

4. Discussion

The discovery of small RNA fragments led to a global research effort to determine its role in cancer [21]. It has been shown to regulate molecular pathways in cancer by targeting various carcinogenic and tumor suppressor genes. It has a role in stem cell biology, vessel formation, Epithelial-Mesenchymal transition, proliferation, and resistance to treatment [21, 22]. Molecular research on miR-370 has been controversy about its role in carcinogenesis. Several studies have shown that this molecule acts as oncomiRNA toward advanced stages of cancer, such as Wilm tumor which is kidneys cancer usually occurs in children) [23], Gastric cancer [24], as well as acute myeloid leukemia (AML) [25]. All of which may occur with the miR-370 effect as an oncogene. In contrast, it may act as an inhibitor of tumors or tumor suppressor genes in laryngeal cell carcinoma and biliary duct cancer [26, 27]. This study highlights the ability of the miR-370 gene expression in benign and malignant tumors to serve as a biomarker in breast cancer patients. This work is considered as the first research conducted to investigate the level of miR-370 expression based on SYBR-Green quantitative qRT-PCR in benign and malignant Iraqi breast patients. Our previous study was showed up-regulate of the miR-328 gene expression level in both benign lesions and breast cancer, suggesting a miR-328 role as a biomarker for early breast cancer detection [28]. The average age of patients with benign and malignant breast cancer in the present study was 34 and 50 years, 52% of malignant breast patients were younger than 50 years and 84% of patients were with moderately differentiated tumors. A high rate (80%) of patients were identified with invasive carcinoma, these results agree with the Iranian study [11]. Based on our findings, in all 25 samples of benign tumors, the fold expression level of miR-370 was increased seven times compared with the fold expression level of control samples with a significant association was found in the level of miR-370gene expression between the ages of less than 50 years and control group (P = 0.047). Depending on the location of the tumor, a high level of the miR-370 fold expression was observed on the right side compared with the fold expression for control samples. There was no significant difference between the groups. Alterations of miR-370 gene expression in benign and malignant breast patients give an

important vision for the miR-370 role in initiating and progressing breast cancer. Significantly associated with high miR-370 expression were found depending on age, tumor location, tumor type, and stage of differentiation. The results indicated that the up-regulated miR-370 can act as oncomiRNA in breast cancer. The overexpression of miR-370 may be responsible for the development of a benign tumor, and the development of breast cancer. Shen with his colleagues observed an increase in miR-370 expression in 60% of colorectal cancer patients depending on age [18]. Mollainezhad and his group [11] showed increased expression of miR-370 in the first and second grades with no significant relation (P = 0.297) in breast cancer. These results refer to the up-regulated miR-370 that may act as oncomiRNA in breast cancer. The overexpression of miR-370 can be responsible for the initiation of a benign tumor and the development of breast cancer. Significantly associated with high miR-370 expression were found depending on age, tumor location, tumor type, and stage of differentiation. The results indicated that the up-regulated miR-370 can act as oncomiRNA in breast cancer, the overexpression of miR-370 may be responsible for the development of a benign tumor, and the development of breast cancer. Shen with his colleagues was observed an increase in miR-370 expression in 60% of colorectal cancer patients depending on age [18]. Mollainezhad and his group [11] showed an increased expression of miR-370 in the first and second grades with no significant relation (P = 0.297) in breast cancer. These results refer to the up-regulated miR-370 that may act as oncomiRNA in breast cancer. The overexpression of miR-370 can be responsible for the initiation of a benign tumor and the development of breast cancer. Increasing evidence showed that miRNAs are involved in cancer pathogens and have given new concepts in the biological pathway to cancer like induced gastric cancer by epigenetic silencing of promoter-proximal CpG island hypermethylation for miRNA 9 gene [31). This miR-370-induced proliferation by down-regulation of cyclin-dependent kinase inhibitors, p27(Kip1) and p21(Cip1), and the up-regulation of the cell cycle regulator cyclin D1 [32]. Moreover, 10 dysregulated miRNAs were identified in both breast cancer cells and chemoresistant tissues, which might be biomarkers for the chemoresistance prognosis of breast cancer. It is useful for developing new strategies for targeted therapies in chemoresistant breast cancer patients [33]. Another study showed that miR-370 plays an important role in the proliferation of prostate cancer cells and direct inhibition of FOX1, which is associated with cellular functions including cellular growth, differentiation, apoptosis, and angiogenesis [15]. It has been known that miR-370 works either as oncomiR or as a suppressor tumor. The miR-370 molecule, as oncomiR, was found in the Pan et al., study because increased miR-370 expression in liver cancer cell lines may inhibit cell proliferation and induce apoptosis. It may inhibit the histological invasion of the tumor, thus, miR-370 acts as a tumor suppressor in the liver cancer cell lines [34]. Mollainezhad with colleagues has been reported that miR-370 could be considered as a new diagnostic factor in breast cancer as a result of its role as an oncogene, and it may be useful both as a diagnostic agent and in targeted treatment [11]. The effect of miR-370 in cancer is controversial, this may be due to its ability to regulate multiple genetic targets, which makes its function in different roles, yet the function of this molecule depends on the type of cell.

5. Conclusion

The present study suggested that miR-370 may serve as an onco-miRNA. Significantly associated with high miR-370 expression were found depending on age, tumor location, tumor type, and stage of differentiation. The level of miR-370 gene expression can be used as biomarkers for breast cancer.

6. Acknowledgement

The authors are grateful for the valuable comments and observations we make in our work.

References

1. Miller KD, Siegel RL, Lin CC, Mariotto AB, Kramer JL, Rowland, JH, Stein, KD, Alteri R. and Jemal A. Cancer treatment and survivorship statistics, *CA Cancer J. Clin*. **2016** ,*66*, 271.
2. Alwan, N.A.S.; Tawfeeq, F.; Maallah, A.S.; Sattar, S.A.; Saleh, W.A. The Stage of Breast Cancer at the Time of Diagnosis: Correlation with the Clinicopathological findings among Iraqi Patients. *J. Neoplasm*. **2017** ,*2*, 22.
3. Imani, S.; Zhang, X.; Hossein, H.; Fu, S.; Fu, J. The diagnostic role of micro RNA-34a in breast cancer: asystematic review and meta-analysis *Oncotarget*. **2017** ,*8*, 23177.
4. Carthew. R.W.; Sontheimer. E.J. Origins and mechanisms of miRNAs and siRNAs. *Cell*. **2009** ,*136* 642.
5. Wang, P.; Chen, L.; Zhang, J.; Chen, H.; Fan, J.; Wang, K.; Luo, J.; Chen, Z.; Meng, Z.; Liu, L. Methylation-mediated silencing of the miR-124 genes facilitates pancreatic cancer progression and metastasis by targeting Rac1. *Oncogene*. **2014** ,*33* 514.
6. Gao, Y.; Cai, Q.; Huang, Y.; Li, S.; Yang, H.; Sun, L.; Chen, K.; Wang, Y. MicroRNA-21 as a potential diagnostic biomarker for breast cancer patients: a pooled analysis of individual studies. *Oncotarget* **2016**, *7*, 34498.
7. Xiong, D.D.; Lv, J.; Wei, K.L.; Feng, Z.B.; Chen, J.T.; Liu, K.C.; Feng, Z.B.; Tian, J.; Chen, J.T.; Liu, K.C.; Chen, G.; Luo, D.Z. A nine-miRNA signature as a potential diagnostic marker for breast carcinoma: An integrated study of 1,110 cases. *Oncol. Rep*. **2017,** *37*, 3297.
8. Tsai, H.P.; Huang, S.F.; Li, C.F.; Chien, H.T.; Chen, S.C. Differential microRNA expression in breast cancer with different onset age. *PloS One*. **2018**, *13*, e0191195.
9. Quan, Y.; Huang, X.; Quan, X. Expression of miRNA-206 and miRNA-145 in breast cancer and correlation with prognosis. *Oncol. Lett*. **2018,** *16*, 6638.
10. Kahraman, M.; Röske, A.; Laufer, T.; Fehlmann, T.; Backes, C.; Kern, F.; Kohlhaas, J.; Schrörs, H.; Saiz, A.; Zabler, C.; Ludwig, N.; Fasching, P.A.; Strick, R.; Rübner, M.; Beckmann, M.W.; Meese, E.; Keller, A.; Schrauder, M.G. MicroRNA in diagnosis and therapy monitoring of early-stage triple-negative breast cancer. *Sci. Rep*. **2018**, *8*, 11584.
11. Mollainezhad, H.; Eskandari, N.; Pourazar, A.; Salehi, M.; Andalib, A. Expression of microRNA-370 in human breast cancer compare with normal samples. *Adv. Biomed. Res*. **2016** ,*5*, 129.
12. Lo, S.; Chen, J. Overexpression of miR-370 and downregulation of its novel target TGFβ-RII contribute to the progression of gastric carcinoma. *Oncogene*. **2012**, *31*, 226.
13. El-Daly, S.M.; Abba, M.L.; Patil, N.; Allgayer, H. miRs-134 and -370 function as tumor suppressors in colorectal cancer by independently suppressing EGFR and PI3K signalling. *Sci. Rep*. **2016**, *20*, 24720.
14. Duan, N.; Hu, X.; Yang, X.; Cheng, H.; Zhang, W. MicroRNA-370 directly targets FOXM1 to inhibit cell growth and metastasis in osteosarcoma cells. *Int. J. Clin. Exper. Pathol.* **2015** ,*8*, 10250.

15. Wu, Z.; Sun, H.; Zeng, W.; He, J.; Mao, X. Upregulation of MircoRNA-370 induces proliferation in human prostate cancer cells by downregulating the transcription factor FOXO1. *PloS One*. **2012,** *7*, e45825.
16. Ye, H.; Kelly, T.F.; Samadani, U.; Lim, L.; Rubio, S.; Overdier, D.G.; Roebuck, K.A.; Costa, R.H. Hepatocyte nuclear factor 3/fork head homolog 11 is expressed in proliferating epithelial and mesenchymal cells of embryonic and adult tissues. *Mol Cell Biol*. **1997,** *17*, 1626.
17. Chen, X.P.; Chen, Y.; Lan, J.Y.; Shen, Z.J. MicroRNA-370 suppresses proliferation and promotes endometrioid ovarian cancer chemosensitivity to cDDP by negatively regulating ENG *Cancer Lett.* **2014**, *353*, 201.
18. Shen, X.; Zuo, X.; Zhang, W.; Bai, Y.; Qin, X.; Hou. N MiR-370 promotes apoptosis in colon cancer by directly targeting MDM4 *Oncol Lett*. **2018**, *15*, 1673.
19. Saberi, A.; Danyaei, A.; Neisi, N.; Dastoorpoor, M.; Birgani, M.J.T. MiR-328 may be considered as an oncogene in human invasive breast carcinoma *IRCMJ*. **2016**, *18*, e42360.
20. Livak, K.J.; Schmittgen, T.D. Analysis of relative gene expression data using real time quantitative PCR and the 2(-Delta Delta C(T)) Method. *Methods*. **2001**, *25*, 402.
21. Johnson, S.M.; Grosshans, H.; Shingara, J.; Byrom, M.; Jarvis, R.; Cheng, A.; Labourier, E.; Reinert, K.L.; Brown. D.; Slack. F.J. RAS Is Regulated by the let-7 MicroRNA Family *Cell* **2005,** *120*, 635.
22. Ahmad, J.; Hasnain, S.E.; Siddiqui, S.M.A.; Ahamed, M.; Musarrat, J.; Al-Khedhairy. A.A. MicroRNA in carcinogenesis & cancer diagnostics: A new paradigm. *Indian J. Med. Res*. **2013**, *137*, 680.
23. Cao, X.; Liu, D.; Yan, X.; Zhang, Y.; Yuan, L.; Zhang, T.; Fu, M.; Zhou, Y.; Wang, J. Stat3 inhibits WTX expression through up-regulation of microRNA-370 in Wilms tumor. *FEBS Lett*. **2013,** *587*, 639.
24. Fan, C.; Liu, S.; Zhao, Y.; Han, Y.; Yang, L.; Tao, G.; Li, Q.; Zhang, L. Upregulation of miR-370 contributes to the progression of gastric carcinoma via suppression of FOXO1. *Biommd. Pharmacother*. **2013**, *67*, 521.
25. Zhang, X.; Zeng, J.; Zhou, M.; Li, B.; Zhang, Y.; Huang, T.; Wang, L.; Jia, J.; Chen, C. The tumor suppressive role of miRNA-370 by targeting FoxM1 in acute myeloid leukemia. *Molec. Cancer*. **2012,** *11*, 56.
26. Yungang, W.; Xiaoyu, L.; Pang, T.; Wenming, L.; Pan, X. miR-370 targeted FoxM1 functions as a tumor suppressor in laryngeal squamous cell carcinoma (LSCC) *Biomed. Pharmacother*. **2014,** *68*, 149.
27. Xu, W.P.; Yi, M.; Li, Q.Q.; Zhou, W.P.; Cong, W.M.; Yang, Y.; Ning, B.F.; Yin, C.; Huang, Z.W.; Wang, J.; Qian, H.; Jiang, C.F.; Chen, Y.X.; Xia, C.Y.; Wang, H.Y.; Zhang, X.; Xie, W.F. Perturbation of MicroRNA-370/Lin-28 homolog A/nuclear factor kappa B regulatory circuit contributes to the development of hepatocellular carcinoma. *Hepatology* **2013**, *58*, 1977.
28. Hasen, M.J.; Mahood, W.S. Evaluation of the microRNA-328 gene expression in some Iraqi breast cancer women. *J. Pharm. Sci. Res*. **2019** ,*11*, 2347.
29. Lu, M.; Wang, Y.; Zhou, S.; Xu, J.; Li, J.; Tao, R.; Zhu. Y. MicroRNA 370 suppresses the progression and proliferation of human astrocytoma and glioblastoma by negatively regulating β catenin and causing activation of FOXO3a. *Exper. Therap. Med*. **2018**, *15*, 1093.
30. Peng, Z.; Wu, T.; Li, Y.; Xu, Z.; Zhang, S.; Liu, B.; Chen, Q.; Tian, D. MicroRNA-370-3p inhibits human glioma cell proliferation and induces cell cycle arrest by directly targeting β-catenin. *Brain Res.* **2016** ,*1644*, 53.

31. Li, Y.; Xu, Z.; Li, B.; Zhang, Z.; Luo, H.; Wang, Y.; Lu, Z.; Wu, X. Epigenetic silencing of miRNA 9 is correlated with promoter proximal CpG island hypermethylation in gastric cancer in vitro and *in vivo Int. J. Oncol*. **2014**, *45*, 2576.
32. Fan, C.; Liu, S.; Zhao, Y.; Yang, Y.; Tao, G.; Li, Q.; Zhang, L Upregulation of miR-370 contributes to the progression of gastric carcinoma via suppression of FOXO1. *Biomed. Pharmacother*. **2013**, *67*, 521.
33. Lv, J.; Xia, K.; Xu, P.; Sun, E.; Ma, J.; Gao, S.; Zhou, Q.; Zhang, M.; Wang, F.; Chen, F.; Zhou, P.; Fu, Z.; Xie, H. miRNA expression patterns in chemoresistant breast cancer tissues. *Biomed. Pharmacother*. **2014**, *68*, 935.
34. Pan, X.P.; Wang, H.X.; Tong, D.M.; Li, Y.; Huang, L.H.; Wang, C. miRNA-370 acts as a tumor suppressor via the downregulation of PIM1 in hepatocellular carcinoma. *ERMPS.* **2007**, *21*, 1254.

Ibn Al-Haitham Journal for Pure and Applied science https://doi.org/10.30526/2021.IHICPAS.2653

Evaluation of Ceruloplasmin Oxidase Activity in Sera of Breast Cancer Individuals in Kurdistan Region/ Iraq

Shahlaa Shafiq Rozoqi
shahla.biochem@epu.edu.iq

Department of Medical Laboratory Technology, Erbil Health Technical College, Erbil Polytechnic University, Erbil, Iraq.

Abstract

Ceruloplasmin is considered the main copper transport protein which is proposed to have a role in cancer. Ceruloplasmin is an acute phase reactant and antioxidant enzyme, has been found to be increased in sera of patients with several types of cancers including breast cancer.
The aim of present study was to determine of ceruloplasmin oxidase activity, specific activity, iron concentration in sera of patients with breast cancer and comparing with healthy group, and the ability of using enzyme as a tumor marker for breast cancer.
This study was performed from November 2018 to January 2019, blood samples were collected from breast cancer patients in Nanakeli Hospital in Erbil city. Study was included (65) female patients with breast cancer and (20) healthy donors as control group. Ceruloplasmin activity, specific activity, serum total protein concentration, serum total iron concentration levels were estimated for all samples by colorimetric methods.
The results shown that there was a significant increase in ceruloplasmin activity level for patients with breast cancer (227.8 U/L) compared with control group (101.1 U/L) while total protein level for breast cancer patients (6.592 g/dl) showed no significant change compared to control group(7.127 g/dL) likewise the result shown that there was a significant increase in specific activity of ceruloplasmin and total iron concentration level for patients with breast cancer (34.74 U/mg) (334.2 mg/dl) compared to control group (14.14 U/mg) (128.6 mg/dl)
The conclusion of this study was the concentration of ceruloplasmin activity, serum total iron concentration and specific activity of ceruloplasmin significantly increase in breast cancer patients while total protein level revealed no significant change.
Serum ceruloplasmin oxidase activity and specific activity were highly significant elevated in patient group when compared with control group. Also the total iron concentration results showed significant increasing ($P<0.0001$) between of patient with breast cancer and control group.

Key words: Ceruloplasmin Oxidase Activity, Breast Tumor, Iron.

1. Introduction

Breast cancer is one of the most common cancers among women around the world, accounting for about 570,000 deaths in 2015 [1]. More than 1,5 million women (25% of all individuals with cancer) were diagnosed with breast cancer worldwide each year [2] . Breast cancer is a metastatic cancer which can usually spread to distant organs such as the bone, liver, lung and brain, which are primarily responsible for its incurability [3]. Early diagnosis of the illness can lead to the best prognosis and increase the chance of survives [4]. Breast

cancer has two main types: non-invasive breast cancer and invasive breast cancer [5] .Ceruloplasmin (Cp) is an enzyme that may play a significant role in the progression of breast cancer [6]. The Cp is an acute-phase protein that is typically produced by hepatic cells [7] and is primarily secreted in the plasma [8], whereas Cp mRNA was found in cell lines of breast cancer patients [9]. It is comprised of angiogenesis and neovascularization thus it has a role in cancer [10]. Cp plays a significant role in iron homeostasis[8], consequently, it has a contribution to the antioxidant mechanism by preventing the formation of free radicals [11] or in oxidative damage mechanisms [12] Ceruloplasmin has two major functions: oxidase and ferroxidase activities [13], by its oxidase activity, play an important role in a variety of processes relevant to the copper metabolism [14] , some organic amines that produce in the body [15], and nitric oxide [16], on the other hand, iron is one of the sources of free radicals which release from Fenton/Haber-Weiss or autoxidation reactions, that lead to the formation of reactive oxygen species (ROS) and lipid peroxidation [17]. Cp acts as an antioxidant by oxidizing iron from its ferrous to ferric state, thus preventing oxidative damage induced by ferrous mediated free radical generation by the Fenton reaction [18]. By ferroxidase activity, Cp assists the export of iron from the cell because only ferric iron can be incorporated with transferrin in the bloodstream [19]; extracellular ferroxidases that included Cp are essential in ferroxidation, which is therefore required for the optimal export of iron, possibly through the production of ion gradients [20].

The present study aimed to find the relation between the oxidase activity of Cp and the specific activity of this enzyme with breast cancer. Also, the relation between the iron concentrations which can cause a high amount of free radicals in breast cancer and ceruloplasmin activity. In addition, the ability to use Cp as a tumor marker for the early diagnosis of breast cancer is possible.

2.Materials and Methods

2.1.Patients and sample age

This study is concerned with malignant breast cancer patients from Nanakeli Hospital-Erbil/Kurdistan region of Iraq from November 2018 to January 2019. The diagnosis of breast cancer was confirmed by 15-3 (CA 15-3) cancer antigen which is a protein formed by normal breast cells; which were carried in the laboratories of the hospital mentioned above.

Eighty-five (85) females were involved in this study. 65 of the human breast cancer patients with age between 20-60 years as a patient group and 20 subjects as a control group with age between 22-56 years old, the distribution of patients age is shown in figure (1). Shows that there were 33% (n=28) of patients in age between (20-35) years & 54% (n=46) of patients in age between (36-55) years and 13% (n=11) of patients (up to 56) years.

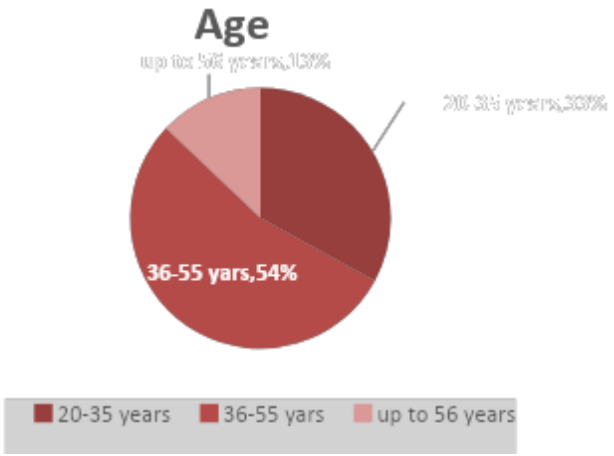

Figure 1. Distribution of patients' age including in this study

2.2. Sample collection

Blood samples were collected by taken 3 milliliters of venous blood from patients was put in a gel tube and left to clot then the serum was separated immediately from the cells by centrifugation at 3000 rpm for 10 minutes, stored until used. The sera which were obtained from blood sample should be un hemolyzed and non-jaundice to avoid any interference with the obtained results. Any case with chronic diseases or chemotherapy treatment were excluded.

2.3.Methods

Ceruloplasmin oxidase activity was performed by using the modified rice method and p-phenylene diamine -2HCL as a substrate [21]. Colorimetric method described by Gornall and et al.[22.23] was used to determine the concentration of total protein in the specimen. The specific enzyme activity is described as follow:

Specific activity (unit/g) = activity of enzyme (U/L) / Protein concentration (g/L)

The colorimetric method was used to estimate the total iron concentration in sera which depend on the dissociation of iron-transferrin bound in an acidic medium, ascorbic acid reduces ferric to ferrous and then to a colored complex of 3-(2pyridyl)-5,-6difuryl-1,-2,-4-triazine-disulfonate (ferene) [24].

2.4.Statistical Analysis

Statistical analysis for this study was done using the Graph Pad prism 7.1 software. The unpaired t-test descriptive statistics was used which is important to test for a statistical significance of the difference in original data.

3.Results and Discussion

3.1.Total protein concentration and total iron concentration

The level of serum total protein concentration was measured in all study groups sera. The results of statistical analysis showed no significant difference (p 0.0108) between the mean total protein concentration of the breast cancer patients (6.596 g / dl) and the mean total protein concentration of the control group (7.127 g / dl), as shown in **Table (1).**

Ibn Al-Haitham Journal for Pure and Applied science https://doi.org/10.30526/2021.IHICPAS.2653

The level of serum total iron concentration was measured in all study groups. According to statistical analysis, the results show a significant increase (P<0.0001) in the patient group compared with the control group as shown in **Table (1).**

Table 1. The concentration of serum total protein and serum total iron in control and patient group.

Parameters	Mean±SD of Control group	Mean(g/dl) ±SD of Patient group	P value
Total Protein (g/dl)	7.127 ± 0.3527 (N=20)	6.592 ± 0.8926 (N=65)	0.0108
Serum total iron (µg/dL)	128.6 ± 46.02(N=20)	338.2 ± 137.7 (N=65)	(P<0.0001)

3.2. Oxidase activity and specific activity ceruloplasmin

The level of serum Cp activity was measured in sera of all study groups, and the statistical analysis of the findings showed a significant difference between the mean concentration of Cp in patients with breast cancer (227.8 U / l) and the mean activity of Cp in the control group (101.1 U / l) as shown in **Table (2).** Cp specific activity was calculated in all study groups. The results appeared a significant increase in enzyme-specific activity for the patient group compared with the control group as shown in **Table (2).**

Table 2: Oxidase activity and specific activity of ceruloplasmin in patient and control group

Parameters	Mean±SD of Control group	Mean±SD of Patient group	P-value
Cp oxidase activity (U/L)	101.1 ± 27.08	227.8 ± 54.99	<0.0001
Specific Activity of Cp (U/mg)	14.14 ± 3.665 N=20	34.74 ± 9.525 N=65	<0.0001

3.3.The relation between smoking and ceruloplasmin oxidase activity.

Figure (2) was shown a slight significant increase (<0.05) between smokers (Mean (U/L) 218.7 ±SD 56. 64) and nonsmoker (Mean (U/L) 229. 6 ±SD 55.) of the patient group.

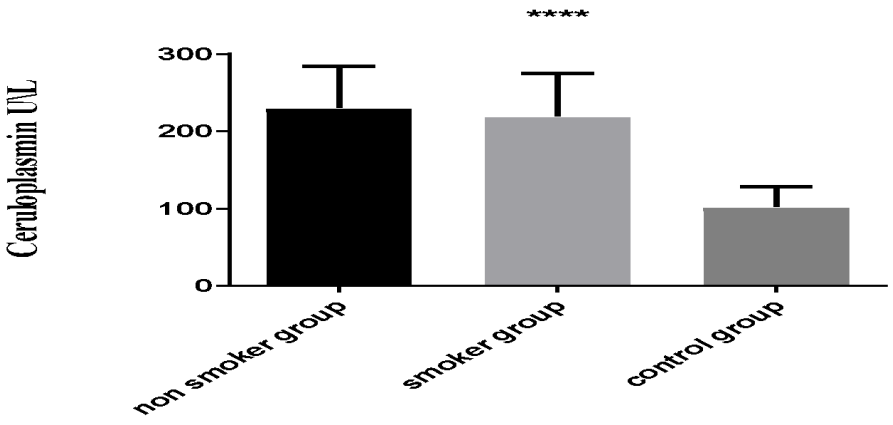

Figure 2. Ceruloplasmin activity in smoker and nonsmoker of the patient group.

In the last decade, researchers have confirmed a significant elevation in free radicals and their role in the micro-environmental tumor[25]. Antioxidants are the major preservation of the body against free radicals and other oxidants, being the substances that stop the attack and the production of radical species inside the cells [26]. The increase of iron concentrations after menopause could be an important etiological factor in the development of breast cancer [27]. The Cp is considered one of important antioxidant that prevents the formation of free radicals by inhibiting Fenton reaction, it can change Fe^{2+} to Fe^{3+} which represent a very important step to load Apo transferrin with iron [18], furthermore, it stimulates the reoxidation of copper I to copper II [28]. Iron imbalance is a distinct physiological phenomenon in women, which is probably to affect their health before, during, and after menopause [27]. There is a possibility that iron deficiency may contribute to a high recurrence of breast cancer in premenopausal women, while iron load may play a role in the incidence of breast cancer in postmenopausal women [28] High concentrations of iron, calculated as plasma iron, transferrin saturation and total iron-binding capacity (TIBC), have been correlated in human studies with elevated overall cancer risk [29] and increased risk of death from any form of cancer[30] . Ceruloplasmin plays a critical role in maintaining the iron level thus it has potential influences in the development of breast cancer [31]. Furthermore, plasma copper rises in the case of malignant tumors level [32], contributes to an increase in the concentration of ceruloplasmin [33] . There is also an increase in the rate of synthesis and secretion of this glycoprotein by the liver[32] in the tumor state. Tumor cells are capable of absorption from plasma so that they contain a relatively large amount of copper that affects pathogenic angiogenesis [34].
Ceruloplasmin was also reported to be associated with different types of cancers [35]. Increased glycoconjugates can be the product of an inflammatory reaction correlated with neoplasm since serum Cp is an acute phase reactant [36], it is also increased in patients of the uterine cervix [37]. Several studies were occurred on sera and solid tumor tissue to figure out the concentration of Cp and some analytes that correlated with this enzyme in cancer patients which emphasizes there is a relation between Cp and prostate, colon cancer patients [38] and with bile duct cancer [35]. The increase of Cp activity in this study has agreed with a study by Ozour et al which found increasing in Cp concentration in breast disease [39]. Further study confirmed that Cp concentration increased in patients with metastatic breast cancer [36] and patients with primary breast cancer [40]. In addition, the result in the current study agrees with research by Jing fan et al which studied the relationship between serum level of copper and Cp concentration in sera of patients with early breast cancer patients by using atomic absorption spectroscopy and immunoturbidimetry assay [41]. On the other hand, the result in the current study disagrees with Debek JT et al which found the Cp activity was significantly decreased in postmenopausal stage I and II breast cancer patients [42].

4.Conclusions

According to the results of this study, serum Cp oxidase activity and specific activity were highly significantly elevated in-patient group when compared with the control group. Likewise, the results showed a significant increase ($P<0.0001$) between the total iron concentration means of a patient with breast cancer and the control group. Protein concentration was increased but insignificantly (p 0.0108) in the patient group when compared with control group.

We propose that ceruloplasmin can use as a tumor marker to diagnose or the follow-up patients with breast cancer. Further study can occur for ceruloplasmin in malignant and benign groups like determination of molecular weight and finding the isomers or forms of this enzyme to find the ability to use this enzyme as a tumor marker. And determine other activities of ceruloplasmin. Finally measure other parameters such as copper, transferrin that related to ceruloplasmin.

Acknowledgment

Thanks to all cancer patients in Nanakali Hospital-Erbil City-Kurdistan region/Iraq as participants.

References

1.Zohre , M.; Hamid S. Epidemiological characteristics of and risk factors for breast cancer in the world, *Breast Cancer: Targets and Therapy.* **2019**, *11*, 151–164.

2.Stewart B,W.; Wild C,P. World Cancer Report .**2014**. Geneva, Switzerland: WHO Press.

3.Yi-Sheng, S.; Zhao ,Z.; Zhang-Nv ,Y.; Fang ,X.; Hang-Jing , L.; Zhi-Yong , Z.; Wen , S.; Jianmin , J .; Ping-Ping , Y.; Han-Ping , Z.; Risk Factors and Preventions of Breast Cancer, *Int J Biol Sci*. **2017**, *13(11)* , 1387–1397.

4.Wang, L. Early Diagnosis of Breast Cancer. *Sensors*. **2017**,*17(7):*1572-1600. Published **2017** Jul 5. doi:10.3390/s17071572

5.Ganesh , N.; Sharma, R. D.; Jyotsana , S.; Piush , S .; Sharma ,K.K. Various types and management of breast cancer: an overview, *J. Adv. Pharm. Technol. Res*. **2010**, *1(2*), 109–126.

6.Ryszard , K .; Bernadeta , D.; Tomasz ,K . The infuence of radiotherapy on ceruloplasmin and transferrin in whole blood of breast cancer patients. *Radiat. Environ. Biophys.* **2017** , *56* , 345-352.

7.Podolsky , D . K .; Isselbacher , K .J. Derangements of hepatic metabolism. Harrison's Principles of Internal Medicine, 12thed, Mc Graw-Hill Co, New York ,**1991**, p1311-1317.

8.Gitlin, J. D. Aceruloplasminemia. *Pediatr. Res.***1998** , *44*,271–276.

9.Kunapuli, S.P. Ceruloplasmin gene expression in human cancer cells, *Life Sci.***1987,** *40(23)*,2225–2228.

10.Stivens, M.D.; Di Silvestro, R.A.; Harris, E.D.; Specific receptor for ceruloplasmin in membrane fragments from aortic and heart tissues, *Biochemistry* , **1984** ,*23(2)*, 261–266.

11.Gutteridge, J. M. Antioxidant properties of caeruloplasmin towards iron- and copper-dependent oxygen radical formation. FEBS Lett.**1983**, *157(1)* ,37–40.

12.Mukhopadhyay, C . K. B.; Mazumder , P .F .L.; Fox, P . L . Identification of the prooxidant site of human ceruloplasmin: a model for oxidative damage by copper bound to protein surfaces. *Proc Natl Acad Sci U S A***.1997**, *94 (21)*,11546–11551.

13.Bento , I .; Peixoto , C .; Zaitsev , V.N.; Lindley , P .F. Ceruloplasmin revisited: structural and functional roles of various metal cationbinding sites. *Acta Cryst. D,* **2007** , *63(2)*, 240–248.

14.Harris, E. D. The transport of copper Review. *Prog. Clin. Biol. Res.* 1993, 380:163–179.

15.Zaitsev, V.N.; Zaitseva, I.;Papiz, M. ; Lindley, P.F. An x-ray crystallographic study of the binding sites of the azide inhibitor and organic substrates to ceruloplasmin, a multi-copper oxidase in the plasma. *J. Biol. Inorg. Chem.* **1999**, *4(5)*, 579 –587.
16.Bianchini, A.; Musci, G.; Calabrese , L. Inhibition of endothelial nitric-oxide synthase by ceruloplasmin. *J. Biol. Chem*. **1999** , *274(29)* , 20265–20270.
17.Huang , X. Iron overload and its association with cancer risk in humans: evidence for iron as a carcinogenic metal. *Mutat Res-Fund Mol M.* **2003** ,*533(1-2)*, 153–171.
18.Osaki, S. Kinetic studies of ferrous ion oxidation with crystalline human ferroxidase (Ceruloplasmin). *J. Biol. Chem* . **1966** , *241(21)*, 5053–5059.
19.Osaki, S. ; Johnson, D . A. ; Frieden, E. The possible significance of the ferrous oxidase activity of ceruloplasmin in normal human serum. *J. Biol. Chem*. **1966**, *241(12)*, 2746–2751
20.Sarkar, J. ; Seshadri, V. ; Tripoulas, N. A. ; Ketterer, M . E. ; Fox, P . L. Role of ceruloplasmin in macrophage iron efflux during Hypoxia. *J. Biol. Chem.***2003** , *278(45)*, 44018- 44024.
21.Rice, E.W. Standardization of ceruloplasmin activity in terms of international enzyme units. *Anal. Biochem.*. **1962**, *3(6)*,452-456.
22.Gornall, A. G.; Bardawill, C. J.; David, M. M. .; Determination of serum proteins by means of the biuret reaction. *J. Biol. Chem.***1949**, *177(2)*, 751-766 .
23.Tietz , N . W. Text book of chlinical chemistry, 3rd ed. C.A. Curtis, E.R. silverman L. M., Christensen R. H.**1995**, p. 523-524.
24.Hennessy, D.J.; Reid, G.R.; Smith, F.E. ; Thompson, S.L. Ferene—a new spectrophotometric reagent for iron. *Can. J. Chem.*. **1984** , *62(4)*. 721-724
25.Ríos-Arrabal, S.; Artacho-Cordón, F.; León, J.; Román-Marinetto, E.; del Mar Salinas-Asensio, M.; Calvente, I. ; Núñez, M.I. Involvement of free radicals in breast cancer. *nvolvement of free radicals in breast cancer. Springerplus.* **2013**, *2*(1), 1-12.
26.Teixeira ,V .; Valente ,H.; Casal , S.; Marques , F.; Moreira , P. Blood antioxidant and oxidative stress biomarkers acute responses to a 1000-m kayak sprint in elite male kayakers. *J Sports Med Phys Fitness*. **2013** , *53(1)*,71–79.
27.Huang, X. Does iron have a role in breast cancer. *Lancet Oncol* .**2008**, *9(8)* , 803–807.
28.Wherland, S.; Farver, O. ; Pecht, I. Multicopper oxidases: intramolecular electron transfer and O_2 reduction. *J. Biol. Inorg. Chem.* **2014** , *19(4-5)* ,541-554.
29.Mainous, A.G.; Wells, B.J.; Koopman, R.J.; Everett, C.J. ;Gill, J.M., 2005. Iron, lipids, and risk of cancer in the Framingham Offspring cohort. *Am. **J**. Epidemiol.***2005**,*161(12)*,1115–1122.
30.Amber , B.M.; Jackilen , S .; David , B. T .Dietary and stored iron as predictors of breast cancer risk: A nested case–control study in Shanghai. *Int J Cancer.* **2009** , *125(5)*, 1110–1117.
31.Vaidya ,S.M .; Kamalakar , P.L. Copper and ceruloplasmin levels in serum of women with breast cancer. *Indian J. Med. Sci*. **1998** , *52(5)*,184-187.
32.Zowczak, M.; Iskra, M.; Torliński, L. ;Cofta, S.,Analysis of serum copper and zinc concentrations in cancer patients. *Biol. Trace Elem. Res.* **2001**, *82(1)*,1–8.
33.Varela, A.S.; Saez, J.B.L. ; Senra, D.Q. Serum ceruloplasmin as a diagnostic marker of cancer. *Cancer Lett.*,**1997** ,*121(2)*,139–145.
34.Pan, Q.; Kleer, C.G. ; Van Golen, K.L. ; Irani, J. ; Bottema, K.M. ; Bias, C. ; De Carvalho, M. ; Mesri, E.A. ; Robins, D.M. ; Dick, R.D. ; Brewer, G.J., Copper deficiency

induced by tetrathiomolybdate suppresses tumor growth and angiogenesis. *Cancer Res.* **2002** , *62(17)*, 4854–4859.

35. Han, I.W.; Jang, J.Y.; Kwon, W.; Park, T.; Kim, Y.; Lee, K.B. ; Kim, S.W. Ceruloplasmin as a prognostic marker in patients with bile duct cancer ,*Oncotarget.* **2017**, *8(17)* , 29028-29037.

36.Schapira , D .V .; Schapira , M . Use of ceruloplasmin levels to monitor response to therapy and predict recurrence of breast cancer. *Breast Cancer Res. Treat.***1983**, *3(2)*,221-224.

37.Upadhya, S.; Upadhya, S. ;Prabhu, K.S. Serum glycoconjugates and ceruloplasmin in cancer of uterine cervix. *Indian J. Clin. Biochem*. **2002,** *17(1):*20-24.

38.Nayak, S.B.; Bhat, V.R.;Upadhyay, D. ;Udupa, S.L. Copper and Ceruloplasmin Status in Serum of Prostate and Colon Cancer Patients. *Indian J. Physiol. Pharmacol.* **2003**, *47(1),* 108-110.

39. Ozyilkan, O.; Baltali, E.; Ozyilkan, E.; Tekuzman, G.; Kars, A. ; Firat, D. Ceruloplasmin Level in Women with Breast Disease Preliminary Results. *Acta Oncol.***1992** , *31(8),* 843-846.

40.Çiğdem , Y.; Meral , F.; Banu , Ö. Serum copper and ceruloplasmin concentrations in patients with primary breast cancer. Biochem. Soc. Trans. **1996**, *24(2)* , 321S.

41.Fan, J.; Wan, Y.; Wang, Y.;Wei, H.; Zhao, G.;Li, S.; Li, M.; Huang, M. ; Wang, T. The relationship between serum level of copper and ceruloplasmin and pathologic and clinical characteristics in early breast cancer patients. *J. Clin. Oncol.* **2018** , *36(15),* e13504-e13504.

42.Dabek , J .T.; Hyvönen ,D . M.; Härkönen , M .; Adlercreutz , H. Evidence for increased non-ceruloplasmin copper in early-stage human breast cancer serum. *Nutr. Cancer.* **1992** , *17(2)*,195-201.

Ibn Al-Haitham Journal for Pure and Applied science https://doi.org/10.30526/2021.IHICPAS.2654

A New Approach of Morgan-Voyce Polynomial to Solve Three Point Boundary Value Problems

Bushra Esaa Kashem

bushra_eesa@yahoo.com , 100047@uotechnology.edu.iq

Department Applied Sciences, University of Technology, Baghdad, Iraq.

Abstract

In this paper, a new procedure is introduced to estimate the solution for the three-point boundary value problem which is instituted on the use of Morgan-Voyce polynomial. In the beginning, Morgan-Voyce polynomial along with their important properties is introduced. Next, this polynomial with aid of the collocation method utilized to modify the differential equation with boundary conditions to the algebraic system. Finally, the examples approve the validity and accuracy of the proposed method.

Keywords: Morgan-voyce, three-point boundary value problem, collocation method, approximation method.

1.Introduction

The three point boundary value problem belongs to the seeming nonlocal or multipoint boundary value problem. This local boundary value problem has a major role in physics, engineering and many phenomena in applied mathematical. An amount of research has been studying the three-point boundary value problem, for example, the positive solution [1], existence and stability [2], discrete first order [3], and variational principle [4].

In this study, we consider the linear three point boundary value problem is:-

$$\ddot{D}Z(x) + F(x)Z(x) = G(x) \quad with\, Z(a) = Z(b) = A\, and\, \dot{Z}(c) = B \;\; x \in (a,b) \qquad (1)$$

Where F, G is a continuous function. a, b, c ∈ R. A, B real constant.

The main purpose of this work is to modify a new algorithm for an approximate solution to three point boundary value problems based on the special case of Morgan-Voyce polynomial. The properties and the method for using are explored. This method decreased the differential equation with its initial and boundary conditions to a system of algebraic equations in the unknown expand coefficients.

2. Morgan-Voyce polynomial

Diametrical polynomial Morgan-Voyce which is introduced recently in 1959 [5] at was used in many interesting papers such as, Functional integro [6], pantograph equation [7], differential-difference equation [8], and nonlinear ordinary differential equation [9].

Ibn Al-Haitham Journal for Pure and Applied science https://doi.org/10.30526/2021.IHICPAS.2654

The Morgan-Voyce polynomials $M_n(x)$ defined by:- [10]

$$M_{n+2}(x) = M_{n+1}(x) - M_n(x) \quad (2)$$

With $M_0(x) = 2$, $M_1(x) = x + 2$

and explicit formulation $(n \geq 1, n > k)$

$$M_n(x) = \sum_{k=0}^{n-1} \frac{2n}{n-k} \binom{n+k-1}{n-k-1} x^k + x^n \quad \ldots(3)$$

on other hand, by using eq.(2) & eq.(3) the first seven Morgan-Voyce polynomials are given:

$M_0(x) = 2$,

$M_1(x) = x + 2$

$M_2(x) = x^2 + 4x + 2$

$M_3(x) = x^3 + 6x^2 + 9x + 2$

$M_4(x) = x^4 + 8x^3 + 20x^2 + 16x + 2$

$M_5(x) = x^5 + 10x^4 + 35x^3 + 50x^2 + 25x + 2$

$M_6(x) = x^6 + 12x^5 + 54x^4 + 112x^3 + 105x^2 + 36x + 2$

$M_7(x) = x^7 + 14x^6 + 77x^5 + 210x^4 + 294x^3 + 196x^2 + 49x + 2$

3- Important Properties of Morgan-Voyce polynomial: [11,12]

1- Connection with Chybechev and Lucas polynomial $T_n(x), L_n(x)$

$$M_n(x) = 2T_n\left(\frac{x+2}{2}\right)$$

$$M_n(x^2) = L_{2n}(x)$$

2- Orthogonality

$M_n(x)$ is an orthogonal polynomial over [0,-4] with weight function $\frac{1}{\sqrt{4-(x+2)^2}}$

3. Integration

Ibn Al-Haitham Journal for Pure and Applied science https://doi.org/10.30526/2021.IHICPAS.2654

$$\int_{-4}^{0} M_{2n+1}(x)dx = 0$$

$$\int_{-4}^{0} M_{2n}(x)dx = \frac{8}{(2n+1)(2n-1)}$$

4-Zeros

$$M_n(x): x_r = -4\,sin^2\left[\frac{2r-1}{2n} * \frac{\pi}{2}\right], \qquad r = 1,2,\dots,n$$

3. Morgan-Voyce Collocation Method

In this section, the solution of three-point boundary value problem can be abstracted by the following steps.

Step 1

The function $\ddot{Z}(x)$ in eq.(1) developed approximately using Morgan-Voyce polynomial:-

$$\ddot{Z}(x) = \sum_{i=0}^{n} C_i\, M_i(x) \qquad (4)$$

Step 2

Integrating eq.(4) twice from 0 t0 x depending the boundary condition to get :-

$$Z(x) = Z(0) + \dot{Z}(0)x + \iint_0^x \sum_{i=0}^{n} C_i M_i(x) \qquad (5)$$

Step 3

Substituting the boundary condition into eq.(5) to reduce the Morgan-Voyce coefficient differential equation.

Step 4

Rewriting eq.(1) by substituted eq.(5) &(4) to get

$$\sum_{i=0}^{n} C_i\, M_i(x) + F(x)\left[Z(0) + \dot{Z}(0)x + \iint_0^x \sum_{i=0}^{n} C_i M_i(x)\right] = G(x) \qquad (6)$$

Step 5

By consider the collocation point $x_j = \frac{j-0.5}{2n}$ j=1,2,3,… can be resulting algebraic system which is solved to find the unknown coefficient M_i.

Step 7

Ibn Al-Haitham Journal for Pure and Applied science https://doi.org/10.30526/2021.IHICPAS.2654

Substituted the calculated coefficients into eq.(5). The solution for eq.(1) will be obtained.

4. Examples Illustrations:-

For showing the accuracy and activity of our approximate method, we consider the following examples.

Example (1):

$$\ddot{Z} - 12\,x^{-2}Z = 0 \qquad Z(1) = Z(-1) = 1\,, \qquad Z(0) = \dot{Z}(0) = 0 \tag{7}$$

Exact solution x^4

For assume $\ddot{Z}(x) \cong \sum_{i=0}^{4} C_i M_i(x)$ (8)

by integrating eq.(8) twice time and applying the steps studied in section(3), the approximate coefficient will be

C_0=36 , C_1=-48 , C_2=12 , C_3=C_4=0.

Applying the approximate coefficient into eq.(8) , we obtain the exact solution $Z(x) \cong x^4$

Example (2):

$$\ddot{Z} - Z = (4x^6 + 12\,x^2)e^{x^2} \qquad Z(1) = Z(-1) = e^1\,, \qquad Z(0) = \dot{Z}(0) = 0$$

Exact solution $x^4\ e^{x^2}$

Assume that $\ddot{Z}(x) \cong \sum_{i=0}^{6} C_i M_i(x)$

by applying the same method and solve a system of equations we approximate the solution. **Table 1** reflects the comparison between the approximate solution with the exact solution and absolute error.

Table 1

x	approximate	Exact	Absolute error
-1	2.718282	2.718282	0
-0.75	0.555381	0.555310	0.000071
-0.5	0.080242	0.080252	0.00001
-0.25	0.004157	0.004158	0.0000001

Ibn Al-Haitham Journal for Pure and Applied science https://doi.org/10.30526/2021.IHICPAS.2654

0	0	0	0
0.25	0.004157	0.004158	0.0000001
0.5	0.080242	0.080252	0.00001
0.75	0.555381	0.555310	0.000071
1	2.718282	2.718282	0

Example (3):

$$\ddot{Z} - \frac{1}{x}\dot{Z} + Z = (4x+1)e^{x^2} + x^2 \qquad Z(1) = Z(-1) = 1 + e^1 \,, Z(0) = 1,$$
$$\dot{Z}(0) = 0$$

Exact solution $x^2 + e^{x^2}$

let $\ddot{Z}(x) \cong \sum_{i=0}^{8} C_i M_i(x)$

the comparison between the approximate and exact solution are showing in **Table 2**.

Table 2

x	approximate	Exact	Absolute error
-1	3.718282	3.718282	0
-0.8	2.536470	2.536481	0.000011
-0.6	1.793318	1.793329	0.000011
-0.4	1.333511	1.333511	0.000000
-0.2	1.080812	1.080811	0.000001
0	1	1	0
0.2	1.080812	1.080811	0.000001
0.4	1.333511	1.333511	0.000000
0.6	1.793318	1.793329	0.000011
0.8	2.536470	2.536481	0.000011
1	3.718282	3.718282	0

4.Conclusion

In this article, a new general formula for Morgan-Voyce polynomial collocation method is employed to solve the three-point boundary value problems. The approached plane is tested by some examples and the results are satisfied in comparison with approximate with existing.

References

1. Yang, C. Positive Solutions for a Three-Point Boundary Value Problem of Fractional Q-Difference Equations. *Symmetry.* **2018**, *10*(9), 358; doi:10.3390/sym10090358.
2. Ali, Z.; Zada, A.; Shah, k. Existence and Stability Analysis of Three Point Boundary Value Problem. International Journal of Applied and Computational Mathematics, **2017**, *3(1),* 651-664. doi:101007/s40819-017-0375-8.
3. Mohamed, M. ; Thompson, H.; Jusoh M. Discrete First-Order Three-Point Boundary Value Problem. *Journal of Mathematics Research*, **2019**, *1, 2*. doi**:**10.5539/jmr.v1n2p207.

4. Liu H.; He J.; Li Z. Variational principle for a three-point boundary value problem. J. Nonlinear Sci. Appl. **2016**, *9(8):*5169—5174. doi:10.22436/jnsa.009.08.02.
5. Morgan-Voyce,A.Ladder-Network Analysis Using Fibonacci Numbers. in IRE transactions on Circuit Theory.**1959**, *6, 3,* 321-322, , doi: 10.1109/TCT.1959.1086564.
6. Özel M, K; Kürkçü, Ö; Sezer M. Morgan-Voyce matrix method for generalized functional integro-differential equations of Volterra type. *Journal of Science and Arts* ,**2019**, *47 (2):* 295-310. Available from: https://search.proquest.com /openview/04dd41f26209638 eae2f4f2 486d359d7/1?pq-origsite=gscholar&cbl=105793.
7. İlhan, Ö.An Improved Morgan-Voyce Collocation Method for Numerical Solution of Generalized Pantograph Equations. *Journal of Scientific and Engineering Research*, **2017**, *4(10):*320-332. Available from: http://oaji.net/articles/2017/4834-1525935151.pdf.
8. Türkyılmaz, B; Gürbüz, B; Sezer, M. Morgan-Voyce Polynomial Approach for Solution of High-Order Linear Differential-Difference Equations with Residual Error Estimation. Düzce University, *Journal of Science and Technology*, **2016**, *4 (1),* 0-0. Available from :https: // dergipark org.tr/tr/pub/dubited/issue/24381/258462.
9. Tarakçi, M.,;Özel, M.; Sezer, M. Solution of nonlinear ordinary differential equations with quadratic and cubic terms by Morgan-Voyce matrix-collocation method. *Turkish Journal of Mathematics,* **2020**, *44*, 906-918,doi:10.3906/mat-1908-102.
10.Swamy ,M.; Bhattacharyya ,B.A Study of Recurrent Ladders Using the Polynomials Defined by Morgan-Voyce. in IEEE Transactions on Circuit Theory, **1967**, *14, 3*, 260-264, doi: 10.1109/TCT.1967.1082705.
11. Horadam A.F.New Aspects of Morgan-Voyce Polynomials. In: Bergum G.E., Philippou A.N., Horadam A.F. (eds) Applications of Fibonacci Numbers. Springer, Dordrecht.**1998**. doi:10.1007/978-94-011-5020-0_20.

12. Swamy, M. RISING DIAGONAL POLYNOMIALS ASSOCIATED WITH MORGAN-VOYCE POLYNOMIALS. Fibonacci Quarterly , 200,)38(1), AMS Classification Available from: https://www..fq.math.ca/Scanned/38-1/swamy2.pdf 0.

Ibn Al-Haitham Journal for Pure and Applied science https://doi.org/10.30526/2021.IHICPAS.2655

Improved Certificate-Based Encryption Scheme in the Big Data: Combining AES and (ECDSA – ECDH)

Omar Salah F. Shareef
omar.alshareef@uofallujah.edu.iq
University of Fallujah, Fallujah, Iraq

Ali Makki Sagheer
prof.ali@alqalam.edu.iq
Qalam University College, Kirkuk, Iraq

Abstract

Big data usually running in large-scale and centralized key management systems. However, the centralized key management systems are increasing the problems such as single point of failure, exchanging a secret key over insecure channels, third-party query, and key escrow problem. To avoid these problems, we propose an improved certificate-based encryption scheme that ensures data confidentiality by combining symmetric and asymmetric cryptography schemes. The combination can be implemented by using the Advanced Encryption Standard (AES) and Elliptic Curve Diffie-Hellman (ECDH). The proposed scheme is an enhanced version of the Certificate-Based Encryption (CBE) scheme and preserves all its advantages. However, the key generation process in our scheme has been done without any intervention from the certificate issuer and avoiding the risk of compromised CA. The Elliptic Curve Digital Signature Algorithm (ECDSA) has been used with the ECDH to handle the authentication of the key exchange. The proposed scheme is demonstrated on a big dataset of social networks. The scheme is analyzed based on security criteria that have been compared with the previous schemes to evaluate its performance.

Keywords: Big Data Security; Certificate-Based Encryption; ECDSA; ECDH; AES.

1.Introduction

The term ‘Big Data’ has been become an essential part of people's lives. The appearance of big data has brought new challenges regarding data security. The collecting, storage, manipulation and retention of huge quantities of data have led to critical security and privacy considerations (Cheng et al.,2017). Accessing the data needs to be controlled to affirm that the non-eligible entities cannot tamper with or access the data. Improving the security and authentication of sensitive data can give the companies new businesses opportunities. Therefore, close attention has been drawn to secure data firmly from any unauthorized access. The main challenge in big data that are using a complicated distributed system, is the multifaceted nature of overseeing wide usage. Verification ought to be overseen by an adaptable, hearty and versatile framework that denies a malevolent client from access big data. Accordingly, new ways to deal with security are required to defeat the security blemishes in the current usage. However, there are two methods to design a secure system and protecting the privacy of the receivers in a communication system; symmetric and asymmetric keys.

The secure cryptosystem is based on effective key management. However, the security of any cryptosystem is dependent upon how securely its keys are managed?

Public Key Infrastructure (PKI) generates and handles a pair of keys in addition to the certificate. The main challenge of managing the digital certificate in public key infrastructure is when we have many nodes in a distributed environment.

To cope with this issue, Shamir (A Shamir, 1984) produced the concept of Identity-Based Encryption (IBE) where the identity was used as a public key, and a third party generates a secret key for the user. This approach eliminates the demand for digital certificates. However, IBE suffers from a key escrow problem, the third party holds the private keys of clients, as a result, it can peek at all communication data of users and successfully disguise himself as any user to sign a message. Alternatively, Certificate-Based Encryption (CBE) overcomes the drawbacks of PKI and IBE.

In 2003, Gentry (Gentry, 2003) presented the idea of CBE. This scheme merges Public-Key Encryption (PKE) and IBE while safeguarding the highlights of schemes. As in conventional PKE, every client produces a pair of keys then asks for a certificate from the Certificate Authority (CA). The significant matter in CBE is a certificate works as a partial private key as well as its work as a certificate. This function produces an effective implicit certificate, thus a recipient wants the certificate together with his/her private key to decrypt a ciphertext, whilst the senders do not need to be concerned about the certificate revocation problem. However, the CBE copes with the limitations of IBE and PKE. The CBE can ignore third-party queries. Then, disregarding a secure channel among the CA and clients. Furthermore, it is avoiding the key escrow problem (since CA does not know the private keys of users). Finally, it fixes the certificate revocation problem.

In recent years, CBE has attracted considerable interest in the community of research and several schemes in CBE have been proposed (Liu and Zhou, 2008; Lu et al., 2008; Galindo et al., 2008; Hyla et al., 2015; Lu and Li, 2014; Le, Kim and Hwang, 2016; Hwang and Le, 2018).

In this paper, we propose an efficient certificate-based encryption scheme that ensures data confidentiality by combining symmetric and asymmetric cryptography schemes. Particularly, using the Advanced Encryption Standard (AES) and Elliptic Curve Diffie-Hellman (ECDH). Moreover, the Elliptic Curve Digital Signature Algorithm (ECDSA) has been used with ECDH to handle the weakness of authentication between the nodes whilst using the ECDH approach. When the system is on a large scale, the task will be computationally intensive. Moreover, the proposed scheme can be supported distributive processing in large-scale key management within a distributed environment.

1. PRELIMINARIES

2.1 ECDSA

ECDSA is the elliptic curve analog of the Digital Signature Algorithm DSA (Johnson et al., 2001). Vanstone proposed the ECDSA scheme as an answer to the request of the National Institute of Standards and Technology (NIST) for feedback on their proposal about the Digital Signature Scheme (DSS) (S. Vanstone, 1992).

DSS is similar to handwritten signatures. The digital signature represents a number based on the private key known only by the signer and on the contents of the signed message, as well as, the signatures should be verified without gain access to the secret key of the signer (Langford, 1995). ECDSA algorithm is defined as follows:

Setup

1. Alice and Bob select a finite field Fq and an elliptic curve E over Fq (E(Fq)).

2. They choose a random base point B ∈ E with order n, such that B generates a large subgroup of E, preferably of the same order as that of E itself.

Key generation

1. choose a secret random integer d in the interval $[2, N]$
2. Computes $Q = dB$
3. Make Q public and keep d secret

Signature generation
Alice sends the signed message to Bob as follows

1. Select random integer k in the interval $[2, N]$
2. Compute $(x, y) = kB$
3. Compute $r = x \bmod n$
4. Compute $e = H(M)$
5. Compute $s = k^{-1}(e + d\,r) \bmod n$
6. The signature for M is (r, s)

Signature verification
Bob verifies Alice's signature (r, s) on message M as follows

1. Compute $e = H(M)$
2. Compute $w = s^{-1} \bmod n$
3. Compute $u_1 = e\,w \bmod n$
4. Compute $u_2 = r\,w \bmod n$
5. Compute $(x, y) = u_1 B + u_2 Q$. If $(x, y) = O$ then reject the signature
6. Otherwise, Compute $v = x \bmod n$
7. Accept the signature if and only if $v = r$

2.2 ECDH

ECDH is a key agreement algorithm that lets two entities generate a shared secret key based on ECC (Anoop, 2001). The following example illustrates how the key establishment will be made.

Suppose A wants to generate a shared key with B through a channel that may be eavesdropped on by a third party. Initially, each entity should agree upon Elliptic Curve domain parameters (q, a, b, G, n, h). Each has a pair of keys; d is a secret key (which is a random integer $< n$, where n is the order of the curve, a domain parameter of the elliptic curve) and a public key $Q = d * G$ (where G is the generator factor, a domain parameter

of the elliptic curve). Suppose $d_A \cdot Q_A$ are the secret/public key of A, and $d_B \cdot Q_B$ are the secret/public key of B.

1. A computes E = $(X_E, Y_E) = d_A \cdot Q_B$
2. B computes F = $(X_F, Y_F) = d_B \cdot Q_A$
3. Since $d_A \cdot Q_B = d_A \cdot d_B \cdot G = d_B \cdot d_A \cdot G = D_B \cdot Q_A$
4. Thus E = F and subsequently $X_E = X_F$
5. As a result, the shared secret is X_E

Because of difficulties regarding discovering the secret key d_A or d_B from the public key E or F, it's difficult to get the shared secret for an outsider.

The algorithm of ECDH Key Exchange is described as following:
Goal: generate a secure shared key
Input: elliptic curve parameter domain
Output: secure shared key E
Step 1:

1. Client A chooses secret random number $X < n$
2. Client B chooses the secret random number $Y < n$

Step 2:

1. Client A computes $PU_A = X * G$
2. Client B computes $PU_B = Y * G$

The two parties share their public keys and the common base point G
Step 3:

1. Client A compute $E = X * PU_B$
2. Client B compute $E = Y * PU_A$

Step 4: Return (E)

3. The Proposed Scheme

In this research, an improved certificate-based encryption scheme has been proposed, and that ensures data confidentiality by combining symmetric and asymmetric cryptography schemes. Particularly, using the Advanced Encryption Standard (AES) and Elliptic Curve Diffie-Hellman (ECDH). Moreover, the Elliptic Curve Digital Signature Algorithm (ECDSA) was used with ECDH to handle the weakness of authentication between nodes while using the ECDH approach. When the system is on a large scale, the task will be computationally intensive.
The proposed scheme will be reduced the workload of the CA by delegating the task of CA to the user level. In other words, the key generation process is done without any intervention from the certificate provider. The keys are generated using the ECDH algorithm and it's derived from the parameters that generate the keys of the certificate and hence avoiding the risk of compromised CA. Accordingly, it can also resolve the problem of violation of any privacy of customers because it resolves the key escrow problem.

Moreover, the proposed scheme can be supported distributive processing in large-scale key management within a distributed environment. The overview of system layers is shown in more detail in **Figure 1**, which presents the block diagram of system operations using the improved CBE.

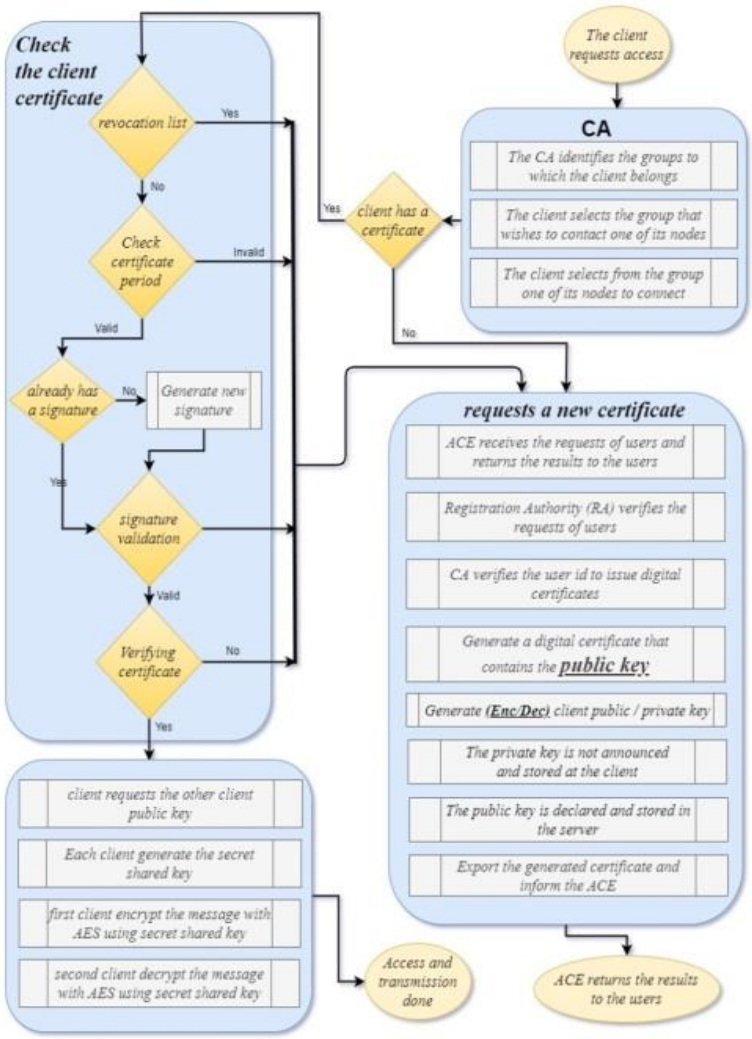

Figure 1 .The Block Diagram of the Proposed Model

By utilizing the benefit of ECDSA, our proposed scheme was built by applying the ECDSA with ECDH that generating the encryption keys. In particular, we designed the setup and certification algorithm by utilizing the key generation as well as the signature generation algorithms of ECDSA. Additionally, by using the key generation algorithm of ECDH, we design the *SetKeyPair* algorithm. Symmetric algorithm AES is used for

constructing encryption and decryption algorithms, in this research AES-128 is used. ECDSA and ECDH are based on some parameters for all network participants.
which:
q = Order of the prime field Fq
E = an elliptic curve y2 = x3 + ax + b defined over the prime field Fq
G = A random non-zero base point in E(Fq)
n = the order of G, typically a prime
h = the cofactor $\frac{|E(fq)|}{n}$
The improved CBE scheme consists of six algorithms:

1. Setup:
ECDSA and ECDH are based on some parameters (params) common for all network participants. Setup run by the CA. It takes the security parameter as input and returns the CA's master secret key *msk*.

2. Certificate *SetKeyPair*:
Input: ID, Domain Parameters.
Output: private key d and secret key Q and master secret key E for encryption/decryption.
private key: $d \in R[1, n-1]$
public key: $Q = dG \in E(Fq)$

3. Encryption/Decryption *SetKeyPair*:
This process has been performed by users without the intervention of the certificate provider. The keys that have been generated will be using the same parameters that are used to generate certificate keys. The shared key is generated using ECDH.

4. Certification:
ECDSA takes ID, params, *msk*, Q and additional identifying information, such as name, as input, and the output is the certificate *Cert* to the user.

A. ECDSA Signature Generation
Input: Domain Parameters, the secret key of the signer d and message M
Output: ECDSA signature (r, s)
k = a haphazardly picked component in $[1, n-1]$ (the session key)
$R = kG$
$r = x(R)$ (the x-coordinate of R) reduced module n
$s = k = 1(H(M) + dr) mod\ n$, H is a cryptographic hash function

B. ECDSA Signature Verification
Input: Domain Parameters, signature (r, s) message M and the public key of signer Q.
Output: accepted or rejected.
$w = s - 1\ mod\ n$
$u = H\ (M)w\ mod\ n$
$v = rw\ mod\ n$
$R = uG + vQ\ \in\ E(Fq\ )$
Accept the signature if and only if $x(R) = r\ mod\ n$

5. Encryption:
Input: ID, params, E, and plain M.

Output: cipher C . AES generate series of AES round keys from E and return (AES_round_key).
Initial Step:
$N_b \leftarrow 4$ (data blocks are of 128 bits)
$N_r \leftarrow$ number of rounds in the cipher (N_r =10 for AES-128)
Step 1:
State ←plain
AddRoundKey (state, w (0, Nb - 1))
Step 2:
For all round do where {1 ≤ round < Nr}
SubBytes (state)
ShiftRows (state)
MixColumns (state)
AddRoundKey (state, w (round * Nb, (round + 1) * Nb - 1))
End for
Step 3:
SubBytes (state)
ShiftRows (state)
AddRoundKey (state, w [Nr * Nb, (Nr+1) * Nb - 1])
cipher_text ← state
Step 4:
Return (cipher)

6. Decryption:
Input: ID, params, Cert, E, and cipher C
Output: plain M
Initial Step:
Nb ← 4 (data blocks are of 128 bits)
Nr← number of rounds in the cipher (Nr = 10 for AES-128)
Step 1:
State ←cipher
AddRoundKey (state, w (Nr * Nb, (Nr + 1) * Nb - 1))
Step 2:
For all-round do where {Nr > round ≥ 1} decrement round by 1
InvShiftRows (state)
InvSubBytes (state)
AddRoundKey (state, w (round * Nb, (round + 1) * Nb - 1))
InvMixColumns (state)
End for
Step 3:
InvShiftRows (state)
InvSubBytes (state)
AddRoundKey (state, w (0, Nb - 1))
Plain← state
Step 4:
Return (Plain)

However, the algorithm of the proposed model is described in detail in **Table 1**.

Table 1: The Algorithm of Proposed Model

Goal: Verify or Generate new Certificate

Input: Access request

Output: The client has access

Step1 *The client requests access.*
Step2 *The CA identifies the groups to which the client belongs.*
Step3 *The client selects the group that wishes to contact one of its nodes.*
Step4 *The client selects from the group one of its nodes to connect.*
Step5 *Check the client certificate*

- *Parse the client certificate*
  - *If the client has a certificate, then go to the next condition*
  - *Otherwise, the client doesn't have a certificate and go to Step 11 or Cancelling request*
- *Check the period of the client certificate*
  - *If valid, then go to the next condition*
  - *Otherwise, expire and go to Step 11 or Cancelling request*
- *Check the certificate signature*
  - *If the client already has a signature from a previous verification, then go to the next condition*
  - *Otherwise, check the signature validation*
    - *If valid, then go to the next condition*
    - *Otherwise, inauthentic and go to Step 11 or Cancelling request*
- *Check the revocation list*
  - *If the client is not revoked in the group to which he belongs, then go to the next condition*
  - *Otherwise, outmode and go to Step 11 or Cancelling request*
- *Check the certificate path until the root certificate*
  - *If the root certificate is valid, then the client has a connection and* ***Done***
  - *Otherwise, invalidate the certificate and go to Step 11 or Cancelling request*

Step6 *The client requests the other client's public key*
Step7 *Each client generates the secret shared key*
Step8 *The first client encrypts the message with AES and using the generated key as encryption key.*
Step9 *The second client decrypt the received message with AES and using the generated key as decryption key.*
Step10 *Access and transmission done.*
Step11 *The client requests a new certificate.*
Step12 *The ACE receives the requests of clients and returns the results to the clients.*
Step13 *The Registration Authority (RA) verifies the requests of clients for a digital certificate and inform the CA to issue it.*
Step14 *The CA verifies the client's id to issue the digital certificates.*
Step15 *Generating a digital certificate which contains its public key.*
Step16 *Generating client's public / private key.*
Step17 *Export the certificate to the server engine.*
Step18 *Store the generated certificate at the certificate service database and inform the ACE.*
Step19 *The ACE returns the results to the clients.*
Step20 *End.*

4. Cryptographic Tool and Dataset

The proposed model was coded in the C# programming language. Also, the open code library "Bouncy Castle" has been used to compose the code. This library is created by the Legion of Bouncy Castle and is a C# usage of cryptographic algorithms.

Friendster social network and ground-truth communities have been used as a dataset for our model (Yang and Leskovec, 2015). Friendster is an online gaming network where clients can create friendship edges with each other. The dataset includes a lot of groups of nodes, each node is either linked to at least one group or is linked to other nodes that belong to different groups. The dataset contains 65,608,366 nodes and 1,806,067,135 edges.

5.System Analysis and Performance

Security Proof

There are two attacks against digital signatures regarding the ECDSA algorithm: a key attack wherein the adversary has a knowledge of the public key and a message attack wherein the adversary has got right of entry to signatures earlier than cracking the function. However, there are various understandings of break a digital signature: recovering the private key, producing an alternative algorithm of signature with a corresponding private key, and then forge a signature for a specific message (Goldwasser et al., 1988).

There are fundamental conditions for ECDSA to make it hard to break and have powerful security (Vaudenay, 2003):

- The discrete logarithm inside the subgroup spanned with the aid of G is difficult. This makes sure it is difficult to resolve the discrete logarithm problem and consequently not possible access the private key.

- The used hash function is a one-way collision-resistant. When could not specify m from $(m) = y$, we can say one-way collision-resistant. However, collision-resistant function has a little opportunity of mapping different messages to be equivalent $(i.e. H(m1) = H(m2))$.

- The generator for k is could not predict. Else, the private key can be acquired using $k, r,$ and s.

Concerning ECDSA, there are two major attacks that either versus the hash function used within the signature generation or against ECDLP (Johnson, Menezes, and Vanstone, 2004). If the algorithm no longer comprises the second bullet point from above, the attacker can discover a collision in the hash function by two messages, and sign a message but claim his signature on the other. ECDLP is described as solving for d in $Q = dG$ within the key generation algorithm. There are common attacks versus ECDLP involving the “Pohlig-Hellman”, “exhaustive seek” and “baby-Step giant-Step” algorithms. Besides these attacks, Pollard’s Rho algorithm has a running time of $(\sqrt{n\pi}) / 2$, in which n is the order of point G. However, this algorithm parallelized and run on r various processors, hence the new running time is $(\sqrt{n\pi})/2r$.

6.Encryption Time Consummation

In this section, a comparative test of the time consumption of our proposed CBE scheme against the RSA algorithm is discussed. Key generation and encryption/decryption of 40 bits' string of characters is tested based on the PC of Core i7 with Frequency 2.2GHz, RAM 8GB, and the operating system is Windows10 with 64bit. These comparisons show the time consumption of the key generation when using ECC of the proposed CBE scheme against RSA as shown in **Table 2**, and the encryption/decryption when using AES of the proposed CBE scheme against RSA algorithm as shown in **Table 3**.

Table 2: Time Consumption of Key Generation (ms)

Key length	Key pair generation	
	RSA	ECC
1024 / 160	237	218
2048 / 224	1440	232
3072 / 256	3377	234
7680 / 384	108718	278
15360 / 512	925284	375

Table 3: Time Consumption of Encryption/Decryption (ms) and (µs)

Key length	Encryption		Decryption		Total (Encryption & Decryption)	
	RSA	AES	RSA	AES	RSA	AES
1024 / 160	680 µs	230 µs	4	1	5	2
2048 / 224	870 µs	440 µs	16	2	17	3
3072 / 256	3	1	32	2	35	3
7680 / 384	6	2	559	2	565	4
15360 / 512	19	3	3456	4	3475	7

Although AES is faster than RSA in encryption, it is noticeable that the gap between ECC and RSA systems grows rapidly as the key sizes increase in key pair generation. Subsequently, the RSA system is much more time-consuming than the ECC system. Hence to obtain an efficient and higher security level, especially in the big data environment, the key sizes must expand and it is advisable to select the ECC-based system.

7.Statistical Analysis

Big Data has a characteristic of the variety, so it may contain images. Therefore, several tests were performed to encrypt the image using the proposed scheme. However, to resist statistical attacks, the encrypted images should possess certain random properties. Independence and uniformity are two properties that should be satisfied by any encryption scheme to ensure high resistance against statistical attacks. To prove the performance of the improved cryptosystem and verify these properties, a statistical analysis has been performed by calculating the correlation, SSIM, MSE, and histograms for the plain image and the encrypted image. Several images have been tested, and it has shown that the intensity values are good as illustrated in **Table 4**.

Table 4. Results of Differential Analysis

Image	Correlation		SSIM	MSE
	Original image	Encrypted image		
Lena	0.9959	0.0009	0.1061	0.3346
Airplane	0.9948	0.0004	0.1112	0.3347
Pepper	0.9966	0.0021	0.1067	0.03345
Tulips	0.9981	0.0061	0.0933	0.3384

The experimental result of the plain image and its corresponding cipher image and their histograms are shown in **Figure 2**. The figure shows the original plain image and its cipher image encrypted by the improving scheme. The result reveals that the improved scheme has reliable encryption and decryption effect. The histogram of the encrypted image is nearly uniformly distributed and significantly different from the respective histograms of the original images, which means that the improved algorithm has an excellent performance in resisting statistical attacks.

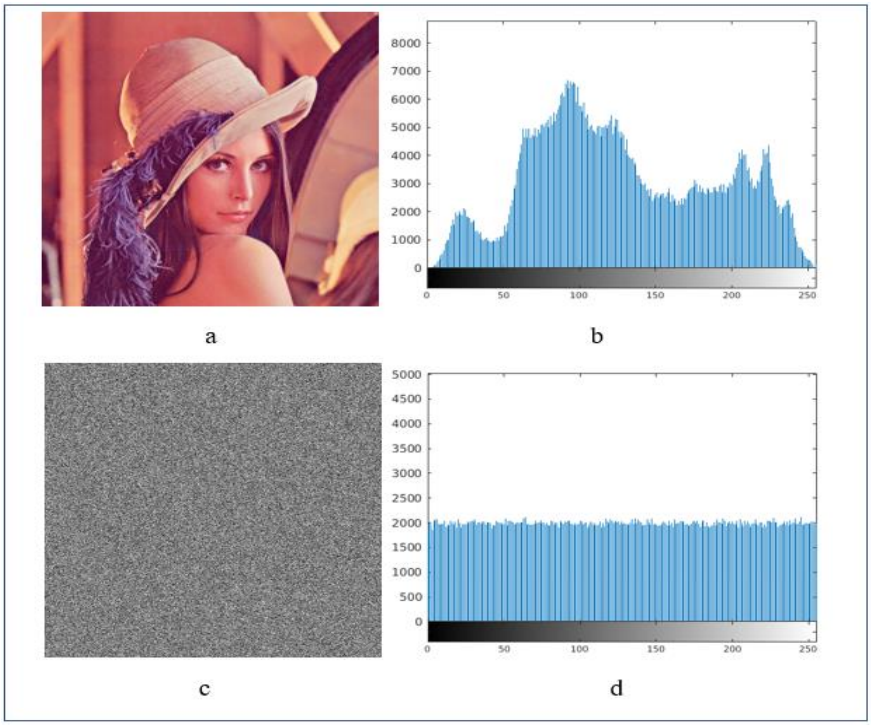

Figure 2. (a) Original Image (b) Histogram of Original Image (c) Encrypted Image (d) Histogram of Encrypted Image

8.Conclusion

An improving algorithm of Certificate-Based Encryption has been presented to using it in the Big Data environment. The system can handle the risks of the compromised CA and key escrow problem, as well as ensure the privacy of communications between clients because the key generation is done at the user level without any intervention from the certificate provider using ECDH, and hence the private key cannot be illegally obtained.

The combining of ECDSA as well ECDH will build a strong system that ensures secure communication among the entities. The key exchange process takes place after the completion of the authentication process, where the authentication is done by verifying the certificate. As a result, the key exchange operation is secured. The keys are then exchanged to generate a shared secret key, which is used as a key to encrypt and decrypt the data.

Consequently, this ensures that two-way data security each one completes the other. The certificate provider cannot decrypt the ciphertext, and at the same time, the user can not send the data without a verified certificate approved by the certificate provider. The proposed scheme tested on a big dataset of social networks. A comparison of the time consumption of the model has been tested and shown to be fast in key generation, encryption, and decryption. However, since the variety is a characteristic of big data, several tests were performed to encrypt the images using the proposed scheme and it has shown that the intensity values are acceptable.

References

1.Ahmed, H. E. H.; Kalash, H. M., ; Farag Allah, O. S. (2007). Encryption efficiency analysis and security evaluation of RC6 block cipher for digital images. **2007** *International Conference on Electrical Engineering,ICEE*. https://doi.org/10.1109/ICEE.2007.4287293.

2.A Shamir ,Identity Based Cryptosystem and Signature Schemes, *Advances in Cryptology Proceedings of CRYPTO*, **1984**, *84*, 7–53. Available at:

http://discovery.csc.ncsu.edu/Courses/csc774-S08/reading-assignments/shamir84.pdf.

3.Anoop, M. S. Elliptic Curve Cryptography – An Implementation Tutorial Elliptic Curve Cryptography An Implementation Guide. **2001** ,1–11. Available at:http://www.infosecwriters.com/text_resources/pdf/Elliptic_Curve_AnnopMS.pdf.

4.Cheng, L., Liu, F. ; Yao, D. D. Enterprise data breach: causes, challenges, prevention, and future directions, Wiley Interdisciplinary Reviews: *Data Mining and Knowledge Discovery*, **2017**, *7(5)*, 1–14. doi: 10.1002/widm.1211.

5.Galindo, D., Morillo, P. ; Ràfols, C. Improved certificate-based encryption in the standard model, *Journal of Systems and Software*, **2008**, *81(7)*, 1218–1226. doi: 10.1016/j.jss.2007.09.009.

6.Gentry, C. Certificate-Based Encryption and the Certificate Revocation Problem, International Conference on the Theory and Applications of Cryptographic Techniques: Advances in Cryptology — EUROCRYPT, **2003**, 272–293. doi: 10.1007/3-540-39200-9_17.

7.Goldwasser, S., Micali, S., ; Rivest, R. L. A digital signature scheme secure against adaptive chosen-message attacks, *SIAM Journal on Computing*, **1988**,*17(2)*, 281–308.

8.Daoud, A. O., Tsehayae, A. A.; Fayek, A. R. A guided evaluation of the impact of research and development partnerships on university, industry, and government. *Canadian Journal of Civil Engineering*, **2017**,*44(4)*,253–263.

9.Hwang, S. O. ; Le, M. H. Efficient certificate-based encryption and hierarchical certificate-based encryption schemes in the standard model, *Journal of Intelligent and Fuzzy Systems*, **2018**, *35(6)*, 5971–5981. doi: 10.3233/JIFS-169838.

10. Hyla T., Maćków W., Pejaś J. Implicit and Explicit Certificates-Based Encryption Scheme. In: Saeed K., Snášel V. (eds) Computer Information Systems and Industrial Management. CISIM 2015. Lecture Notes in Computer Science, vol 8838. Springer, Berlin, Heidelberg. **2014**, 651-666. doi:10.1007/978-3-662-45237-0_59.

11.Johnson, D.; Menezes, A. ; Vanstone, S. The Elliptic Curve Digital Signature Algorithm Validation System (ECDSAVS).**2004**, 56. Available at: http://cs.ucsb.edu/~koc/ccs130h/notes/ecdsa-cert.pdf.

12.Langford, Susan K. Threshold DSS signatures without a trusted party." *Annual International Cryptology Conference*. Springer, Berlin, Heidelberg, **1995**.

13.Lehmann, E. L.; Casella, G. Theory of Point Estimation , Second Edition *Springer Texts in Statistics In Design*. **1998**,*41*. https://doi.org/10.2307/1270597

14.Le, M. H., Kim, I. ; Hwang, S. O. 'Efficient certificate-based encryption schemes without pairing', *Security and Communication Networks*. **2016**, *9(18)*, 5376–5391. doi: 10.1002/sec.1703.

15.Liu, J. K. ; Zhou, J. Efficient certificate-based encryption in the standard model, *Lecture Notes in Computer Science (including subseries Lecture Notes in Artificial Intelligence and Lecture Notes in Bioinformatics)*, 5229 LNCS, **2008**, 144–155. doi: 10.1007/978-3-540-85855-3_10.

16.Lu, Y. ; Li, J. Efficient certificate-based encryption scheme secure against key replacement attacks in the standard model, *Journal of Information Science and Engineering*, **2014**,*30(5)*, 1553–1568.

17.Lu, Y., Li, J. and Xiao, J. (2008) Generic construction of certificate-based encryption, *Proceedings of the 9th International Conference for Young Computer Scientists*, ICYCS

2008,1589–1594. doi: 10.1109/ICYCS.2008.11.
18.*S. Vanstone,* Responses to NIST's Proposal, *Communications of the ACM, 35, July* **1992**, *50-52 (communicated by John Anderson).*
19.Yang, J., ; Leskovec, J. Defining and evaluating network communities based on ground-truth. *Knowledge and Information Systems*, **2015**, *42*(1), 181-213.Retrievedfrom https://snap.stanford.edu/data/com-Friendster.html
20.Vaudenay, S. (2002) The security of DSA and ECDSA: Bypassing the standard elliptic curve certification scheme, *Public Key Cryptography — PKC* **2003**, 2567, 309–323.